

30703



National Library  
of Canada

Bibliothèque nationale  
du Canada

CANADIAN THESES  
ON MICROFICHE

THÈSES CANADIENNES  
SUR MICROFICHE

NAME OF AUTHOR/NOM DE L'AUTEUR GEORGE EDWARD NEWTON HEAL

TITLE OF THESIS/TITRE DE LA THÈSE THE WRIGLEY-LOU AND POLARIS-TRURO LEAD ZINC DEPOSITS,  
N. W. T.

UNIVERSITY/UNIVERSITÉ UNIVERSITY OF ALBERTA

DEGREE FOR WHICH THESIS WAS PRESENTED/  
GRADE POUR LEQUEL CETTE THÈSE FUT PRÉSENTÉE MASTERS OF SCIENCE

YEAR THIS DEGREE CONFERRED/ANNÉE D'OBTENTION DE CE DEGRÉ 1976

NAME OF SUPERVISOR/NOM DU DIRECTEUR DE THÈSE DR. R. E. FOLINSBEE

Permission is hereby granted to the NATIONAL LIBRARY OF  
CANADA to microfilm this thesis and to lend or sell copies  
of the film.

*L'autorisation est, par la présente, accordée à la BIBLIOTHÈ-  
QUE NATIONALE DU CANADA de microfilmer cette thèse et  
de prêter ou de vendre des exemplaires du film.*

The author reserves other publication rights, and neither the  
thesis nor extensive extracts from it may be printed or other-  
wise reproduced without the author's written permission.

*L'auteur se réserve les autres droits de publication; ni la  
thèse ni de longs extraits de celle-ci ne doivent être imprimés  
ou autrement reproduits sans l'autorisation écrite de l'auteur.*

DATED/DATE September 8, 1976 SIGNED/SIGNÉ *George Edward Newton Heal*

PERMANENT ADDRESS/RÉSIDENCE FIXE Box 339, Oliver, British Columbia

#### INFORMATION TO USERS

THIS DISSERTATION HAS BEEN  
MICROFILMED EXACTLY AS RECEIVED

This copy was produced from a microfiche copy of the original document. The quality of the copy is heavily dependent upon the quality of the original thesis submitted for microfilming. Every effort has been made to ensure the highest quality of reproduction possible.

PLEASE NOTE: Some pages may have indistinct print. Filmed as received.

Canadian Theses Division  
Cataloguing Branch  
National Library of Canada  
Ottawa, Canada K1A 0N4

#### AVIS AUX USAGERS

LA THESE A ETE MICROFILMEE  
TELLE QUE NOUS L'AVONS RECUE

Cette copie a été faite à partir d'une microfiche du document original. La qualité de la copie dépend grandement de la qualité de la thèse soumise pour le microfilmage. Nous avons tout fait pour assurer une qualité supérieure de reproduction.

NOTA BENE: La qualité d'impression de certaines pages peut laisser à désirer. Microfilmée telle que nous l'avons reçue.

Division des thèses canadiennes  
Direction du catalogage  
Bibliothèque nationale du Canada  
Ottawa, Canada K1A 0N4

THE UNIVERSITY OF ALBERTA

THE WRIGLEY-LOU AND POLARIS-TRURO LEAD ZINC DEPOSITS, N.W.T.

by



GEORGE E. NEWTON HEAL

B.A. (Victoria)

B.Sc. (Alberta)

A THESIS

SUBMITTED TO THE FACULTY OF GRADUATE STUDIES AND RESEARCH

IN PARTIAL FULFILMENT OF THE REQUIREMENTS FOR THE DEGREE

OF MASTER OF SCIENCE

DEPARTMENT OF GEOLOGY

EDMONTON, ALBERTA

FALL, 1976

THE UNIVERSITY OF ALBERTA  
FACULTY OF GRADUATE STUDIES AND RESEARCH

The undersigned certify that they have read, and  
recommend to the Faculty of Graduate Studies and Research, for  
acceptance, a thesis entitled The Wrigley-Lou and Polaris-  
Truro Lead Zinc Deposits, N.W.T.  
submitted by George E. Newton Heal  
in partial fulfilment of the requirements for the degree of  
Master of Science

R.E. Johnson  
(Supervisor)  
M. Helch  
G. Canning

Date July 16, 1976



## ABSTRACT

The Cominco-owned Wrigley-Lou ore deposits, hosted in Middle Devonian carbonates and shales, are structurally controlled and lie in close proximity to the Camsell Fault, which is basement controlled.

Fluid inclusion studies of sphalerite and fluorite reveal that the fluids are 16 to 26 equivalent weight percent NaCl, homogenize in the range of 80 to 156°C, and have a density of 0.95 to 1.05 g/cc. The characteristics revealed by the two-phase inclusions provide parallels to those of North American Mississippi Valley type deposits.

Sulphur isotope analyses yield  $\delta^{34}\text{S}$  values averaging +10.3% for pyrite, +7.5% for sphalerite, +3.8% for galena, and -15.7% for sedimentary pyrite. The sulphur is in isotopic disequilibrium, thereby implying bacteriogenic reduction of sea water sulphate. The probable source of the sulphide is the latest Emsian-earliest Eifelian Bear Rock Formation and it is very likely the sulphur source is independent of the metal source. From sphalerite-galena sulphur isotope pairs the mean temperature of sulphide precipitation is 176°C.

Lead isotope analyses of galena-lead indicate that the lead is anomalous, comparable to Illinois-Kentucky district and some Appalachian Valley lead. The lead-model age (time  $t_2$ ) is  $58 \pm 142$  m.y. or late Cretaceous to early Tertiary in age. The time  $t_1$  is  $2,213 \pm 260$  m.y., an age which relates with Kenoran and/or Hudsonian orogenic event(s) of the Slave Province. This model age indicates that the probable source of the lead was from the Precambrian basement, and the Kenoran and/or Hudsonian event(s) released the metals. The pyrite anomalous lead line intersects the growth curve at  $674 \pm 198$  m.y. which implies that the

Middle Devonian argillaceous sediments were derived from the Bear Province to the north, and had been shed by the rising Minto and Coppermine Arch in Paleozoic time.

Sulphur and lead isotope determinations from the Polaris and Truro deposits of Little Cornwallis and Truro Islands, Arctic Archipelago, reveal a comparable source of sulphur and metals to that of the northern Camsell Range deposits. The sulphur isotope analyses give sphalerite  $\delta^{34}\text{S}$  values which average +7.8%, galena  $\delta^{34}\text{S}$  values which average +4.0% and one pyrite  $\delta^{34}\text{S}$  value which is +8.9%. The sulphur is in isotopic disequilibrium and likely was derived from the Baumann Fiord and/or Bay Fiord evaporites through bacterial reduction. The temperatures from sphalerite-galena sulphur isotope pairs is in the range of 143° to 170°C.

The lead isotope analyses lie close to the growth curve indicating an approximate model age of 525 m.y. This age relates to the age of metamorphic rocks of northern Ellesmere Island, and suggest a period of metamorphism in Cambrian or Hadrynian time. The time relationship indicates that the source of metals was likely Precambrian rock; however, a deep-seated source cannot be disregarded.

The fluid inclusion studies along with the sulphur and lead isotope studies indicate that the Wrigley-Lou and Polaris-Truro deposits have many similarities.

### ACKNOWLEDGEMENTS

This study was completed under the supervision of Dr. R.E. Folinsbee for whose assistance, guidance and encouragement I am most grateful. Dr. R.D. Morton provided expertise and invaluable suggestions in the areas of fluid inclusion and sulphur isotope studies and Dr. C.R. Stelck offered many helpful suggestions as well as critical commentary. Dr. G.L. Cumming and Dr. J. Gray of the Department of Physics permitted the writer to use the mass spectrometer facilities and provided both assistance and constructive criticism in the field of isotope study.

Dragan Krstic of the Physics Department generously provided expertise and assistance in operating the solid source mass spectrometer as well as critical commentary in interpreting the lead isotope data. Say-Lee Kuo provided suggestions, ideas and direction in the analytical phases of the research, which I greatly appreciate. Steve Burnie provided helpful advice during the sulphur isotope phase of the experimental work.

Cominco Ltd. provided employment in the principal study area and permitted free access to the records and drill cores of the Wrigley-Lou properties. The Polaris-Truro samples were freely given to Dr. R.E. Folinsbee by Cominco Ltd. Special thanks go to R.G. McEachern, Dr. Hugh Morris, W.T. Irving, D. Heddle and J. Ryznar of Cominco Ltd. for their interest, generosity and support.

The writer is indebted to Mrs. L. Hauer and Ms. Val Stephansson for their assistance in drafting, editing and typing.

# TABLE OF CONTENTS

	PAGE
ABSTRACT . . . . .	iv
ACKNOWLEDGEMENTS . . . . .	v
CHAPTER	
I.    INTRODUCTION . . . . .	1
A.    HISTORY OF THE WRIGLEY-LOU PROPERTIES . . . . .	2
B.    LOCATION AND ACCESS . . . . .	2
C.    HISTORY, LOCATION AND ACCESS OF THE POLARIS- TRURO PROPERTIES . . . . .	3
D.    PURPOSE AND SCOPE OF THE STUDY . . . . .	5
E.    METHOD OF STUDY . . . . .	6
F.    METHOD OF DRAWING CROSS-SECTIONS . . . . .	8
II.   GENERAL GEOLOGY . . . . .	9
A.    REGIONAL STRUCTURE . . . . .	9
B.    CONSIDERATION OF BASEMENT FAULTING . . . . .	13
C.    SURFICIAL GEOLOGY . . . . .	18
D.    GENERAL STRATIGRAPHY . . . . .	19
E.    STRATIGRAPHY . . . . .	24
1. Delorme Formation . . . . .	25
2. Arnica Formation . . . . .	25
3. Manetoe Formation . . . . .	26
4. Landry Formation . . . . .	27
5. Headless Formation . . . . .	28
6. Nahanni Formation . . . . .	29
7. Hare Indian and Fort Simpson Formations . . . . .	31
III.  ORE AND GANGUE MINERALS AND THEIR CONTROL . . . . .	33
A.    PRIMARY ORE MINERALS AND ASSOCIATED TRACE ELEMENTS . . . . .	33

# TABLE OF CONTENTS (cont'd)

CHAPTER	PAGE
1. Galena, Sphalerite . . . . .	34
2. Pyrite . . . . .	38
B. OXIDIZED ZONE . . . . .	38
C. GANGUE MINERALS . . . . .	39
1. Dolomite . . . . .	40
2. Spar Calcite . . . . .	40
3. Silica . . . . .	41
4. Sedimentary Pyrite . . . . .	42
5. Bitumen . . . . .	42
6. Fluorite . . . . .	43
D. CONTROLS TO MINERALIZATION . . . . .	43
IV. FLUID INCLUSION STUDIES . . . . .	48
A. PREVIOUS FLUID INCLUSION STUDIES . . . . .	48
B. MATERIAL STUDIED . . . . .	49
C. ORE FLUID SALINITIES FROM FREEZING TEMPERATURES . . . . .	52
D. ORE FLUID TEMPERATURES FROM HOMOGENIZATION TEMPERATURES . . . . .	56
E. POSSIBLE ORIGIN OF THE WRIGLEY DEPOSIT, REVEALED THROUGH FLUID INCLUSION STUDIES . . .	59
F. CONCLUSIONS . . . . .	63
V. SULPHUR ISOTOPE STUDIES . . . . .	64
A. SAMPLES USED IN THE STUDY AND RESULTS . . . .	66
B. SOURCE OF SULPHUR (THEORY) . . . . .	67
C. CONSIDERATION OF THE WRIGLEY SULPHIDE SULPHUR AND THE DEVONIAN SEA WATER SULPHATE . . . . .	71
D. TO TEST THE VALIDITY OF $\Delta\delta^{34}\text{S}$ . . . . .	74

# TABLE OF CONTENTS. (cont'd)

CHAPTER	PAGE
E. CONSIDERATION OF THE CONTROL OF THE CHEMISTRY OF THE ORE SOLUTION(S) . . . . .	75
F. CONCLUSION . . . . .	80
G. SULPHUR GEOTHERMOMETRY . . . . .	81
VI. LEAD ISOTOPE STUDIES . . . . .	82
A. THEORY OF LEAD DATING . . . . .	82
B. AGE OF THE EARTH . . . . .	86
C. CONSIDERATION OF THEORETICAL MODELS . . . . .	87
D. CONSIDERATION OF 'NEW GROWTH CURVES' . . . . .	94
E. ANOMALOUS LEADS . . . . .	95
F. RESULTS AND DISCUSSION . . . . .	98
1. Possible Source of Lead . . . . .	101
2. Age of Source Rocks . . . . .	103
3. Age of Sulphide Mineralization . . . . .	104
4. Consideration of the Lead Isotopes of Sedimentary Pyrite . . . . .	105
G. CONCLUSION . . . . .	107
VII. SUMMARY - WRIGLEY-LOU LEAD-ZINC MINERALIZATION . . . . .	108
VIII. SULPHUR AND LEAD ISOTOPES FROM LITTLE CORNWALLIS ISLAND, ARCTIC ARCHIPELAGO . . . . .	111
A. GENERAL GEOLOGY . . . . .	113
B. MINERALIZATION . . . . .	117
C. SULPHUR ISOTOPES . . . . .	120
D. SULPHUR GEOTHERMOMETRY . . . . .	124
E. LEAD ISOTOPES . . . . .	124
F. MODEL FOR MINERAL EMPLACEMENT . . . . .	133

# TABLE OF CONTENTS (cont'd)

CHAPTER	PAGE
IX. CONCLUSIONS . . . . .	135
***	
MICROPHOTOGRAPHIC PLATES . . . . .	137
REFERENCES . . . . .	141
APPENDIX I. SAMPLE DESCRIPTION . . . . .	155
APPENDIX II. SULPHUR ISOTOPE . . . . .	158
Sulphur Isotope Sample Preparation . . . . .	158
Preparation of Sulphur Dioxide for Mass Spectrometer . . . . .	159
Mass Spectrometer . . . . .	159
APPENDIX III. LEAD ISOTOPE . . . . .	162
Lead Isotope Preparation . . . . .	162
Chemical Methods . . . . .	162
Mass Spectrometer . . . . .	165
Error Consideration and Data Standardization . . . . .	166
Broken Hill Standard Ratios . . . . .	169

# LIST OF FIGURES

FIGURE		PAGE
1.	Index map	4
1A.	Wrigley property map	in pocket
2.	Elliptical pattern of en échelon folding in Mackenzie Plain, western district of Mackenzie	16
3.	Interpreted environment of deposition of Landry, Headless and Nahanni Formations in relation to the energy regime of an epeiric sea	20
4.	North Camsell Range, cross-section	in pocket
5.	Zonation of Devonian in Mackenzie Mountains, Camsell Range and Norman Wells area	21
5A.	Schematic cross-section, southern Mackenzie Mountains to Tathlina High, showing formational names	22
6.	Wrigley cross-section A-A'	in pocket
7.	Paragenesis: Wrigley and Lou properties	36
8.	D.D.H.B.-73-2: 'Zebra Zinc' fault	45
9.	Generalized diagrammatic interpretation of faulting in crystalline basement in foreland corner north of Norman Wells, N.W.T.	47
10.	H <sub>2</sub> O-NaCl phase diagram	53
11.	Freezing temperature °C and equivalent weight percent NaCl of the Wrigley deposit sphalerite, fluorite and calcite fluid inclusions	54
12.	Homogenization temperature °C of the Wrigley deposit sphalerite and fluorite fluid inclusions	54
13.	Histogram of the freezing temperatures of the Wrigley deposit sphalerite and fluorite fluid inclusions	57
14.	Histogram of the homogenization temperatures of the Wrigley deposit sphalerite and fluorite fluid inclusions	57
15.	The density of sodium chloride solutions for concentrations up to 3 molar and temperatures up to 350°C	62



# LIST OF FIGURES (cont'd)

FIGURE		PAGE
16.	Pressure corrections for homogenization temperatures: a - for 15% solution; b - for 20% solution; c - for 25% solution; d - for 30% solution of NaCl	62
17.	The sulphur isotope age curve of Holser and Kaplan (1966)	69
18.	Histogram of the sphalerite-galena $\delta^{34}\text{S}$ values, Wrigley property	73
19.	Variation of $\delta^{34}\text{S}$ of sulphate (ion or mineral), $\text{H}_2\text{S}$ , and sulphide minerals with variation in $\text{H}_2\text{S}/\text{SO}_4^{2-}$ of the hydrothermal solution at $T = 175^\circ\text{C}$ , $\delta^{34}\text{S}_{\text{SS}} = 20\%$ .	77
20.	Comparison of the positions of $\delta^{34}\text{S}$ contours with the stability fields of Fe-S-O minerals, calcite and graphite. $T = 150^\circ\text{C}$ and $I = 1.0$	79
21.	$^{207}\text{Pb}/^{204}\text{Pb}$ vs $^{206}\text{Pb}/^{204}\text{Pb}$ ratio plot of galena-lead and pyrite-lead isotope data of Wrigley-Lou properties	100
22.	Lead-zinc occurrences of the Canadian Arctic	112
23.	Table showing formations north of Cape Airy-Snowblind Bay line of facies change	116
24.	Paragenesis: Polaris and Truro deposits, N.W.T.	119
25.	$^{207}\text{Pb}/^{204}\text{Pb}$ vs $^{206}\text{Pb}/^{204}\text{Pb}$ ratio plot of the lead isotope data of the Polaris-Truro deposits, Canadian Arctic	127
26.	$^{207}\text{Pb}/^{204}\text{Pb}$ vs $^{206}\text{Pb}/^{204}\text{Pb}$ ratio plot of the lead isotope data of Pine Point, N.W.T.	128
27.	Range of uranium derived lead isotope compositions observed for the Polaris-Truro, Wrigley-Lou, Pine Point, Red Sea, and other Mississippi Valley type deposits	130
28.	Method of analysis of standard ratio values	167
29.	Measured correction factors, plotted ratio distribution against mass unit	171
30.	Standard Broken Hill measured values plotted relative to $^{204}\text{Pb}$ and fractionation error lines, and the true Broken Hill ratio values (Cooper <i>et al.</i> , 1969)	172

# LIST OF TABLES

TABLE		PAGE
1.	Fluid inclusion freezing and homogenization temperatures	51
2.	$\delta^{34}\text{S}$ per mil values in the Wrigley deposit	68
3.	Lead isotope symbols and constants	85
4.	Wrigley-Lou galena-lead and pyrite-lead isotopic data	99
5.	Summary of the geology of lead-zinc occurrence of the central Canadian Arctic Islands	114
6.	Unconformities affecting the Cornwallis belt	115
7.	Polaris-Truro sulphur data	121
8.	Polaris-Truro lead isotope data	125
9.	Broken Hill lead isotope data	170

## Chapter I

### INTRODUCTION

Carbonate hosted lead-zinc deposits in northern Canada are significant, although there are few large tonnage deposits. The Pine Point deposit had held the foremost position with respect to size until the Cominco-Bankeno discovery of the stratabound lead-zinc district on Little Cornwallis Island. In contrast, the relatively small, structurally controlled Wrigley-Lou mineral deposits of the northern Camell Range are typical of most of the base metal deposits of the Northwest Territories.

This thesis considers fluid inclusion and lead-sulphur isotope experimental results of the Wrigley-Lou and Polaris-Truro deposits in the context of structure and stratigraphy. The principal goal was to ascertain: (1) the sulphur and lead source rocks; (2) the types of brines which transported the sulphur and base metals; (3) the probable controls to fluid movement; (4) the temperature of ore deposition; and (5) the model ages of the respective leads. From these data, comparative knowledge of the two mineral districts may be attained, which, taken in a larger context, allows for comparison with other Mississippi Valley type deposits of North America. In the practical field of ore exploration, it is hoped that the information assembled will provide a guide to future exploration.

Primary consideration is directed at the geology and ore-genesis of the Wrigley-Lou properties, and secondarily to the Polaris-Truro deposits. The writer has had greater access and extensive sample suites from the Wrigley-Lou property showings. The provided Polaris-Truro sample suite was not extensive and therefore, did not merit indepth consideration.

### A. HISTORY OF THE WRIGLEY-LOU PROPERTIES

Cominco Ltd. began field work in the Wrigley area in March, 1971. Initial work was carried out on the 'Berg' Group, optioned by the Company in 1970. Impetus for further work arose from detailed study of oil wells drilled in the general area. The presence of galena-sphalerite mineralization in Middle Devonian carbonates indicated that the stratigraphy merited further examination. Subsequent field work revealed in situ Pb/Zn mineralization on the north end of 'Mount Barrett' and the 'Fry' Group of 37 claims was staked in September, 1971. Cominco Ltd. then acquired a three-year prospecting Permit No. 273, from Ottawa, in April, 1972. The area of the Permit was 169,990 acres (271.5 square miles) exclusive of the 38 'Berg' claims, which were subsequently dropped, and the 37 Cominco-owned 'Fry' claims. The Permit expired March 31, 1975 and Cominco Ltd. staked 448 claims (36.16 square miles) to maintain control.

The Lou property of 20 claims (1.62 square miles) is located approximately 14 miles south of the southern boundary of the Wrigley property, and just north of the Root River, within the Camsell Range. Originally staked in 1972, field work commenced in August, 1973. Examination centered on mapping, geochemistry and general prospecting.

The Lou property is located within one of the Union Oil permit areas. Giant Yellowknife also holds permits in the area. At the time of writing, (1976), large portions of these permits have been dropped.

### B. LOCATION AND ACCESS

The area of detailed consideration, the Wrigley Claim Group, is composed of two claim units: the Wrigley property and the Lou property.

The geographical center of these claim units are:

Wrigley property - Longitude 63°08'N; Latitude 123°37'W

Lou property - Longitude 62°53'N; Latitude 123°47'W

The general area of the Camsell Range, herein considered, is bounded by the Wrigley River to the north, the Root River to the south, the Mackenzie River to the east, and the Mackenzie Plain to the west. The entire area so enclosed includes crown land and land staked by Cominco Ltd. Fig. 1 indicates the respective property locations within this regional setting.

The only settlement in the area is the town of Wrigley, situated on the east bank of the Mackenzie River. The community centers around an airport operated by the Department of Transport. This community is 114 miles northwest of Fort Simpson, which is the main supply center for the surrounding area. Air service is the principal means of travel to and from Wrigley; however, during the winter it is serviced by a winter road from Fort Simpson, and during the summer by the government barging system (NTCL) on the Mackenzie River. An all-weather highway is being constructed from Fort Simpson to Wrigley and beyond, which, when completed, will reduce operating costs for companies in this area.

#### C. HISTORY, LOCATION AND ACCESS OF THE POLARIS-TRURO PROPERTIES

The Polaris-Truro lead-zinc deposits of the Little Cornwallis and Truro Islands are located near the geographic center of the Canadian Arctic Archipelago. The lead-zinc discoveries are jointly owned by Cominco Ltd. and Bankeno Mines Ltd. They were first drilled in 1971. Subsequent exploration located additional mineral occurrences (Fig. 22).

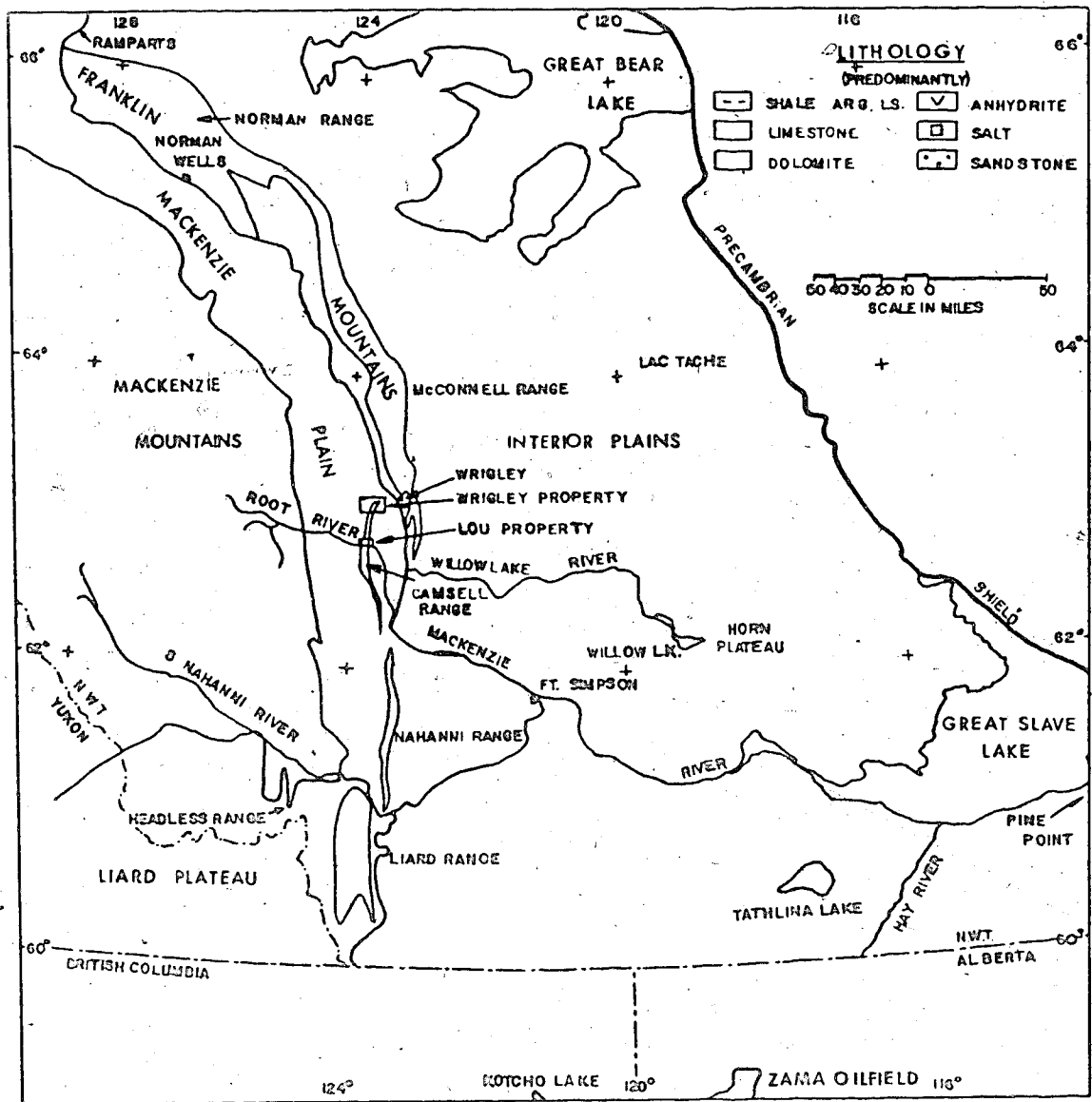


Fig. 1. Index map.

The Polaris deposit is the largest, proven to 20 million tons of 20% lead-zinc combined. The mineral discoveries are under the control of Arvik Mines Ltd.

Resolute, situated near Resolute Bay on the south-central coast of Cornwallis Island, is the principal settlement. Resolute is serviced by an airport operated by the Department of Transport, and is accessible by ship for part of the summer and fall. This center is the principal base of activity for governmental agencies and is the supply center for commercial companies operating in the Canadian Arctic Islands north of Perry Channel and just south of the channel (Thorsteinsson and Kerr, 1967).

#### D. PURPOSE AND SCOPE OF THE STUDY

(1) To consider briefly the structure and stratigraphy of the northern Camshell Range.

(2) To consider the petrology of the ore and host rock of the Wrigley and Lou properties in order to determine the paragenetic sequence of sulphide and gangue minerals.

(3) To consider the sulphur isotopes to ascertain the probable origin of the sulphur, and the temperature of sulphide formation.

(4) To consider fluid inclusions to indicate the probable type of mineralizing fluids and to corroborate the temperature of mineralization.

(5) To consider lead isotopes to ascertain the approximate source and age of mineralization.

(6) To consider the Polaris-Truro deposits in terms of the structure, stratigraphy, paragenesis, and sulphur and lead isotopes to

ascertain the probable origin of the sulphur and metals, the model age of the lead and a possible model for mineral emplacement.

(7) To consider the two mineral districts in a comparative sense.

The structure of the Wrigley-Lou properties is considered in the regional context. Definitions of the lithologies and of the stratigraphic units are primarily based on the work carried out by the writer in the summer of 1974, while employed by Cominco Ltd. The lists of identified fossils for the Headless and Nahanni Formations are from the Cominco properties and are not as extensive as those listed by H. Gabrielse, S.L. Blusson and J.A. Roddick (1967).

In the isotope and fluid inclusion studies, attention is focussed upon the Nahanni Formation as it is the most prominent formation with regard to mineralization. This focus, however, is not intended to negate the presence of mineralization in the other Devonian formations -- namely, the Hare Indian Shale, Headless Shale, Landry-Manetoe and Arnica.

#### E. METHOD OF STUDY

The Wrigley property and the Lou property are located about 14 miles apart, in the northern Camsell Range. The Mackenzie Plain, which essentially surrounds the Camsell Range, is muskeg-covered and outcrop is minimal. The range rises above the plain, and varies in elevation from less than 500 feet along the Mackenzie River to 2,750 feet on 'Mount Grotch'. The heavy forest growth and mantling glacial debris, which masks the plain, extends up the westward-dipping slope of the range and good outcrop is restricted to the eastern cliff scarp above the Camsell Fault. Information as to the geology was derived from surface mapping and examination of drill cores.



Diamond drilling has been carried out only on the Wrigley property. A total of 39 exploration holes were drilled in the summers of 1973 and 1974. The writer examined many of the cores in 1974 and mapped both the Lou and Wrigley properties. Measured sections on the Lou property allowed for the comparison of stratigraphic thicknesses between the two properties.

The locations of the diamond drill holes have in general been numbered according to the property line grid coordinates and this numbering system will be retained in the present study. Map Fig. 1-A (in pocket) provides the locations of the diamond drill holes used in this study and the location of cross-section A-A' (Fig. 6).

Thin sections and polished sections were prepared for examination from selected intervals of the core of the Wrigley property, while the veins on the Lou property were sampled to provide a surface cross-sectional picture. Unfortunately, these surface samples were weathered. A representative selection of diamond drill core and of surface samples was cut and stained using the Friedman (1959) method to test for iron-free calcite, iron-rich calcite, iron-poor dolomite and ankerite.

Ten pairs of 'co-existing' sphalerite-galena samples were prepared and run for sulphur isotopes. The samples are from diamond drill core and are representative of the Wrigley property.

Field inclusion sections were prepared from samples of good sphalerite and fluorite crystal development. Wherever possible, the sphalerite samples for these sections were taken from the same location as that for sulphur isotopic determination. This was done to provide valid comparisons for the temperature determinations arrived at using these two analytical methods.

Twenty galena and pyrite samples were isotopically examined for lead. Thirteen of the galena samples are from diamond drill cores and give a vertical and horizontal indication of isotopic change. Three surface samples are included. The four pyrite samples represent diagenetic sedimentary pyrite.

The Polaris-Truro deposits were considered in a similar fashion. Only a few samples of these galena-sphalerite ore bodies were available, with no specific map locations. Considerable dependence has been placed upon the literature since the writer did not visit or work on these properties.

#### F. METHOD OF DRAWING CROSS-SECTIONS

Tectonism associated with the Laramide orogeny (late Upper Cretaceous-early Oligocene) has resulted in broad folds, basement block faults and thrust faults in the general area of this study. In the stratigraphic section A-A' (Fig. 6) the tectonic deformation is removed and the top of the Headless Shale Formation is the datum. The north Camsell Range cross-section (Fig. 4) is more extensive and the datum is the top of the Nahanni Formation. The sections are drawn from field data, diamond drill logs and oil well logs.

## Chapter II

### GENERAL GEOLOGY

#### A. REGIONAL STRUCTURE

The general area may be divided into two tectonic provinces. East of the Mackenzie River the structure is not complex, while west of the river en échelon folding and faulting is prevalent. This latter area is characterized by mountain ranges and plateaus which are separated by flat intermontane valleys. The visible tectonic deformation is a result of the Laramide orogeny, and faulting has exposed the formations. Some of the areally exposed formations are traceable into the plains east of the Mackenzie River.

Bostock (1958) and Law (1971) have defined the main structural elements of the general area:

- (1) The Interior Plains, known in this area as the Great Slave Plain, and,
- (2) The Disturbed Belt
  - a) A narrow zone east of the Franklin Mountains,
  - b) The Franklin Mountains, the four ranges of which are, from north to south, the Norman, McConnell, Camsell and Nahanni Ranges,
  - c) The Mackenzie Plain, between the Franklin and Mackenzie Mountains,
  - d) The Mackenzie Mountains,
  - e) The Liard Range, south of the Mackenzie Mountains,
  - f) The Liard Plateau, south of the Mackenzie Mountains and west of the Liard Range (Law, 1971).

The northern structural area was considered by Hume and Link (1945), Hume (1954); the southern portion by Douglas and Norris (1959, 1960, 1961, 1963). The following is the précis presented by Law (1971) relative to the two areas.

"The anticlines are broad, sinuous, up to 100 miles long and commonly arranged en échelon. Dips vary from gentle to steep but are usually in the range  $10^{\circ}$  to  $50^{\circ}$ , being relatively gentle in the north half of the area and steeper in the south. The synclines are broad and flat with dips in the order of  $10^{\circ}$  to  $20^{\circ}$ .

The anticlines may be symmetrical or asymmetrical either to the east or to the west. They are frequently cut by high angle thrust faults near their crests. The thrusts may dip either to the east or to the west, depending usually on the asymmetry of the fold. The folds are crossed by high angle reverse and thrust faults of small displacement.

In contrast to the southern Rocky Mountain foothills, with their low angle thrust faults, the faults of the Mackenzie Plain and related areas dip at fairly steep angles. Movement in this area has been vertical rather than horizontal. The anticlines are usually parallel folds with rounded flanks."

The Camsell Range, within the Mackenzie Plain, appears to fit within this description, illustrating the en échelon folding, high angle thrust and block faulting. The tectonic controls responsible for these Laramide structures have been considered by many workers; among these are Goodman (1951), Gabrielse (1967), Molchanova (1968), Norris (1972) and de Wit et al. (1973).

A brief summary of the tectonic evolution of the northern Canadian Cordillera, based upon the work of Gabrielse (1967), will indicate the structure that has been over printed by the Laramide orogeny.

Tectonism in the northern Cordillera area commenced in the late Proterozoic and persisted through Devonian time. The latest orogenic event (Laramide) took place from Cretaceous to Oligocene time. Much of the tectonic activity is recorded as structural deformation and/or clastic sedimentation.

The oldest rocks recognized in the northern Cordillera are Proterozoic (Purcell) which outcrop in the Mackenzie, Wernecke and Ogilvie Mountains. Deformation of the rocks is caused by uplift, folding and block faulting of the Racklan orogeny. Unconformably overlying the 'Purcell-like' deformed rocks, is the Rapitan Formation. The lower unit of this formation is composed of bedded chert, conglomerate, and conglomeratic mudstone. Iron formation occurs in the thick 'tilloid' conglomerate in the north flank of the Mackenzie Mountains (Dahlstrom, 1976). The lower unit is overlain, locally unconformably, by dominantly fine-grained clastic and volcanoclastic rocks. The lower Rapitan Formation is very similar to the Upper Purcell Series of southeast British Columbia, while the 'Grit' unit of the Selwyn Basin has correlative similarities to the Windermere and Miette rocks of the southern Canadian Rocky Mountains. Likely the late Proterozoic 'Grit' unit was deposited following tectonism of the Racklan orogeny.

Subsequent sedimentation developed within connected and unconnected basins (Handfield, 1965) of the Franklin Mountains and Redstone Arch areas through the duration of the Cambrian, the process being broken by uplift and erosion. Late Cambrian (pre-Franconian) uplift is evident in the eastern Selwyn Basin, and represents the last event of the period.

Early and Middle Ordovician shales, cherts and siltstones were deposited in the west, while thick carbonates accumulated on the flanks of the Ogilvie and Redstone arches and in the Root Basin (Gabrielse, 1967). In the westernmost part of the northern Canadian Cordillera a widespread unconformity separates Late Ordovician and Silurian rocks from the older strata. In the Franklin Mountains the comparative unconformity truncates the Franklin Mountain Formation.

Not until the Middle Devonian are any of these unconformities regional in extent. Douglas and Norris (1963) record a regional Middle Devonian unconformity on the Franklin Mountain Platform, and Gabrielse (1967) notes that no significant angular relationships have been recorded. The early-Middle Devonian lithologies are characterized by dolomite, limestone, shales and evaporites, while the late-Middle Devonian consists primarily of carbonates and shales. Although tectonic differentiation is lacking during the Middle Devonian (Martin, 1959), the Late Devonian and Mississippian tectonic activity was widespread in the west (Selwyn Basin and Pelly-Cassiar Platform) and in north-central and central British Columbia. This period of deformation was followed by the Late Pennsylvanian and Early Permian (Melvillian) orogeny (?), indicated by K-Ar dates of 225 and 265 m.y. (Douglas *et al.*, 1970), which affected the northern Yukon Territory and continued as far south as the Liard Basin (Harker, 1963). Permian sequences unconformably overlie the older strata.

Gabrielse and Reesor (1964) considered K-Ar dates of plutonic rocks in the southern Yukon and concluded they do not indicate that tectonic and plutonic evolution occurred in a single Mesozoic cycle. They consider an evolutionary structural development took place in which structural reworking of older plutons by successively younger tectonic events resulted. The events do not accommodate a specific orogeny, such as Laramide orogeny of White (1959). They obtained a large number of dates in the range of 100 m.y. to 60 m.y. (Cretaceous) which may reflect an increase in plutonism during the progressive development of the tectonic cycle. This mid- and Upper Cretaceous plutonic and associated tectonic evolution, which resulted in the Canadian Rocky Mountain development,

has been corroborated by the eastern Yukon 1851 batholith dates of about 95 m.y. (Baadsgaard et al., 1961a). These latter dates tend to indicate that the principal tectonic and plutonic activity occurred during the mid-Cretaceous. Baadsgaard et al. (1961a) consider this mid-Cretaceous orogeny "continued on into Late Cretaceous times with the emplacement of small plutons such as Bayonne (British Columbia), Boulder (Montana), and Marysville (Montana, ..., believed to be Late Cretaceous and assignable to the Laramide orogeny." (Baadsgaard et al., 1961a). Within the generalities of the preceding, this Cretaceous period of deformation may be referred to as the Laramide orogeny, as applicable to the tectonic evolution of the northern Canadian Cordillera.

The various tectonic events of the northern Cordillera have resulted in a cumulative structural overprint. The Laramide structures are the most recent and therefore are dominant. The structural style of the southern Canadian Rockies changes in the vicinity of the Liard River from low angle thrust faults in the south to basement controlled faulting in the north, the latter displaying more structural symmetry. Gabrielse (1967) summarizes the northern Cordillera regional development in the following manner: "... regional compression combined with dominantly vertical, or in places, transcurrent movements of basement blocks could have produced the characteristic structural style of the Mackenzie Mountains."

#### B. CONSIDERATION OF BASEMENT FAULTING

The Precambrian basement fault control of the foreland ranges of the northern Canadian Cordillera was initially suggested by M.Y. Williams in 1927 (Goodman, 1951). He envisaged up-thrust edges of basement fault

blocks. Goodman (1951) similarly considered block faulting of the basement to have produced 'most of the mountain-building stresses' in the Mackenzie Mountain forelands. The compressive stresses operative during the Laramide orogeny affected the basement along existing lines of weakness, and never reached the over-thrusting stage. Thus, comparatively gentle structures developed.

Molchanova (1968), in considering zones of resonance-tectonic block structure along the periphery of the circum-Pacific Belt, believes that the tectonic movements of the northern Canadian Rockies were less intense than those operative in the American Rockies. She implies, by comparison with the American Rockies, that vertical displacements "led to the formation of block and arched uplifts ...".

Eardley (1954) and King (1961), in studies of the American Rockies, have considered the ~~crystalline~~ basement movement to be significant in the mountain building. The decreased degree of vertical movement in the northern Canadian Rockies prevents accurate visual proof of the basement involvement. Lowell (1974) considered Laramide foreland basement deformation in the area of Wyoming-Idaho thrust-fold belt, where horizontal compression, vertical movement, and strike-slip movement within the basement has transpired. He proposes "in addition to tangential compression and strike-slip, a lithostatic slab subducted well beneath the foreland...", thereby accounting for the uplift of the basement.

From the above studies it is apparent that the Precambrian basement was not passive during the Laramide orogeny. The actual cause of movement is not known. As an illustration of this basement movement, the Helvillian orogeny (?) (225-265 m.y., Baadsgaard et al., 1961b; Wanless, 1964) caused displacement on the southwest extension of the MacDonald fault system, and the movement is expressed in the Paleozoic structure.



The structure of the Interior Plains in large part has been determined by the underlying Precambrian basement. de Wit et al. (1973) believe the erosion of the Precambrian and subsequent block faulting have been instrumental in the development of the basement topography, and thereby controlled the overlying, generally southwest-dipping Paleozoic stratigraphy. Examples of the basement control are found in the area of the Celebeta High and within a triangular area between the Nahanni Range and the Liard and Mackenzie River. However, de Wit et al. (1973) do not assign significance to vertical basement displacement in the mountain belt. They envisage truncation of the dominant Precambrian basement control to lie at the eastern extremity of the foreland or disturbed belt. Goodman (1951) does not consider a clearly defined demarcation line to exist. The basement control may be the explanation for the sinuous Nahanni-Camsell Ranges of some 160 miles in length, which display minor offsets, block rotations and reverse faulting.

D.K. Norris (1972), in the light of an examination of the fold patterns of the northern Cordillera, considered the kinematics and dynamics of the Laramide orogeny. The Mackenzie Plain west of the Wrigley property (Fig. 2) illustrates right-hand en échelon anticlines and synclines and Norris considers the folding to be the result of slippage of the sedimentary strata over detachment surfaces at the top of the passive basement. The folding was likely the precursor to the mountain building.\* In this way the cross-cutting structural relationship of

---

\*Douglas et al. (1970) consider the folding of the Mackenzie Plain may have been of the early phase of the Laramide orogeny or earlier, and a décollement zone at the level of the Cambrian salt and anhydrite may be significant.

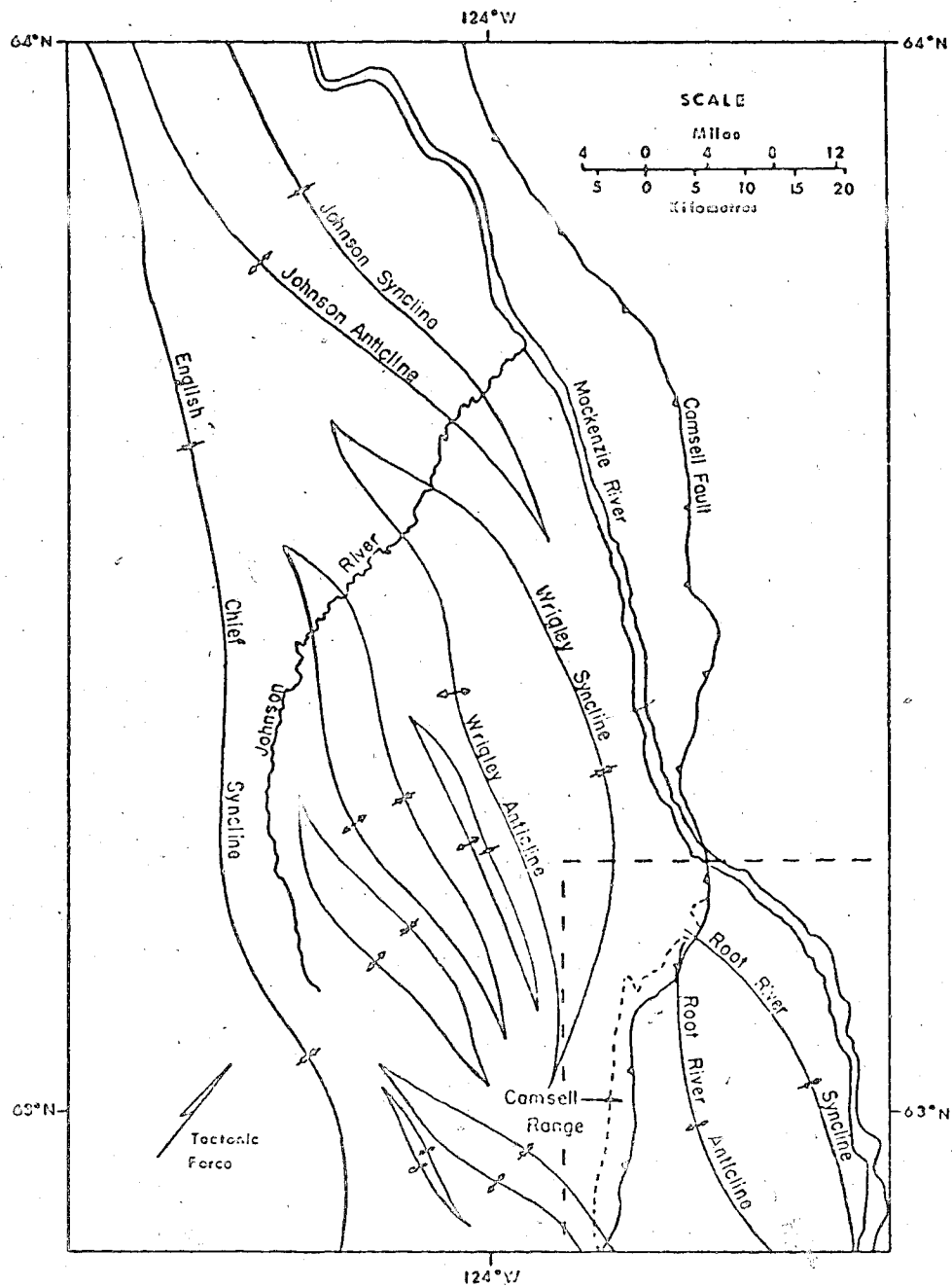


Fig. 2. Elliptical pattern of en échelon folding in Mackenzie Plain, western district of Mackenzie (after Douglas and Norris, 1961, 1963; Norris, 1972).

the broad Root River anticline and syncline of the Mackenzie Plain (see Fig. 2) to the Camsell Fault may be explained. The en échelon folding preceded the basement controlled faulting, and the latter controlled the mountain building development. This sequence of events did not result in the folds being faulted along the flanks of the folds; instead, the large Camsell Fault cross-cuts the fold patterns. Evidence of thrusting and horizontal shortening is not evident. The Root River anticline, as traced in the Mackenzie Plain, and the northern extension of the anticline in the hanging wall of the Camsell Fault in the Wrigley property area (see dotted enclosure - Fig. 2) reveal essentially no horizontal displacement. This indicates that the displacement along the Camsell Fault is vertical, or near to vertical, with a degree of strike-slip movement.

The effect of the above mentioned basement faulting in controlling the structural development of the northern Cordillera foreland ranges extends into the realm of base metal mineralization. Neil Campbell (1950) and Cumming and Robertson (1969) consider a possible relationship to exist between the MacDonald Fault and the Pine Point deposit. A.V. Heyl (1972) assigns significance to the 38th parallel basement wrench fault zone, which extends from northeastern Virginia to south-central Missouri, because of the intimately associated Pb/Zn/Ba/F mining districts. Kanasewich (1968b), in the study of a Precambrian rift valley in southern Alberta, found that the rift may be traced into southeastern British Columbia where it passes through the Kimberley ore field. He considers the stratiform lead-zinc deposits at Kimberley formed within the bounds of the rift "under conditions similar to those prevailing in the hot-brine areas of the modern Red Sea".

In this regard, faulting of the basement permits brine circulation (White, 1968) and/or release of interstitial fluids and provides a heat source for those fluids by way of increase in the geothermal gradient. The significance of these fluids with respect to mineralization will be considered in Chapter IV.

### C. SURFICIAL GEOLOGY

Craig (1965), as a result of his studies of the areas covered by the Slave River - Redstone River map sheets, found evidence for at least two glaciations. The evidence rests on the presence of glacial striae, drumloid features, and glacial erratics, including volcanic and metamorphic shield derived boulders which may be found at elevations in excess of 5,000 feet. Similar glacial features and erratics are found within the study area and are considered to be the result of Laurentide ice-sheet transport. The direction of ice movement is variable in the vicinity of the examined properties but drumlins and ground moraine substantiate a northwest direction of ice movement. Near the headwaters of the Wrigley River the ice movement is considered to be almost due north, following the Wrigley River valley. Precise measurement of glacial striae in the Hay River area to the south indicate approximate directions of S50°W and N50°W (Craig, 1965).

The Wrigley and Lou properties possess a veneer of glacial till at lower elevations on which a growth of vegetation occurs. This growth is composed of an assortment of low bushes and of miniature coniferous and deciduous trees. Within the Plains area the land is poorly drained and additional water is added from springs (hot and cold) which issue from the Camsell Fault zone.

#### D. GENERAL STRATIGRAPHY

The Devonian stratigraphy of the Camsell Range rests upon the shelf-edge of a Paleozoic sedimentary basin which extends west from the Precambrian Shield. Bostock (1948) considers the orientation of the shelf-edge to be north-south through the Wrigley area, thereby approximately parallel to the Mackenzie River valley.

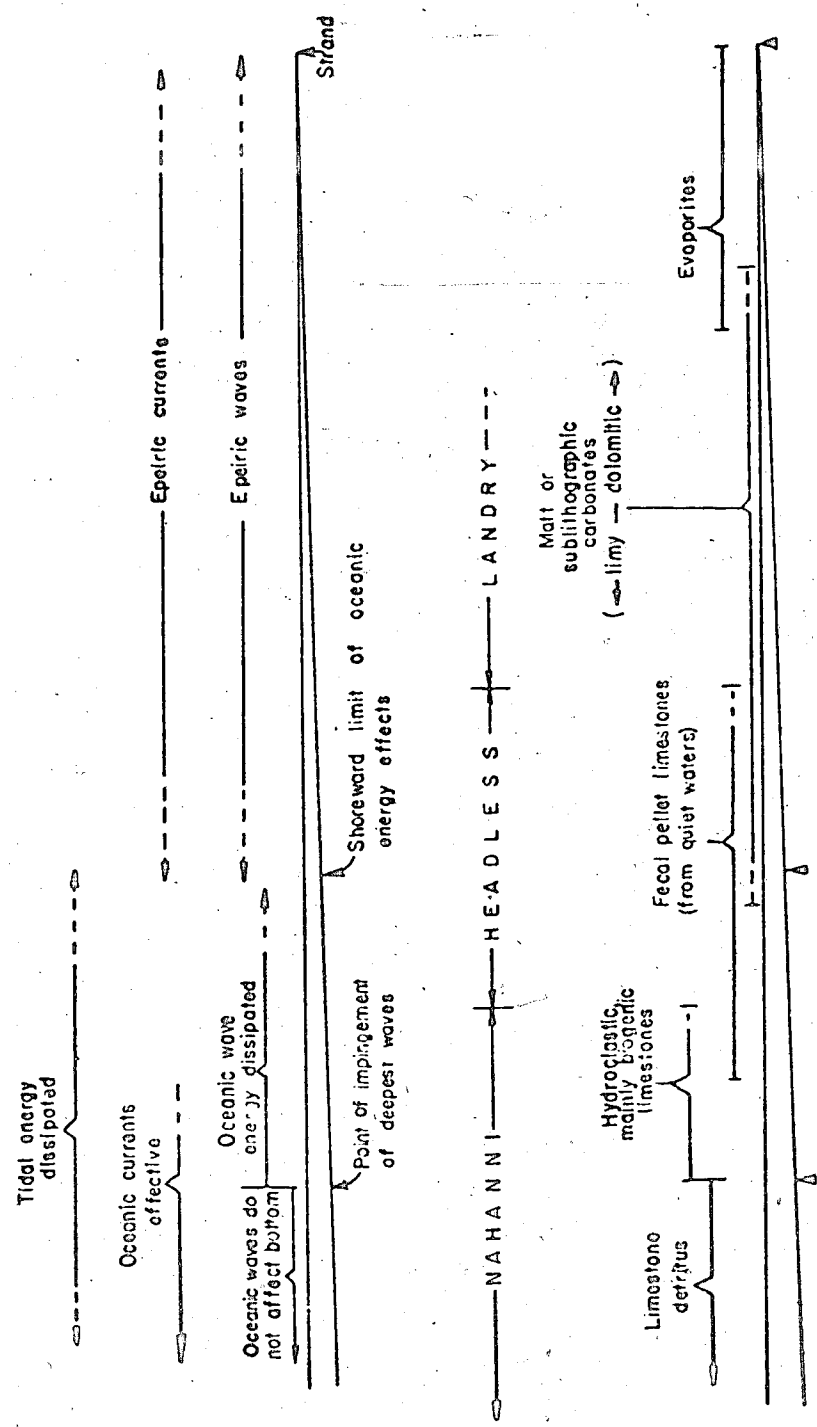
The Paleozoic sediments are of shallow marine deposition. Deposition has been on a shelf between the craton to the east and a mobile shelf to the west. From a study of thin sections and paleo-fauna of the Middle Devonian stratigraphy, Simpson (1975) deduced that the zone of deposition was a shallow shelf subject to oceanic wave and current action. Diagrammatically the environment of deposition is shown in Fig. 3.\*

The marginal cratonic basin to the west of the shelf edge received thicker deep-water carbonates and shales presumably from some extra-cratonic source, whereas eastward on the epeiric shelf thin sequences of evaporites and restricted carbonates were laid down (see Fig. 4, in pocket). Within this Devonian time period of deposition, the sea alternately transgressed and regressed resulting in a large number of depositional breaks and erosional cycles. Notation of the various formational changes and depositional breaks are found in Fig. 5.

It is not the writer's intention to give detailed consideration to the formational relationships within the study area; however, brief consideration of those relationships relative to the Camsell Range will be included (Fig. 5a).

---

\*Noble and Ferguson (1973) consider that the models II and III from LaPorte (1969, Fig. 14) are applicable for the depositional environment of the Nahanni and Arnica Formations.



Vertical scale greatly exaggerated

Fig. 3. Interpreted environment of deposition of Landry, Headless and Nahanni Formations in relation to the energy regime of an epeiric sea. Adapted from Shaw (1964).

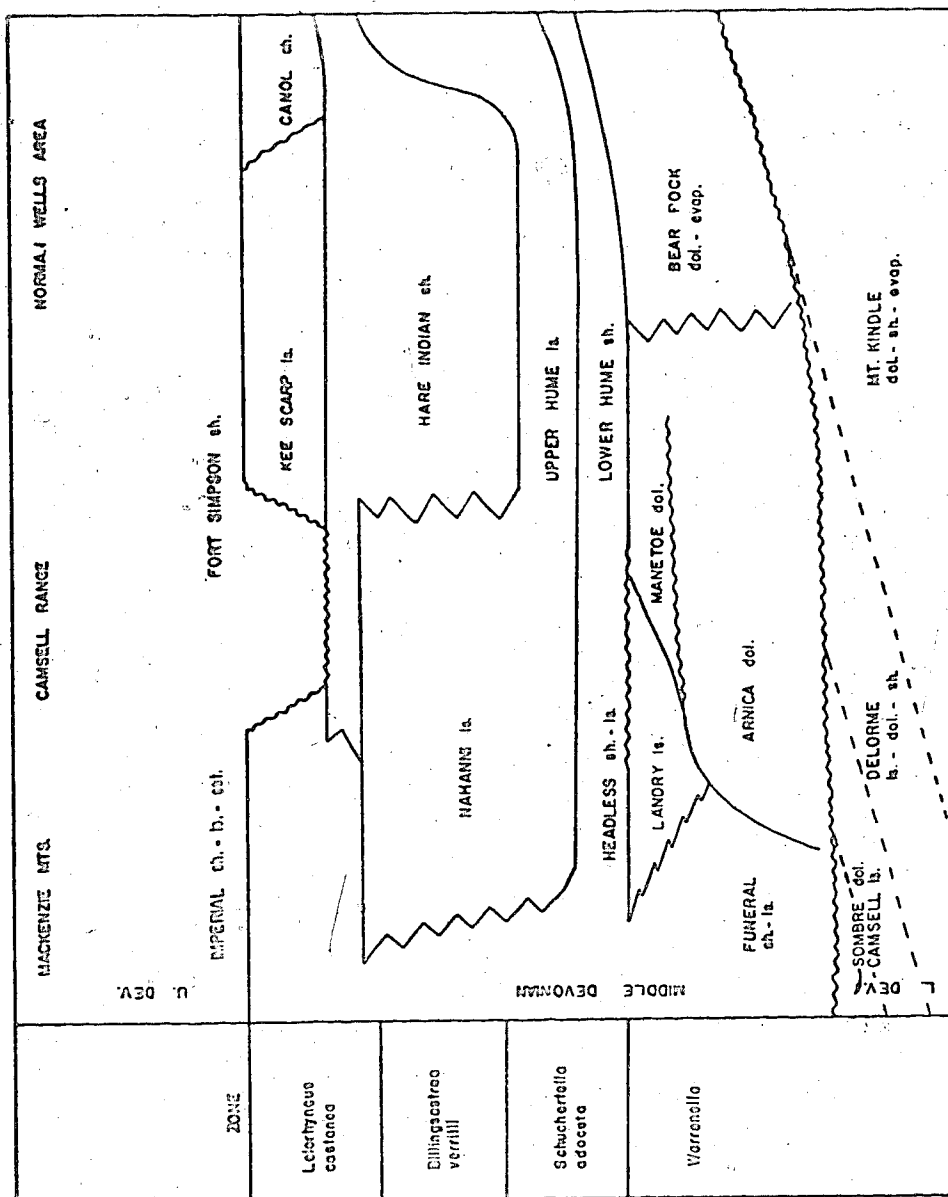


Fig. 5. Zonation of Devonian in Mackenzie Mountains, Camsell Range and Norman Wells area. Adapted from Law (1971), Noble and Ferguson (1973), and Caldwell (1971).

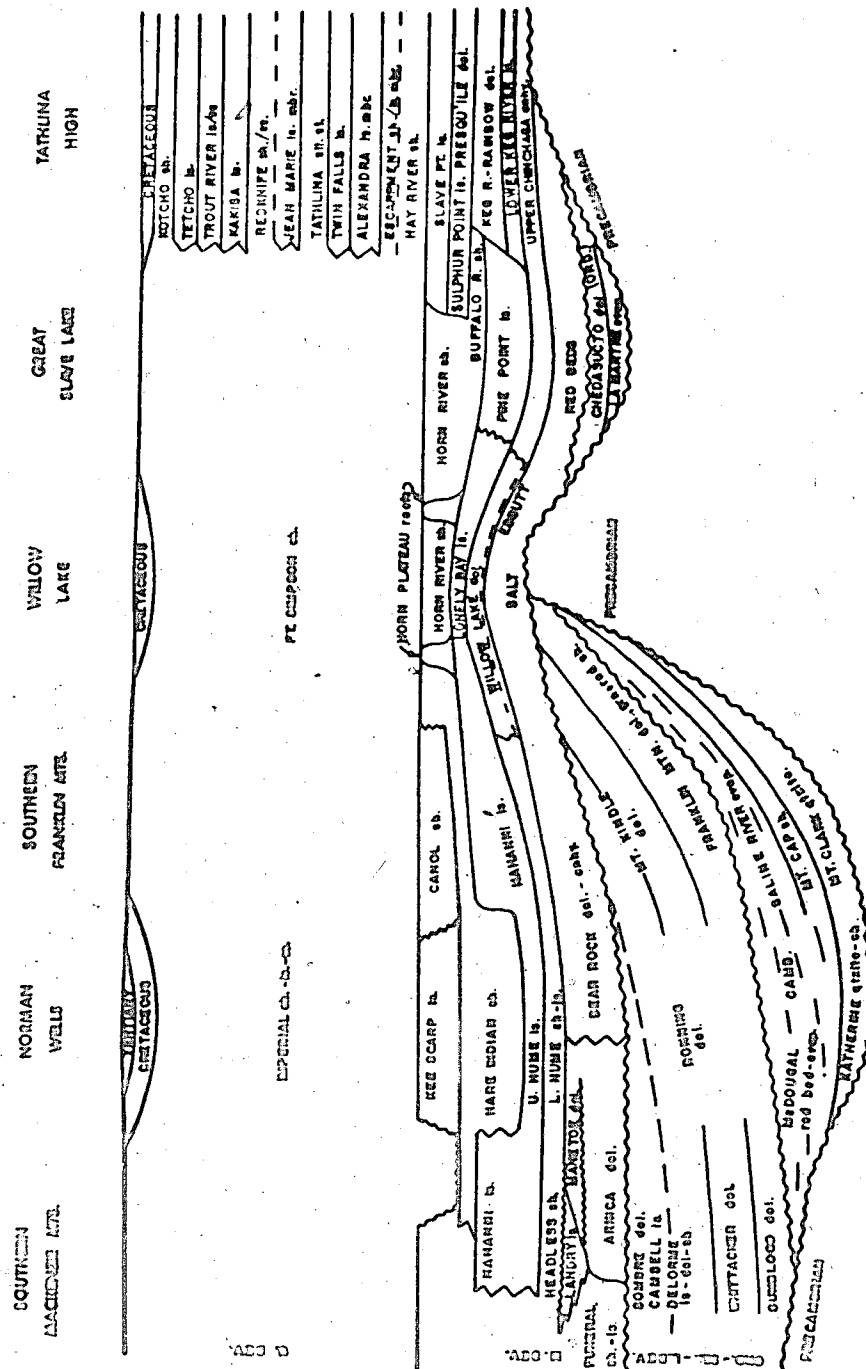


Fig. 5A. Schematic cross-section, southern Mackenzie Mountains to Tathlina High, showing formational names.



In the eastern part of the Interior Plains Paleozoic sediments overlie the granitic Precambrian basement, and the basement extends westward under the Camsell Range. This is revealed in oil well drill core from east of the range. There are Proterozoic strata outcrops near Wrigley on the northwest flank of Cap Mountain. Overlying the Proterozoic with an angular unconformity is fine-grained, white quartzose sandstone of the Mount Clarke Formation, which in turn is conformably overlain by grey, green and red shales of the Mount Cap and evaporites of the Saline River Formations. Overlying these formations, with angular unconformity, are the Ordovician-Silurian Franklin Mountain and Mount Kindle Formations. The thickness of these formations is variable, governed primarily by differential erosion related to unconformities (Norford and MacQueen, 1975). To the west of the study area these widespread formations are stratigraphically equivalent to the carbonate Sunblood and Whittaker Formations. These formations are overlain by the Silurian to Lower Devonian Delorme, Camsell and Sombre Formations, with angular unconformity. The Delorme Formation is the only Lower Devonian-Silurian formation to outcrop in the Camsell Range of the Franklin Mountains. To the west, however, the Delorme, Camsell and Sombre are revealed in outcrop.

The Bear Rock Formation is extensive in the Interior Plains and has been described in the literature. It is comprised of dolomite and anhydrite. Law (1971) and Noble and Ferguson (1973) have equated the Bear Rock Formation to the Middle Devonian (Eifelian) Arnica, Manetoe, Funeral and Landry Formations west of the Franklin Mountains. The exact stratigraphic relationship of the Arnica Formation to the Bear Rock is questioned by Douglas and Norris (1961). They say "the formation may be overlain, interbedded with, or grade laterally into the Funeral and Bear Rock Formations, and may be overlain by and partly laterally equivalent to the Landry and Manetoe Formations".

The Eifelian Headless Formation is the facies equivalent to the tan-grey, micro to finely crystalline Willow Lake dolomite, which correlates with the Upper Chinchaga Formation (Law, 1971). The Lower Nahanni Formation of the Franklin Mountain area correlates with the Lonely Bay Formation of the Willow Lake area and therefore with the Pine Point Formation of the Great Slave Lake area. Correlation with the Hume Formation of Norman Wells, N.W.T., is on the basis of the zone fossil Billingsastraea verrilli (Crickmay, 1960; Bassett, 1961; Warren and Stelck, 1962). The Eifelian-Givetian age is delineated at the upper boundary of the Hume Formation (Law, 1971; Bassett, 1961) which places the uppermost Nahanni and the Hare Indian Formations as Givetian in age. These two formations contain localized reefal development and may be related to the Upper Pine Point Formation of the Great Slave Lake area and to the Horn River Shale Formation northwest of Great Slave Lake. It is impossible to accurately trace the latest Emsian to early Givetian faunas in detail from the Mackenzie Mountains to the Great Slave Lake area (Caldwell, 1971) because of unexposed facies changes in the Interior Plains. Consequently, there is a lack of unanimity with regard to the above formational correlations.

#### E. STRATIGRAPHY

The Paleozoic stratigraphic sequence of the northern Camell Range is as follows.

Upper Devonian	2000'	Ft. Simpson Shale		Disconformity
	350'	Hare Indian Shale		
	450'	Nahanni Limestone		
Middle Devonian	100'	Headless Shale		Hiatus
	150'	Landry Limestone	Complex	
	100-300'	Manetoe Dolomite		Unconformity-Karst
	2000'	Arnica Dolomite		Unconformity-Angular
Lower Devonian		Delorme Dolomite		

1. The Delorme Formation is exposed along the base of the Camsell Fault trace and represents the oldest outcropping formation in the northern Camsell Range. The type section was measured at the headwaters of Pastel Creek in the Delorme Range and on the east flank of the Whittaker Range (Douglas and Norris, 1961). The age is considered to be Upper Silurian-Lower Devonian. The lithology is a variable grey, fine-grained limestone and dolomitic limestone, with a few thin beds of buff weathered shale and sandstone. Contorted bedding is common and intra-formational breccia is usually seen in outcrop. The recessive weathering of this formation and the rusty iron coloration, in varying intensities of brown, provide a certain distinctiveness to the formation.

It should be noted that the exposures of the Delorme Formation in the Camsell Range revealed no fossils. Douglas and Norris (1963), however, state that the basal beds of the Delorme carry fossils which were identified by Norford as Silurian, probably Ludlovian in age, while beds positioned higher stratigraphically contain fossils of Silurian to Devonian age. Chatterton (1976) places the upper part of the Delorme Formation at Whittaker anticline as Gedinian, based upon conodont collections.

2. The Arnica Formation unconformably (angular) overlies the Delorme Formation. The type section is located at First Canyon on the South Nahanni River. Douglas and Norris (1963) state that this stratigraphic unit comprises part of the Lone Mountain Formation of Kindle and Bosworth (1920).

The formation consists of a dense, fine- to crypto-grained, grey to black, finely porous, thick-bedded dolomite. The rocks are characterized by a colour banding of grey and black, while the weathered surface is muted dark grey in colour. Tectonic breccia and slump breccia

are common in the lower portions of the formation, while toward the top of the unit solution collapse breccia is evident. The clasts are cemented by white spar dolomite, which may be related to the overlying unconformity. Gabrielse et al. (1973) note that the distinctive dark weathering and well-bedded nature of the Arnica stands out in contrast with the massively bedded, light grey weathering habit of the Bear Rock Formation.

Some fossils are present in the Arnica Formation of the Camsell Range, particularly the echinoderm ossicle with double axial canals, designated Gasterocoma (?) bicaula Johnson and Lane, which is noted by Gabrielse et al. (1973). Norris (1968) noted that this fossil is most abundant in late to mid-Eifelian age (late Lower-Middle Devonian) but may extend to late Emsian (late Lower Devonian) age. Chatterton (1976) found latest Emsian to earliest Eifelian age conodonts in this formation.

3. The Manetoe Formation is composed of massive, coarsely crystalline dolomite. The name, adopted from the Manetoe Range in the Virginia Falls map area, was assigned by Douglas and Norris (1961). The type section is located at First Canyon on the South Nahanni River.

The formation is of variable thickness, usually in excess of 150 feet, porous, and cross-cut by fractures and veins, welded by secondary white calcite and dolomite. Generally, the formation consists of a grey and white banded coarse crystalline dolomite with banded algae horizons. The coarse dolomitization has obliterated much of the previous texture and biogenic features. Law (1971) considers the formation to represent reef or bank deposits, of a shallow water biostromal nature, since the dolomites grade into the Funeral limestones and shales to the west. The Landry Formation, considered within this context, represents the inter

and back reefal equivalents. This interpretation for the Manetoe formation in the Camsell Range is questionable because of the lack of biohermal structural development, which, if present, would rise more or less abruptly from the sea floor, whereas the Manetoe is quite consistent in thickness. Manetoe bioherms, however, do occur about 30 miles to the west of the study area.

Gabrielse et al. (1973) restrict the formational name 'Manetoe' to outcrop in the Thunder Cloud Range and in this paper the 'Manetoe' will be considered a dolomitized portion of the Landry Formation rather than an entity unto itself. The composite name that will be used is 'Landry-Manetoe Complex' (see Fig. 6, in pocket).

4. The Landry Formation, so named by Douglas and Norris (1961), overlies the Manetoe. It is crypto- to fine-grained, in places pelletoid limestone of thin to thick bedding and weathers a buff to light grey. It is non-fossiliferous in the study area; however, Gabrielse et al. (1973) refer to it as poorly fossiliferous, while Douglas and Norris (1961) indicate the formation is fossiliferous containing fossil fragments.

An unconformity is considered to exist at the top of the Landry due to uplift and erosion. Support for this contention is found in the vicinity of Norman Wells where Hume (1954) noted a possible unconformity.

The age of this formation assigned by Gabrielse et al. (1973) is late Eifelian or early Givetian. Chatterton (1976) assigned the age latest Emsian to earliest Eifelian.

Everywhere in the Camsell Range, the Landry Formation is overlain by the Headless Formation, separated by a hiatus. The Landry-Manetoe Complex, Funeral, and Arnica Formations are stratigraphic equivalents of the Bear Rock Formation to the east of brecciated dolomite and anhydrite.

5. The Headless Formation, first recognized by Douglas and Norris (1960) in the Headless Range, unconformably overlies the Landry, and is equivalent to the basal Hume Formation to the east. It represents the shaley, calcareous-argillaceous facies of the Nahanni Formation and is correlated with the Lower Hume due to the presence of the Eifelian brachiopods, Schuchertella adoceta (Crickmay, 1960).

Within the northern Camsell Range, the Headless shales are from 70 to 80 feet thick, while to the south and west (southern Franklin and Mackenzie Mountains) they thicken to about 200 feet (Law, 1971). These persistent calcareous-argillaceous shales, which are interbedded with limestone beds, are recessive weathering, and are usually tree-covered. The fossiliferous limestone at the top of the unit is thin- to medium-bedded, medium to dark grey, weathering a grey-buff to buff colour, due to iron staining. The calcareous shale, which forms the major portion of the formation, is black and is often deformed due to tectonism. The basal part of the formation reveals interbeds of black, bituminous, microclastic limestone.

The limestone beds in the upper part of the formation contain an abundant micro and macro fauna, which is itemized below. The lack of fossil breakage is indicative of a relatively low energy environment (Simpson, 1975). This environmental condition appears to have persisted throughout the deposition of the formation, although the sea was undergoing minor transgressions and regressions which resulted in interbedded limestone and shale.

The limestone beds in the lower part of the formation have a high argillaceous and bituminous content. A limited faunal assemblage is

present in these beds. Deposit feeders such as Palaeoneilo and a few Actinopteria have been identified. This assemblage is indicative of a restricted, shallow water environment. The presence of dessication cracks attest to these conditions..

The limy shale beds are essentially non-fossiliferous. Thin section petrographic studies indicate that the shales at the base of the formation consist of fecal pellet muds or pelmicrite with a considerable argillaceous content.

The Headless Shale fauna identified by Simpson (1975) follows.

Corals:

Hexagonaria  
Digonophyllids  
Coenites or Thamnopora  
Favosites limitaris  
Alveolites

Algae:

Charophytes:  
Trochiliscus  
Eochara  
Chovanella

Brachiopods:

Schuchertella adoceta  
Spinulicosta stainbrooki  
Emanuella sp.  
Atrypa desquamata

Pelecypods:

Actinopteria  
Palaeoneilo

Ostracods:

Moelleritia canadensis

Crinoids

Trilobites:

Proetus  
Dechenellids

Gastropods:

Bellerophon  
Mastigospira  
small, high-turreted  
form

Cephalopods:

small, orthoconic  
forms

D.J. McLaren (1970), on the basis of Billingsastraea sp., suggests an age of Middle Devonian. This genus was not noted in the Headless Shale of the study area, but was noted in the Nahanni Formation. Chatterton (1976), on the basis of conodont collections, suggests the age of Eifelian.

6. The Nahanni Formation (Hage, 1945; Douglas and Norris, 1961) is composed of massive resistant, medium- to thick-bedded, light grey weathering, fossiliferous limestone, which forms the westerly-dipping flank of the Franklin Mountain range. Within the formation are several

semi-resistant thin-bedded limestone beds, which appear to contain thin argillaceous partings. The more massive beds are bioclastic to varying degrees, more so near the base where black, silicified corals such as Thamnopora, Coenites, and stromatoporoids are generally associated with bitumenization.

The formation has been structurally deformed. The evident minor strike-slip faulting and 'crackle' development (irregular but complete fracturing of the rock with essentially no displacement of the fragments) most likely are related to the Laramide orogeny. Often the 'crackle' zones are more fossiliferous than the massive, non-fractured limestone beds. The fossils may be broken but are not rotated. The presence of these zones throughout the formation, devoid of dolomitization and not associated with sulphide mineralization, indicate that this deformation followed the period of mineralization.

The depositional environment of the Nahanni Limestone has been variable as revealed by the varying amount of intra-formational argillaceous material. The non-persistent depositional conditions are also reflected by the variable faunal population. Although the fauna, a mixed fossil assemblage (residual and transported community), reflect significant current and wave action, these conditions were not persistent throughout all of the depositional period. The organoclastic nature of the limestones, viewed in thin section, and the bulbous stromatoporoids suggest that the more fossiliferous units probably formed the biohermal structures at a depth within the sphere of influence of current and wave action (Simpson, 1975).



In thin section study, the Nahanni limestone is found to be composed of fossil fragments with a micritic matrix and to have varying degrees of quartz crystal development. By the classification of Folk, the rock is laminated micrite to organoclastic biomicrite.

The following fossils were collected on the Wrigley and Lou properties and were identified by Simpson (1975).

Corals:

Billingsastrea verilli  
Hexagonaria atypica  
Syringopora  
Eridophyllum  
Thamnopora  
Coenites  
Chaetetes  
Favosites limitaris

Stromatoporoids:

circular (bulbous)  
 laminar

Brachiopods:

Atrypa arctica  
Atrypa aperanta  
Emanuelia sp.  
Ambocoelia meristoides  
Spinulicosta stainbrooki

Pelecypods:

Paracyclas elliptica  
Ontaria clarkei

Trilobites:

Proetus

Ostracods

Crinoids

Gastropods:

Euomphalus  
Buchelia  
Bellerophon  
 numerous small forms

Cephalopods:

orthoconic nautiloid  
 form

According to Gabrielse et al. (1973) direct lithologic and faunal correlation is possible between the combined Headless and Nahanni Formations and the Hume Formation. An Eifelian age is assigned to the Nahanni Formation (Chatterton, 1976).

7. The Hare Indian and Fort Simpson Formations. The Nahanni Formation is conformably overlain by very fine-grained pyritiferous, fissile black shale and calcareous shale. Douglas and Norris (1961) proposed the name Fort Simpson Formation, based upon the term 'Simpson' proposed by Cameron (1917), which covered "the shales occupying the stratigraphic interval between the Middle Devonian limestones and the overlying siltstones and shales of the 'D<sub>4</sub> unit' of Hume (1921)". Gabrielse et al. (1973) have

refrained from assigning a name to the recessive, thin-bedded pyritic, slaty shales conformably overlying the Nahanni Limestone in the southern Mackenzie Mountains. They say that only when the Nahanni Limestone and the underlying Funeral Shale are present can these shales be distinguished from the Road River Shale of the Mackenzie Mountains. Caldwell (1971) has considered historically the biostratigraphy of the various Middle and Upper Devonian formations. He contends that the Frasnian Fort Simpson Shales overlie the Givetian Hare Indian Shale\* disconformably. The Hare Indian Formation is designated by a Leiorhynchus castanea and probably 'Emanuella' meristoides fauna, as is the Horn River Shale on the north-west side of Great Slave Lake (McLaren, 1970).

Within the consideration of this thesis the shales which conformably overlie the Nahanni limestone will be referred to as the Hare Indian Formation. Diamond drilling has indicated their thickness in the Wrigley area to be about 350 feet, which agrees with the Hare Indian - Horn River isopach map (Law, 1971) for the Wrigley area. Outcrop of the shales in the northern Camell Range is minimal, exposure being mainly along Wrigley Creek. One local reef structure is known to exist in this sequence, about 15 miles north of Wrigley (E.G. Olfert, personal communication).

The Fort Simpson Formation disconformably rests upon the Hare Indian Formation and has been revealed in diamond drill holes in the Mackenzie Plain. These shales lack fossils and may be designated as a distinct unit representing shale deposition in an euxinic environment. They appear to be a distinct formation but may well represent in part a lateral time equivalent to the Hare Indian Shale.

---

\*Chatterton (1976) obtained conodont collections of early Givetian age from the base of the Hare Indian Formation.

### Chapter III

#### ORE AND GANGUE MINERALS AND THEIR CONTROL

The Wrigley mineralization is oxidized in surface outcrop and at depth within the structurally controlled deposit. Diamond drill hole data indicated the deposit may be divided into an upper supergene zone and a lower hypogene zone. No intermediate zone of enrichment is noted, the usual indication of enrichment being the presence of wurtzite and marcasite (Bateman, 1967).

##### A. PRIMARY ORE MINERALS AND ASSOCIATED TRACE ELEMENTS

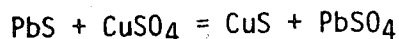
The primary ore minerals are sphalerite ( $ZnS$ ) and galena ( $PbS$ ) with minor silver, cadmium and copper. Due to the small quantity of trace elements, exact determination of the minerals would require use of the electron microprobe which lay outside the scope of this study.

The silver values are on the whole less than 2 oz per ton. According to Ramdohr (1950), galena is a well-defined 'carrier of silver' and therefore it may be assumed that the silver values are carried by the galena.

Cadmium is a minor element in these polymetallic ores. Sphalerite is generally the main carrier of cadmium; however, it may also be found in zincian tetrahedrite, stannite, chalcopryrite and in some lead minerals (Ivanov, 1961). The percentage cadmium, as determined in two drill core sulphide sections, ranges between 0.04 and 0.13%.

The copper is primarily in the oxidized form of malachite and azurite and is usually in close association with galena. The silver-bearing

tennantite-tetrahedrite ( $\text{Cu}_{12}\text{As}_4\text{S}_{13}$  -  $\text{Cu}_{12}\text{Sb}_4\text{S}_{13}$ ) appears to be responsible for the copper. Covellite ( $\text{CuS}$ ) is present and most likely is due to the reaction of copper sulphate ( $\text{CuSO}_4$ ) with galena or tetrahedrite, in a reaction such as:



On the whole, copper values of the deposits are low, occasionally reaching 0.5%.

### 1. Galena and Sphalerite

The galena and sphalerite of the properties are often closely associated or intergrown. The crystallization of the major sulphides ranges from very fine disseminated grains to massive, as representative of the extremes. Consideration of the manner of occurrence of the galena and sphalerite will be given in two parts: the 'Hammer' and 'Shelter' showings on the Lou property, and the Wrigley samples taken from diamond drill core.

(a) 'Hammer' and 'Shelter' showings. The 'Hammer' showing reveals a mineralized vein in which almost no original carbonate host rock is present, replacement by silica and sulphides being almost complete. Coarse crystalline secondary quartz and some diagenetic quartz (about 70-80%  $\text{SiO}_2$ ) rimmed with bitumen predominated in the vein, and the vein silica contact with the host Nahanni limestone is very sharp. The sphalerite and galena occur within the vuggy inter-crystalline areas or as small grains disseminated within the quartz crystalline mass.

It should be noted that study of the same vein a distance of some 40 feet along strike revealed a mineralogic compositional change from that described above. Instead of the sphalerite-galena ratio being 2:1,

galena predominates, occurring as massive aggregate. The carbonate host is brecciated, along with post-mineral calcite filled hairline fractures. The quartz content is less than 10% and the silver values within this vein are not consistent relative to the lead assays.

The 'Shelter' showing, about 900 feet to the north of the 'Hammer' showing, demonstrates vein sphalerite and galena, both disseminated and massive, inter-crystallized with diagenetic quartz, coarse crystals of secondary spar calcite and dolomite, with a crypto- to micro-crystalline calcareous matrix. Ring cement is evident, and all mineralized and non-mineralized rock is cross-cut by hairline fractures (to 1 mm) cemented by spar calcite, related to post-mineral deformation. The silica content ranges from 1-75%, while the bituminous material is in the range of 10-15%. The bitumen is peripheral to the silica grains, and is intimately associated with secondary grey dolomite. Euhedral silica crystals often penetrate the sphalerite and galena in a later crystal growth manner and euhedral dolomitic rhombs (less than 5 microns) may be seen in the sphalerite crystals, indicating dolomite formation in the post-mineral stage.

In general, it may be said that where the percentage silica is high, the percentage sulphide content will be low; where the percentage dolomite is high, the percentage sulphide content will be high; and where the percentage secondary calcite is high, the degree of sulphide mineralization will be low.

(b) Wrigley samples. Most of the mineral relationships mentioned above may be found in the Wrigley diamond drill core. Galena and sphalerite are the major sulphides and are primarily associated with dolomite.

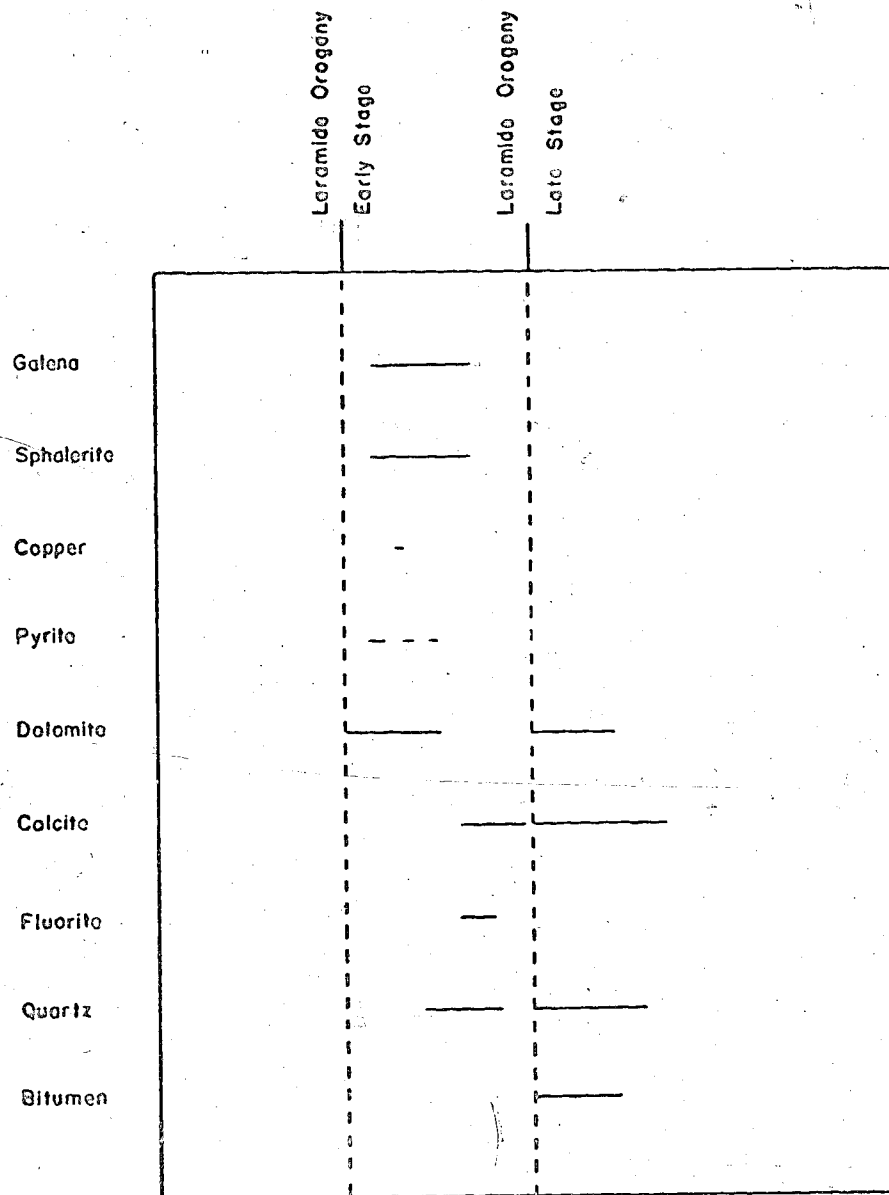


Fig. 7. Paragenesis: Wrigley & Lou Properties

Section 36-3 (46.5) reveals barren unfragmented white spar dolomite and calcite in proximal relation to mineralized grey fragmented and silicified dolomite. This implies that the (Pb/Zn) mineralization was deposited by Mg-Si rich brines. The grey colour is imparted by the quartz crystals and the bitumen. Subsequent iron-free, non-siliceous, and non-mineralized dolomite and calcite fill the remaining vugs and fractures. Stylolites are formed throughout the rock increasing the porosity and permeability of the host. The stylolitic development is due to tectonic forces of post-mineralization age which have fractured the mineralized veins. On the microscopic scale, the tectonic forces are revealed by strain shadows in the quartz crystals and by bent rhombohedral cleavage traces of the secondary spar calcite and dolomite.

From thin section studies the following paragenetic sequence has been constructed (see Fig. 7) within the context of the tectonic events of the Laramide orogeny.

Generally, the galena and sphalerite crystallization ranges from very fine- to coarse-grained mineralization and occurs as disseminations within the host Nahanni limestone conformable to bedding (i.e., pseudo-stratiform mineralization of the Zebra-Zinc showing, Wrigley) or as disseminations within silicified dolomite vein fillings of a cross-cutting nature. The mineralization may also be found as disseminations within calcite veins (very minor) and as massive galena in association with minor 'vesicular' (massive silicification) silica development, as is evident at the Bourne showing. The predominant host rocks of the epigenetic mineralization include brecciated Nahanni limestone, siliceous Nahanni limestone, spar dolomite, brecciated spar dolomite and very rarely spar calcite. Illustrations of the latter host rock may be found on the Lou property.

## 2. Pyrite

Pyrite is a minor constituent of the deposits. Very fine-grained disseminated pyrite is evident in the mineralized veins, and sample 12-4 (255) reveals the largest samples of pyrite viewed in intimate contact with galena and sphalerite. It is usually closely associated with silica and/or dolomite.

### B. OXIDIZED ZONE

The oxidized zinc minerals include the following: carbonates of zinc-smithsonite ( $\text{ZnCO}_3$ ), hydrozincite ( $2\text{ZnCO}_3 \cdot 3\text{Zn}(\text{OH})_2$ ) and a silicate of zinc-hemimorphite ( $\text{Zn}_4(\text{OH})_2\text{Si}_2\text{O}_7$ ).

The host rocks in which the carbonates of zinc usually form are limestone and dolomite, whereas the silicate, hemimorphite, is present when the gangue is rich in silica (i.e., quartz). Within the Wrigley deposit the gangue rock is predominantly limestone and dolomite with varying amounts of quartz as crystalline 'needles' and/or amorphous silica.

Smithsonite is the principal oxidized zinc mineral and reveals a well developed 'gnarled root texture' in surface outcrop and in core samples. Thin section (i.e., S-73-1 (171)) examination reveals that the oxidized minerals are intimately associated with calcite, silica and iron oxide.

Smithsonite development occurs in the upper part of the Nahanni Formation where chemical conditions are favourable to its formation within the open fracture systems. Erosion of the enveloping host limestone has resulted in exhumation, in the form of extensive outcrop, of the silicified smithsonite. According to Sangster (1975), the smithsonite mineralization in the Yukon-Northwest Territory area represents a pre-glacial



weathering product of a sphalerite-bearing deposit, preserved because of insufficient glacial scour.

Hydrozincite and hemimorphite are relatively minor in the deposit. The oxidized lead minerals, cerussite ( $\text{PbCO}_3$ ) and anglesite ( $\text{PbSO}_4$ ) and less often pyromorphite ( $\text{Pb}_5\text{Cl}(\text{PO}_4)_3$ ), are derived from the lead sulphide ( $\text{PbS}$ ). The lead carbonate, lead sulphate and lead chloro-phosphate are only of academic interest in the Wrigley deposit and are not considered in this study as they are not uniformly distributed.

Malachite ( $\text{Cu}_3(\text{CO}_3)_2(\text{OH})_2$ ) and azurite ( $\text{Cu}_2\text{CO}_3(\text{OH})_2$ ) are often to be seen in close proximity to sulphide mineralization, which may be due to the oxidation of sulphosalts - tennantite-tetrahedrite - which are noted for malachite, azurite and antimony oxide alteration (Berry and Mason, 1959).

### C. GANGUE MINERALS

Dolomite, quartz and occasionally calcite are to be found in close association with mineralization ( $\text{Pb/Zn}$ ). The relationship of dolomite to ore deposition is not fully understood (Hewett, 1928; Sonnenfeld, 1963); however, the proximity of dolomite to the sulphides in many metalliferous deposits (such as the Mississippi Valley type deposits) signifies a connection. Sonnenfeld (1963) observed a relationship between phreatic groundwaters which carry magnesium compounds, the area of dolomitization and sulphide mineralization. He noted that within the Upper Devonian Leduc-Rimbey reef trend in Alberta, magnesium-rich groundwaters transported sphalerite, galena, tetrahedrite and other copper sulphides. Dolomite therefore may be considered significant in the northern Camell Range and merits further consideration.

## 1. Dolomite

Dolomitization, as it occurs in the study area, is evidence of permeating Mg-rich brines within the Nahanni, Headless and Landry Formation fracture systems. The Manetoe and Arnica Formations are totally dolomitized. The textural range of this dolomitization is from sucrosic to sandy, friable in places, with high inter-crystalline porosity, to a granular, coarsely crystallized texture in which the original grain and depositional fabric is largely destroyed. Mineralization, to varying degrees, is related to the areas of dolomitization within the respective formations.

Dolomite, structurally controlled within faults and veins, may be genetically associated with the pervasive dolomitization of the underlying formations. In both, it is intimately associated with sulphide mineralization and often cements mineralized fault breccias. The association of the mineralization with the dolomitization implies the mineralizing process took place over a period of time as indicated by the determined periodicity of the associated dolomitization.

## 2. Spar Calcite

Spar calcite (secondary) is extensive throughout the study area. Occasionally it is found as a host to disseminated galena mineralization in small fracture veins. It is often the cementing matrix in mineralized breccia and 'crackle' fragments and is most often the matrix of post-mineral tectonic fractures and fissures. The first above-mentioned association of vein calcite with mineralization is very rare, which indicates that calcification is primarily post-sulphide in the paragenetic sequence and that the brine is very depleted in magnesium salts.

The spar calcite ranges from coarsely granular in vuggy areas, to a finer, saccharoidal texture in surface exposed fissures. In all cases the calcite is white except on the exposed surface where it takes on a cream colour.

### 3. Silica

Silica, both diagenetic and secondary in origin, is prominent within the Nahanni Formation. The silicification concentration is irregular (0-80%). Quartz crystals are usually associated with mineralization but the presence of silica does not signify sulphide mineralization. It may pervade the sulphides, the dolomite and the host formational limestone. The concentration appears to be highest within the environs of the tectonically deformed areas, i.e., faults, fractures and veins, and may also be well developed, of euhedral habit, within vugs of the dolomitized host formation.

Primary or diagenetic silica may be considered within the category of 'quartz needle rock' which signifies carbonate rock composed of varying concentrations of silica (up to 50%), the silica occurring as subhedral to euhedral quartz crystals of  $<5-30\mu$  in size. The diagenetic crystal development transpired in the post-sedimentation stage, and the presence or absence of argillaceous material in the carbonate sediment is considered the determining factor in the formation of the quartz crystals (Smirnov et al., 1969). Silicification of fossils is an illustration of the diagenetic quartz, although such silicification can occur after lithification depending upon the physico-chemical conditions. The high silica concentration in the cross-cutting mineralized veins, however, is only partially attributed to pre-mineral mobilization of silica, the majority due to syn- and post-mineral silicification. This epigenetic silica usually possesses a habit indistinguishable from that of the pre-mineral or diagenetic silica.

Massive silica, which lacks a crystalline euhedral habit, referred to herein as 'vesicular' silica, is epigenetic and is associated with massive

sulphide mineralization in outcrop. Core samples of the 'vesicular' silica, which is usually spatially separate from 'quartz needle rock' tend to indicate that massive silica is not always in association with mineralization. This indicates a period of post-mineral silicification.

#### 4. Sedimentary Pyrite

Pyrite appears within the shale horizons of the Headless, Nahanni and Hare Indian Formations. It occurs as early diagenetic framboids and as isolated euhedral grains. The crystallization of the pyrite commenced during early stages of sediment deposition, signified by diagenetic load casting. The question of the origin of the diagenetic framboids and the pyrite crystals is the subject of this work but has been considered by Kaplan (1967), Berner (1964, 1970) and Kalliokski (1965), as well as by Chauhan, (1974).

The sedimentary pyrite is different from the pyrite associated with the galena and sphalerite. The latter pyrite is localized within structural veins and is often in dolomitized rock.

#### 5. Bitumen

Bitumen is present within the Nahanni Formation, in the form of solidified, black hydrocarbons. Certain horizons, such as the base of the formation, reveal ovoid bituminous pods which may reach a size of 10-20 inches across. Where these large pods are located, the fossil population is usually high, signifying an area in the host rock which possessed greater porosity and permeability. Bituminous material is also present interstitially in carbonate and silica rocks hosting sulphide mineralization. Bitumen, however, is absent from the white secondary dolomite and calcite. This tends to indicate a bituminous intrusion into

the host rocks that post-dates the mineralization (no bituminous matter occurs in the sphalerite fluid inclusions, see Chapter IV), post-dates the post-mineral structural deformation that developed the 'crackle' zones but pre-dates the white, secondary spar calcite and dolomite.

#### 6. Fluorite

Fluorite is associated with sphalerite mineralization in two local areas as revealed in Wrigley outcrop. No fluorite has been noted on the Lou property. It represents a minor constituent in close association with dolomite and silica. The crystals, which sit in a carbonate boxwork, may exceed 3 mm in diameter and are mauve to blue in colour. Paragenetically, they may represent a late stage of mineralization.

#### D. CONTROLS TO MINERALIZATION

The lead-zinc mineralization within the Devonian carbonate formations occurs as veins within fracture systems of tectonic derivation and therefore the mineralization may be considered to be structurally controlled.

Throughout the region paleo-karst features are to be noted, indicated by sink hole development and breccia-filled caverns, controlled by unconformities. Solution collapse breccias within the Arnica Formation, exposed on the cliff face between the Lou and Wrigley properties, reveal the effect of connate and/or meteoric waters. Similar collapse structures in the Bear Rock Formation are noted by E.O. Olfert (personal communication). However, none of these karst features have, to date, been found to host lead-zinc mineralization.

The fracture lineations, normal faults and shears mapped on the Wrigley property (Fig. 1-A) represent structural deformation of more than one generation. Some of the structural breaks lack mineralization, while others are mineralized locally along the exposed strike length, the most

prominent of these is the 'Zebra Zinc' fault. By inference, the north-east extension of this fault forms a linear through areas of mineralization (Fig. 1-A); for example the 12-North and 36-North areas of mineralization. This localization of mineralization along the linear fault may be due to pinch and swell phenomena; however, little evidence of lateral strike-slip displacement is to be seen in the field.

Consideration of diamond drill hole B-73-2, which was drilled to transect the 'Zebra Zinc' fault, tends to indicate block or reverse faulting when the Nahanni, Headless and Landry Formations are correlated across the fault (Fig. 8). A vertical displacement of 466 feet is indicated, the eastern side of the fault representing the hanging wall. A similar, unmineralized fault is visible on the cliff scarp of the Lou property, and the vertical throw is approximately 250 feet (see Plate I). These two examples indicate that this type of faulting is significant in understanding the structural controls of mineralization within the northern Camstell Range. The fact that the former fault is related to mineralization while the latter is not, may be indicative of an extended period of structural deformation in which the block faulting took place.

The mineralized structures (veins and fissures) are closely related to the early Laramide phase of folding. The veins and fissures are parallel or near to parallel to the axial plane of the folds which implies that the mineralization was emplaced in the host structures subsequent to the folding. The structures may be linear flexure breaks and therefore are related to the folding.

The presence of post-mineral deformation of the mineralized veins on the Urigley and Lou properties implies that the extended deformational period of the Laramide orogeny transcends the period of sulphide deposition. This post-mineral deformation has brecciated the mineralization

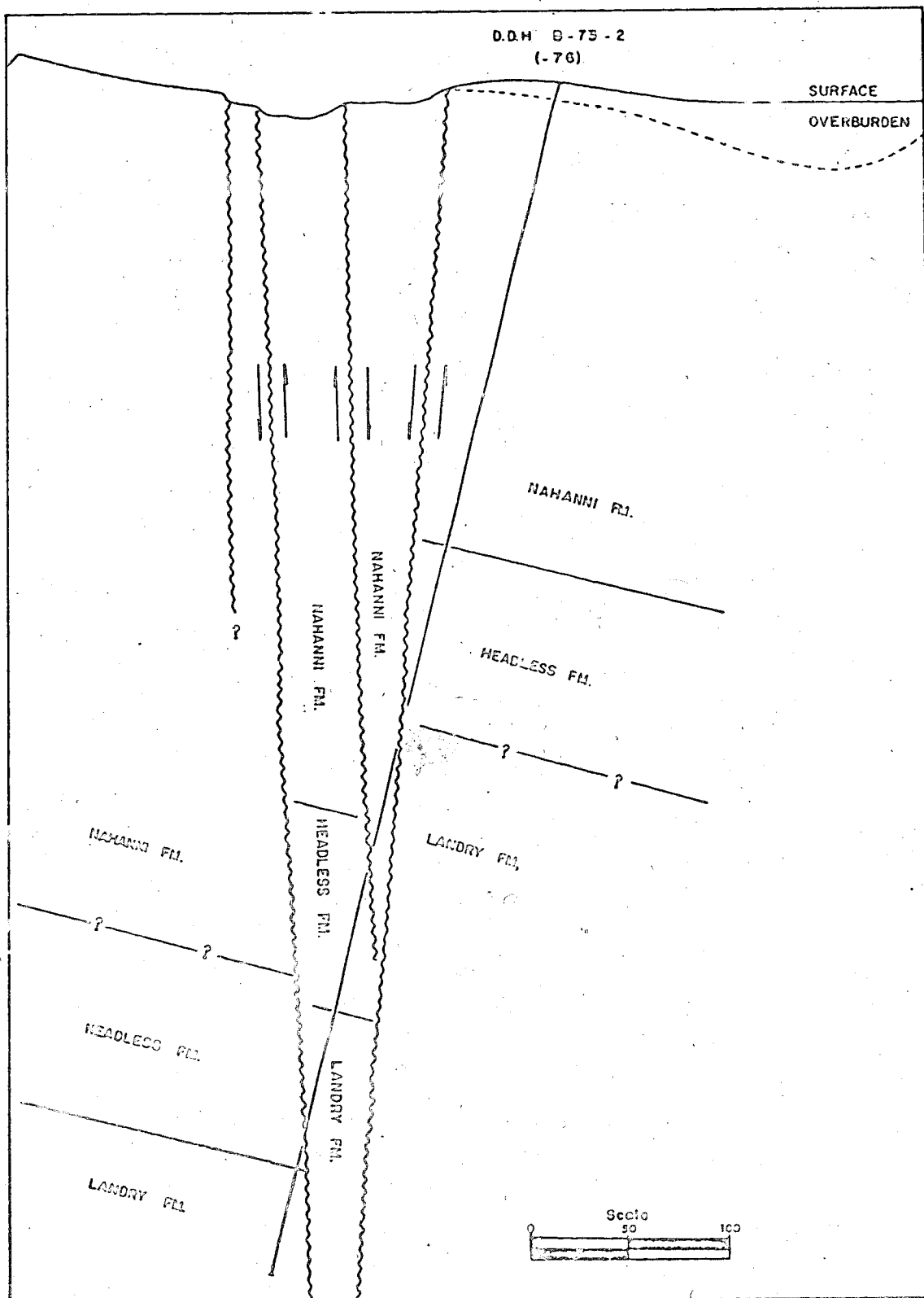


Fig. 8. D.D.H. B-73-2: 'Zebra Zinc Fault'.

and contorted the veins, thereby increasing porosity and permeability allowing entry of secondary spar calcite, dolomite and silica-bearing fluids. It is most probable that this late deformational period produced the non-mineralized 'crackle' zones of the Nahanni Formation.

The formation of the mineral controlling structures is therefore intimately related to the Laramide orogenic event. The possible sequence of events within the orogenic period is as follows:

(1) En échelon folding of the Paleozoic sediments result with décollement at the level of the Cambrian salt and anhydrite (Douglas et al., 1970; Norris, 1972).

(2) The folds become broken by faults with small thrust or strike-slip component. Douglas et al. (1970) consider that a fracture system was present in the rocks as faults or zones of fractures prior to the Laramide tectonics. Therefore, the breakage of the folds may be due to the reactivation of this earlier fracture system.

(3) Zones of weakness within the basement (Goodman, 1951) are reactivated as block and/or reverse fault, with certain strike-slip movement, such that block rotation may result. This period is related to the mineralization of the fracture-fault system. The reactivated basement releases saline interstitial fluids or formation brines containing lead ions which mobilize updip along the fault planes. This is also the period of the Camsell Range development.

(4) Subsequent deformation along lines of weakness, of decreased magnitude, causes strike-slip and minor reverse faulting (i.e., Lou property). The resulting deformation fractures and contorts the mineralized veins and fissures and permits oxidation of the sulphides which have not been rewelded by the post-sulphide phase of calcite, dolomite and silica. Secondary minerals therefore formed with no specific depth pattern.



The block faulting, which aids the preparation of the stratigraphy for reception of the mineralizing fluids, may be related to the east-west basement faults of the Interior Plains region, some of which have been mapped by de Wit et al. (1973). Illustration of this possible connection is brought out in the diagram presented by Goodman (1951) relative to the Norman Wells, N.W.T. area (see Fig. 9).

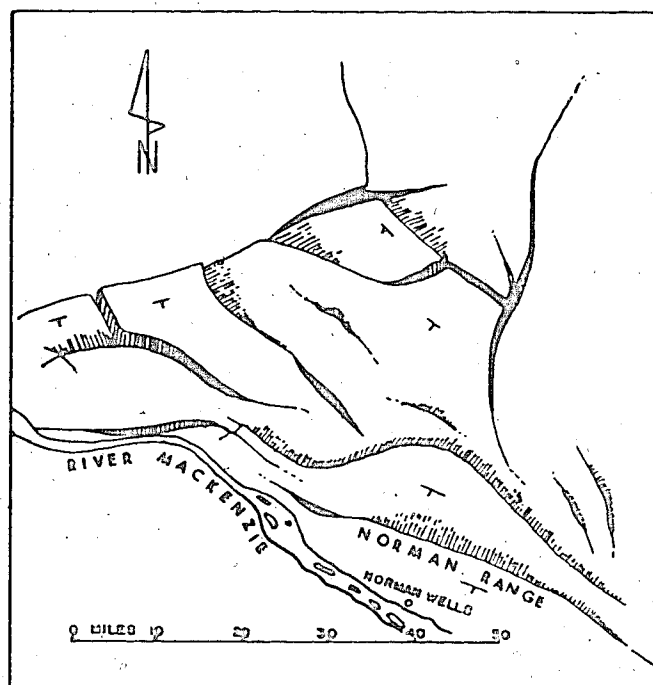


Fig. 9. Generalized diagrammatic interpretation of faulting in crystalline basement in foreland corner north of Norman Wells, N.W.T. (Goodman, 1951).

## Chapter IV

### FLUID INCLUSION STUDIES

Fluid inclusion studies have been used in this study with three major objectives: the determination of the density, salinity and the temperature of the mineralizing fluids. Using this information, the nature and the environmental source of the ore-bearing brines can be established and along with the data of sulphur and lead isotopes, comparisons can be made with other mineral deposits, such as Mississippi Valley type deposits.

#### A. PREVIOUS FLUID INCLUSION STUDIES

The literature on fluid inclusions is voluminous and Roedder (1972) has presented a very good bibliography. The application of fluid inclusion studies to mineral-forming solutions is very ably presented by Yermakov et al. (1965). Roedder (1972) has considered the composition of the fluids in inclusions. The study of sphalerite fluid inclusions has interested a number of researchers, Newhouse (1932), Roedder (1968, 1971), Skinner (1967), Skinner et al. (1967), Jowett (1975), because they felt that fluid inclusions truly represent the ore-bearing brines.

Previous sphalerite fluid inclusion studies of northern Canadian lead-zinc deposits may be summarized as follows.

The Pine Point Mine, located some 55 miles east of Hay River, N.W.T. and southeast of the Wrigley lead-zinc deposit, was considered in terms of the origin of the ore-forming fluids by Roedder (1968). His study centered upon crystals of replacement, vug and 'colloform' crust sphalerite. The homogenization temperatures cover a range of 51 to 97°C, and the salinity

is 25 weight percent equivalent NaCl (as revealed by low freezing temperatures).

The Little Cornwallis Island, N.W.T., Polaris lead-zinc deposit was examined by Jowett (1975). The two phase sphalerite inclusions studied reveal a homogenization temperature range of 52 to 105°C. The ore fluid salinity is estimated to be in the range of or less than 26.3 weight percent NaCl.

#### B. MATERIAL STUDIED

Detailed descriptions of the respective samples used in this study are provided in Appendix I. Initially, samples of well developed sphalerite crystals were selected from the diamond drill cores of the Wrigley property, representing various horizons within the Nahanni Formation. The twelve selected samples were prepared as doubly polished plates 1/2 to 3/4 mm thick, some of which nearly duplicate the 'coexisting' sulphide pairs used in the sulphur geothermometry. Sample selection centered upon well-developed, light-coloured sphalerite crystals which appeared to have the greatest possibility of providing useable fluid inclusions. These sphalerite crystals represent vug and fissure mineralization. Post-mineral tectonism has caused fracturing of the sphalerite crystals, along which secondary inclusions have developed. The majority of the primary and pseudo-secondary inclusions have not been affected by this tectonism, as indicated by essentially no leakage of the inclusions. Consequently, the fluids in these inclusions are considered to represent the original mineralizing brines and the experimental findings are believed to reflect the conditions existing at the time of ore deposition.

The sphalerite crystals varied from colourless, through light yellow to orange red, in concentric bands within individual crystals. The reason for the zonation is not known; however, variation in iron content is not considered to offer a full explanation (see Appendix II). The dark colour of the sphalerite crystals, the small size ( $<1-8\mu$ ) of the inclusions and the numerous secondary inclusions, some opaque, some void and others filled with gas and liquid phases, often hamper detection and study of the primary and pseudo-secondary inclusions. Due to these reasons only five of the sphalerite samples proved to be suitable. Only the studied sections are listed in Table 1.

Tests for high pressure fluids were performed using a crushing stage and the minor amount of gas so released is considered to be carbon dioxide, because the gas bubble dissolved very slowly in  $\text{CO}_2$  saturated kerosene. In the microscopic examination of the inclusions, only one three-phase primary inclusion was observed. Presumably most of the  $\text{CO}_2$  gas is contained within secondary inclusions. Daughter crystals are generally absent. One exception was noted - the daughter crystal was considered to be halite in this case.

One fluorite crystal from a mineralized surface sample was studied. The inclusions in the fluorite are larger than those of sphalerite (of diameter  $8\mu \times 16\mu$ ) and are easily visible on the heating and cooling stage. Paragenetically the fluorite is late stage in mineral development (at the end of the sulphide phase), but the temperature and salinity data agrees well with that from the fluid inclusions in sphalerite (see Table 1).

Table 1.  
Fluid Inclusion Data

Sample No.	Freezing T°C	Homogenization T°C
48-1 (345)	-25.1	120
	-24.6	118
	-24.7	107
	-23.4	103
	-24.8	87
	-23.2	90
	-20.0	96
	-20.3	
48-1 (379.5)	-17.7	116
	-23.6	154
	-24.4	155
	-21.9	94
	-17.8	141
	-23.7	156
	-20.9	141
	-18.8	109
36-1 (54)	-25.2	134
	-17.5	82
	-14.3	80
	-18.2	140
	-18.6	151
36-8 (166)	-20.4	86
	-27.7	102
	-21.9	98
	-25.2	
	-20.1	91
	-24.8	136
	-24.7	120
	-24.8	135
	-24.7	126
	-24.7	130
B-73-5(586)	-17.5	118.
	-17.1	118
	-11.2	89
	-11.3	87
	-10.9	84
	-19.9	128
Fluorite	-16.9	135
	-17.5	136
	-18.0	134
Calcite	- 8.5	
	- .2	

Post-mineral calcite vein samples were prepared, but they were very translucent and consequently accurate results with regard to freezing experiments could not be attained. Leakage along the rhombohedral cleavage traces is believed to have caused homogenization temperature determination failures. The freezing temperature determinations indicate that the post-mineral fluids were very low in salinity (Fig. 11), approaching pure water. Leakage of groundwaters into the inclusion may explain freezing temperatures close to  $0^{\circ}\text{C}$  (Roedder, 1963).

The studied sphalerite and fluorite inclusions were of two phases, and the vapour bubble seldom exceeds a size of 4-5 volume percent. The high salinity of the inclusions necessitated supercooling to a temperature of at least  $-76^{\circ}\text{C}$  before freezing was attained. In this regard, the inclusions are similar to those of Pine Point (Roedder, 1968) and of the Polaris lead-zinc deposit (Jowett, 1975). Another similarity lies in the lack of evidence of organic matter in the inclusions, even though the Nanhani stratigraphy contains large bitumen pods, and bitumen is surficially in association with the dolomite and silica.

### C. ORE FLUID SALINITIES FROM FREEZING TEMPERATURES

Mississippi Valley type deposits are noted for their very saline brine inclusions of sodium-calcium-chloride composition. White (1968) notes in the Illinois and upper Mississippi Valley Zn-Pb district that during the fluorite and sulphide stages the salinity reaches 4 to 10 times that of sea water but declines to 3 or less times that of sea water in the post-ore stages. Due to this high salinity, difficulty is often encountered in freezing the inclusions, as mentioned earlier. Roedder (1963)

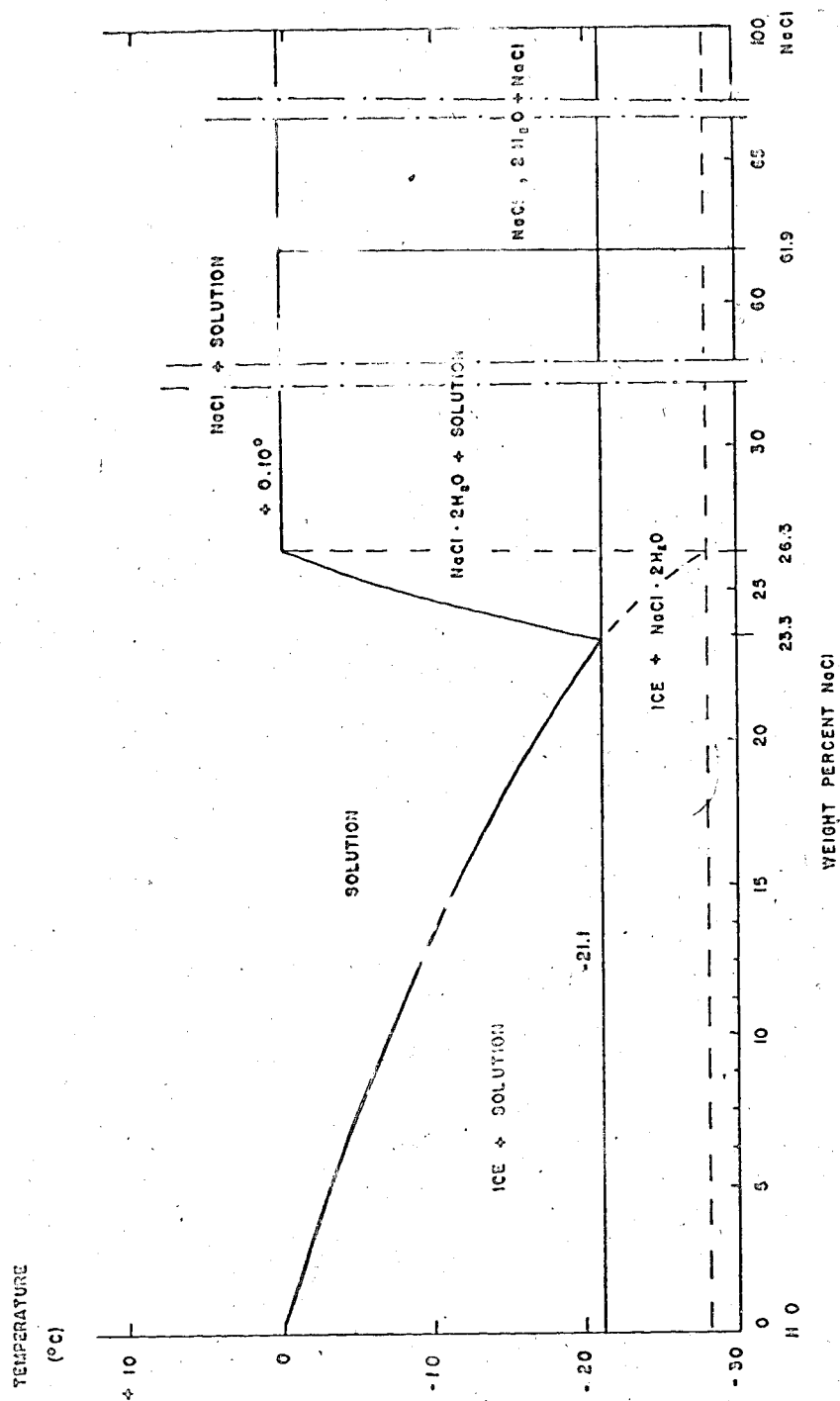


Fig. 10: H<sub>2</sub>O-NaCl phase diagram (from Roedder, 1962).

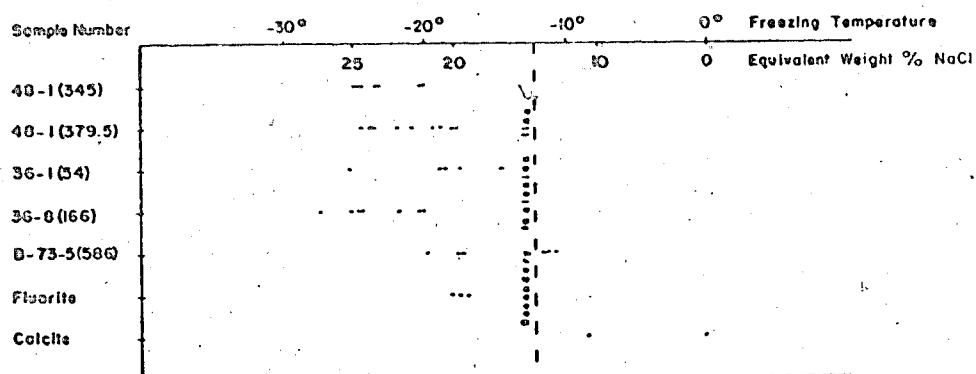


Fig. 11. Freezing temperature and equivalent weight percent NaCl of the Wrigley deposit sphalerite, fluorite and calcite fluid inclusions.

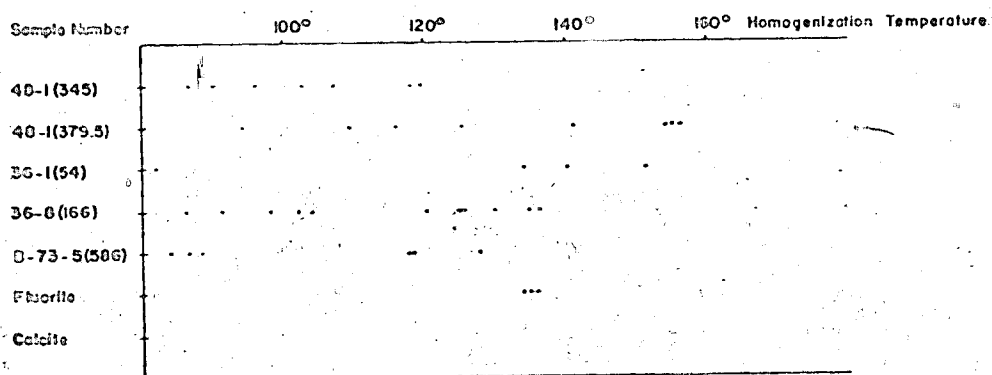


Fig. 12. Homogenization temperature of the Wrigley deposit sphalerite, fluorite fluid inclusions.



considers the necessary supercooling required to freeze the inclusions is indicative of fluids that are quite clean and 'free from suitable extraneous solid nuclei such as dirt and dust', quite unlike surface waters.

The salinity of the Wrigley sphalerite samples was determined from the experimentally derived freezing point, with reference to the  $H_2O$ -NaCl phase diagram presented by Roedder (1962) (Fig. 10). The salinity determination is based upon the premise that the only dissolved salt is sodium chloride. This premise becomes suspect when it is noted that the freezing temperatures, on the whole, fall below the minimum temperature ( $-21.1^{\circ}C$ ) obtainable with NaCl as the only solute (Roedder, 1962). Therefore, the Wrigley sphalerite inclusion fluids must contain salts other than NaCl. Roedder (1971), in an examination of southern Appalachian Valley mineral deposits, found freezing temperatures to exceed  $-28^{\circ}C$  and he concluded such depression of temperature could be explained by the presence of calcium chloride. This may explain the low freezing temperatures of the Wrigley deposit fluid inclusions.

From five sphalerite, two fluorite and one calcite sections, forty-four fluid inclusions were tested on the freezing stage (Table 1, Fig. 11). With the exception of three sphalerite inclusions of sample B-73-5 (586), the inclusions are considered to be primary or pseudo-secondary as defined by Yermakov et al. (1965). The three exceptions are thought to be secondary due to abnormally small weight percent salinities. The low salinities most likely indicate a later introduction of essentially non-saline fluids along fracture planes.

The primary and pseudo-secondary inclusions have NaCl contents in the range of 16 to 26 weight percent. The data of the inclusions are presented

in histogram form (Fig. 13), the mean salt content being 24 equivalent weight percent NaCl (excluding secondary inclusions).

#### D. ORE FLUID TEMPERATURES FROM HOMOGENIZATION TEMPERATURES

Subsequent to the freezing runs, filling (homogenization) temperatures were determined on the same inclusions. The homogenization theory is based upon the assumption that the inclusions now partly filled with a liquid phase were initially entirely filled by a single fluid phase, with no gaseous phase, representative of the ore fluid, at the time of mineralization. Upon cooling, the single fluid phase changed to a simple two-phase system of liquid and gas. The gas formed due to the phenomena of 'shrinkage'. Roedder (1967a) explains shrinkage in the following manner: "As the volume coefficient of thermal expansion for most minerals is one to three orders of magnitude lower than that for water, on cooling from the temperature of trapping to room temperature the container for the inclusion shrinks much less than the fluid inside. As soon as the pressure in the inclusion drops below the total vapour pressure of the multicomponent fluid at that temperature, at equilibrium, a bubble will nucleate and grow." Therefore, through the process of heating the inclusion until the single phase inclusion is attained, the temperature of the original ore-forming fluid will be indicated. This deductive reasoning is valid so long as the inclusion does not leak. In order to insure against a 'leaky' inclusion, following the initial heating test, the sample is cooled until the gaseous bubble reappears, of the same size as at the commencement of the experiment. Reruns of the homogenization determination on questionable inclusions is the conclusive test. Any data obtained from 'leaky' inclu-

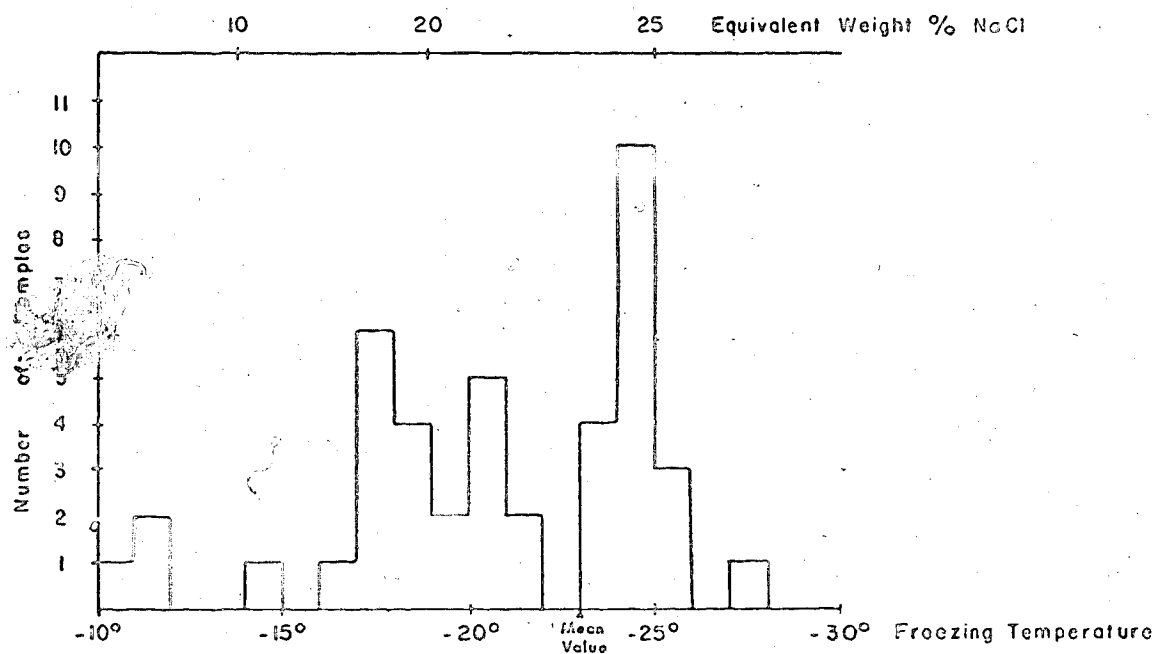


Fig. 13. Histogram of the freezing temperatures of the Wrigley deposit sphalerite and fluorite fluid inclusions.

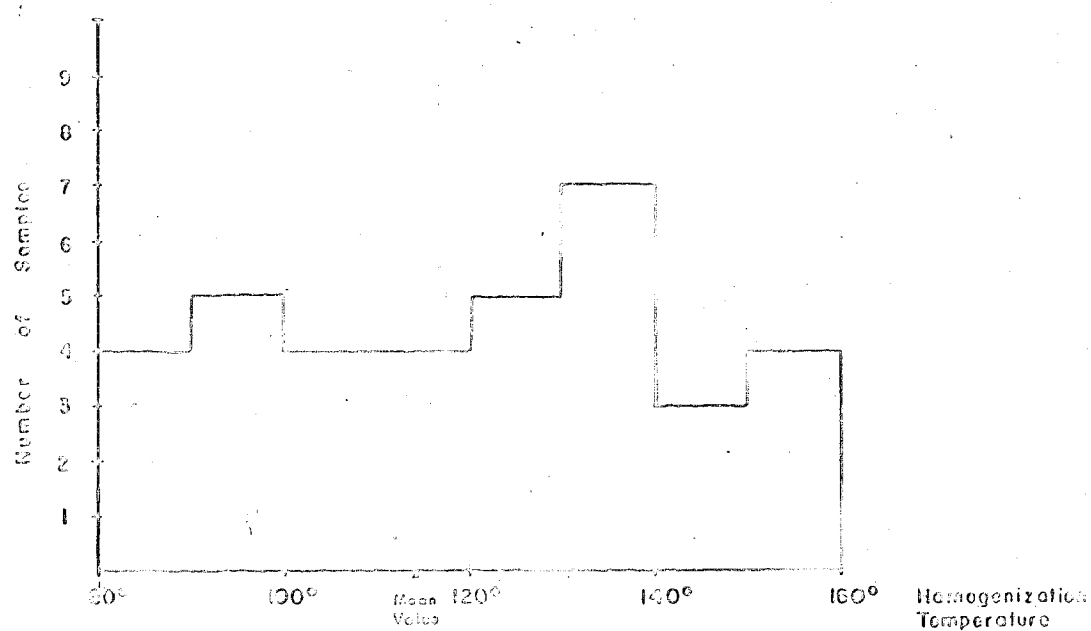


Fig. 14. Histogram of the homogenization temperatures of the Wrigley deposit sphalerite and fluorite fluid inclusions.

sions was discarded. Reruns showed accuracy to be within the range of 2 to 3°C.

Determination of the true trapping temperature of the inclusion requires a pressure correction to be taken into account. This will be considered later although the correction in the case of Wrigley samples is very small (<5°C) and could reasonably be omitted, particularly if hydrostatic pressures dominated as in open vugs, fissures, etc. (Yermakov et al., 1965).

In order to avoid temperature gradient effects, very small polished slices were used and very gradual temperature increases were maintained

to permit the equilibration of the temperature within the sphalerite and/or fluorite inclusion. Any possible errors from temperature gradients are cancelled by the poor optical quality of the sphalerite crystal, by the reduced optical resolution due to the heating stage cover glass, and by the small amount of light available through the aperture of the heating stage. To counteract this latter problem some investigators have adopted the use of flexible optics illuminators (Roedder, 1971). Such an optic illuminator did not noticeably improve the optical quality. Due to the decreased resolution, the optical uncertainty is in the range of  $\pm 2^\circ\text{C}$  as revealed in duplicate runs.

The homogenization temperatures are listed in Table 2 for sphalerite and fluorite. Tests on vein calcite were inconclusive due to leakage. The temperature distribution for sphalerite lies within the range of 80 to 156°C (excluding pressure correction, see Fig. 12). The fluorite homogenization temperatures reveal a narrower range of 134 to 136°C. The histogram (Fig. 14) illustrates the temperature distribution over the above

range with the mean at 119°C. This wide range of temperature values is characteristic of Mississippi Valley type deposits (Roedder, 1968, 1971; Jowett, 1975).

The assumed lithostatic pressure for the Wrigley sphalerite fluid inclusions is based upon an estimated depth of burial of less than 1/2 km. Considering this depth, a salinity weight percent of 16 to 26, the pressure would be in the range of 30 to 65 bars and the fluid density would be within the range of .9 to 1.02 g/cc (Haas, 1971). Using the density diagram presented by Ellis and Golding (1963) (Fig. 15), the density range for 3 molar sodium chloride solution is .97 to 1.05 g/cc. Consideration of the pressure correction diagrams presented by Lemmlein and Klevtsov (1961) (see Fig. 16) reveal that the pressure correction is less than 10°C, most likely 3-5°C. The correction factor is so small, almost within the experimental error range, that it will not be applied to the Wrigley deposit data. As mentioned earlier, the open fracture system of the deposit may have allowed hydrostatic pressures to dominate, in which case the pressure correction should be ignored.

#### E. POSSIBLE ORIGIN OF THE WRIGLEY DEPOSIT, REVEALED THROUGH FLUID INCLUSION STUDIES

The origin of the Wrigley ore deposit cannot be determined by fluid inclusion studies alone, but the mechanisms of ore deposition that could have been operative are limited by the various data. Thus the theory of origin must be compatible with the data.

The density of the brines at the time of inclusion fluid trapping ranged between 0.95 and 1.05 g/cc, which is comparable to the range of fluid densities in many Mississippi Valley type deposits. The significance

of the density lies in understanding the behavior of brines in the deposit. Roedder (1967a, 1971) considers the density in respect to the slow rate of movement of the ore-forming fluids and the ore textural developments, such as abraded sphalerite crystals and large crystal development in fissures. He contends that the density of ore-forming fluids is the most important variable in the explanation of fluid movement and ore crystal development.

Lange and Murray (in press) consider brine density in terms of the problem of moving a dense, saline, potential metal-bearing brine upward in the stratigraphy. The dense brine will not displace the overlying lighter formational fluids unless there is a mechanism to drive the hot saline brine upward. They propose a mechanism which involves two dense saline brines. The brine, possibly derived from overlying evaporite deposits, descends in the stratigraphy due to the density contrast with formational fluids. The rate of downward flow will depend upon permeability and the distance traversed will depend upon the density of the fluid encountered. The displaced fluids will represent an earlier brine, which has had time to increase in temperature and to leach metals from the surrounding rock. This metal-bearing brine could represent the potential ore-forming solution. The second downward moving saline brine is therefore the means by which the hot saline brines are moved upwards.

The Wrigley filling (homogenization) temperatures fall within the range of 80 to 156°C. According to Roedder (1967b) and White (1967, 1968), the fluid temperature range of Mississippi Valley type deposits is in the vicinity of 100-150°C but may be as low as 70°C (Wisconsin and Tri State district) or as high as 180°C (southern Illinois - Kentucky deposits). These high temperatures are difficult to reconcile with normal geothermal

gradients when depth of burial is usually less than 1,500 m, and in the case of Wrigley, is less than 900 m. Haas (1971) considered the effect of salinity on the temperature-depth relation of a brine within a hydrothermal system (vein type), open to the surface, where the hydrostatic pressure permitted boiling of the brines. From adoption of a mathematical model he was able to ascertain the minimum depth and pressure at which crystal development took place, provided the inclusion(s) of the sample indicate that boiling of the brine actually occurred. Roedder (1967a) describes this type of inclusion. The inclusion indicates boiling by the presence of 'simultaneously formed inclusions of both liquid and vapour'. This type of inclusion is identified by very minor amounts of liquid, that may be visible as a lining to the inclusion, or may not be visible. Upon freezing ice is formed. This was the case for two fluid inclusions in the Wrigley deposit (see sample 36-8 (166), Table 2).

The salinity of the sphalerite fluid inclusions varies between 16 and 26 equivalent weight percent NaCl. This saline content is comparable to that of Pine Point (Roedder, 1968) and to Mississippi Valley type deposits which frequently exceed 20 weight percent (Roedder, 1967b). This comparison may indicate that the depositing brines have comparable origins. Craig (1966) considered that the dissolution of evaporites is the reasonable explanation of highly saline brines in the Mississippi Valley type deposits, and White (1968) concurs with this hypothesis. Davidson (1966) has considered the movement and redeposition of heavy metals in sedimentary terrains, by way of chloride-rich brines derived from the solution of evaporites. This concept, although strongly questioned by Dunham (1966), has been examined further (Jackson and Beales, 1967; Billings et al., 1971), and is applicable to the Wrigley deposit.

Above 100°C in Water and in Sodium Chloride Solutions

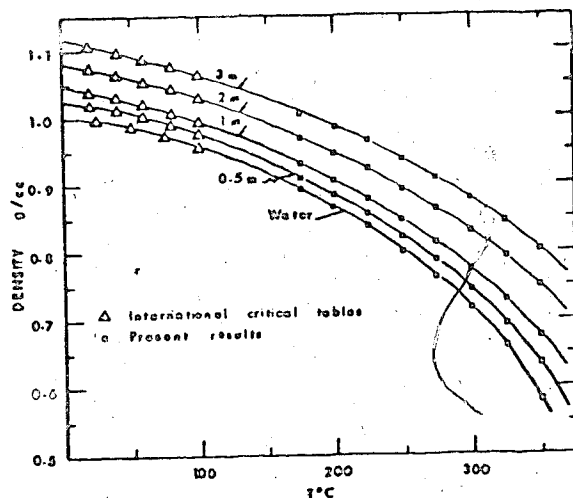


Fig. 15. The density of sodium chloride solutions for concentrations up to 3 molar and temperatures up to 350°C (from Ellis and Golding, 1963).

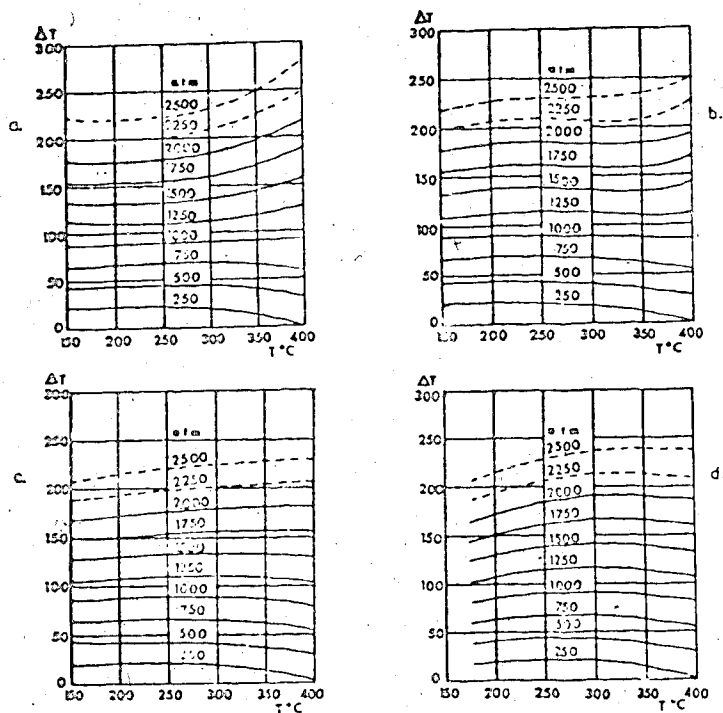


Fig. 16. Pressure corrections for homogenization temperatures: a - for 15% solution; b - for 20% solution; c - for 25% solution; d - for 30% solution of NaCl (from Lermlein and Klevtsov, 1961).



### F. CONCLUSIONS

The study of fluid inclusions within sphalerite and fluorite of the Wrigley lead-zinc deposit reveals that:

(1) The sulphide minerals crystallized from highly saline brines (Na-Ca-Cl) which had either a meteoric or connate origin, the salt most likely being derived from evaporites of the Bear Rock Formation.

(2) The pressure environment was hydrostatically controlled due to the shallow depth of the deposit and to the open-ended nature of a boiling vein-fissure fluid system.

(3) The high density of the brines is assumed to have contributed to the upward migration of the ore fluids and to the displacement of the less dense, less saline formational waters.

(4) The high salinity of the fluid inclusions implies that transport of the heavy metals was as a soluble salt, such as a chloride complex.

(5) The minimum temperature range of ore deposition was 80-156°C.

The inclusion data are, in many respects, similar to those reported from North American Mississippi Valley type deposits. The data, however, do not provide the complete answer to ore genesis. When combined with sulphur and lead isotopic data, it is hoped that greater understanding of the genesis will be attained.

## Chapter V

### SULPHUR ISOTOPE STUDIES

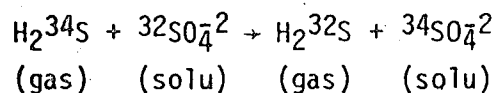
Following the work of Thode, MacNamara and Collins (1949) and of MacNamara and Thode (1950), subsequent workers have attempted to provide a greater understanding of the physio-chemical conditions of mineralization processes. Particular consideration has centered upon the source of sulphur; prominent within this area is the work of Holser and Kaplan (1966) which considered the sulphur isotopic composition of ocean sulphate through geological time, based upon evaporitic sulphur. Subsequently, Sangster (1968) related sea water sulphates ( $\delta^{34}\text{S}$ )\* to that of sedimentary and stratabound sulphide deposits, which revealed relatively constant  $\delta^{34}\text{S}$  relationships, perhaps indicative of genetic relations through bacterial reduction of sea water sulphur. Jensen and Dessau (1967), through examination of the broad variation in  $\delta^{34}\text{S}$  values of Mississippi Valley type deposits, concluded that bacteriogenic reduction of sulphur was a significant process in the genesis of such sulphide deposits. Rye and Ohmoto (1974), however, demonstrated that complete genetic hypotheses for ore deposits may not be based solely upon comparative sulphur studies. These authors showed that sulphides precipitated from magmatic sulphur, contrary to earlier theories, may have wide ranging  $\delta^{34}\text{S}$  values, whilst non-magmatic sulphur may have a narrow range near to the value for meteoritic sulphur or 'average crystal' sulphur.

These studies, considered in the geological realm, are intimately concerned with isotopic fractionation of sulphur. The studies of Thode

---

\*See Appendix II for definition of  $\delta^{34}\text{S}$ .

et al. (1954), Harrison and Thode (1958), Jensen (1958), Sakai (1957), Ault (1959), Kemp and Thode (1968), to mention a few, have increased the understanding in this area. The significance is revealed in the following general equation:



which indicates that the lighter isotope favours the sulphide species while the heavier isotope favours the sulphate. Generally one may conclude that fractionation is controlled by two processes, namely, kinetic isotopic effects and isotopic exchange equilibria. The kinetic effect is most significant in the bacteriogenic reduction of sulphate to sulphide; however, consideration of the kinetic effect must not be to the exclusion of the chemical effect as applied to the rate of the isotopic exchange reaction (Sasaki and Kajiwar, 1971).

Trudinger et al. (1972) assessed the physio-chemical limits of bacterial sulphate reduction and concluded that there are few geochemical factors which would prevent operation of the process in sedimentary environments. He considers Desulfovibrio and Desulfotomaculum to be the principal genera which convert sulphate to hydrogen sulphide gas.

The possible sources of sulphur in ore deposits are: (1) sulphate from evaporites; (2) connate-formational brine sulphate from sea water; (3) petroleum sulphur (which includes free sulphur, hydrogen sulphide, and/or organic sulphur compounds, such as thiols, or mercaptans (Levorsen, 1967)); (4) sulphide minerals in sedimentary rocks; (5) magmatic sulphur (Heyl et al., 1974). Within this frame of reference the probable source(s) of the sulphur of the Wrigley deposit will be discussed. Particular em-

phasis will be placed upon the work of Thode and Münster (1965), Holser and Kaplan (1966), Sangster (1968, 1971), Sasaki and Kajiwarra (1971), Ohmoto (1972), Robinson and Ohmoto (1973), and Rye and Ohmoto (1974).

From the sulphur isotope geothermometry based upon the work of Czamanske and Rye (1974), the sphalerite-galena sulphur isotope fractionation curve will be considered as applicable to the Wrigley deposit. The determined temperatures for sulphide deposition have been corroborated by fluid inclusion work in the style of Rye (1974).

#### A. SAMPLES USED IN THE STUDY AND RESULTS

Ten 'coexisting' galena-sphalerite pairs and two pyrite samples, representative of the Nahanni Formation sulphide vein type mineralization, were chosen for isotopic study. One sedimentary pyrite sulphur from the Hare Indian Formation was also analyzed. The diamond drill hole locations are indicated on map 1-A, and the choice of holes was based on the desire for good areal distribution. The vertical distribution was controlled by the available 'coexisting' sulphide pairs; however, where possible a distribution with respect to depth was attained.

The sphalerite-galena pairs were separated by employment of the Hallimond tube flotation system (Fuerstenau *et al.*, 1957) because the low iron sphalerite would not separate from the galena using the Franz magnetic separator (see Appendix II). The core samples from which the sulphide pairs were taken are described in Appendix I. In general, the sulphides are intimately associated with coarse-grained, white and grey dolomite and/or white calcite, with variable amounts of finely disseminated euhedral crystalline quartz. Only one sample (12-4 (255)), revealed pyrite in association with galena and sphalerite in other than a very finely disseminated state.

Table 2 summarizes the results of the sulphur determinations as  $\delta^{34}\text{S}$ . The overall  $\delta^{34}\text{S}$  per mil range (exclusive of sedimentary pyrite) is 1.5% to 16.2%. The sphalerite range is 4.1% to 16.2%, while that of galena is 1.5% to 10.1%. The mean sphalerite value is 7.5%; the mean galena value is 3.8%; the mean ore-pyrite value is 10.3%. The composite mean  $\delta^{34}\text{S}_{(\text{gn-sl})}$  value is 5.7%, and of  $\delta^{34}\text{S}_{(\text{gn-sl-py})}$  is 7.2%. The one sedimentary pyrite value is -15.7%. In all of the sphalerite-galena samples the theoretical fractionation prediction of Bachinski (1969) based on  $\delta^{34}\text{S}$  is valid, namely sphalerite > galena. The ore pyrite samples also follow the fractionation pattern with pyrite being heavier than sphalerite.

The sedimentary iron sulphide from the Hare Indian Formation formed within reducing muds and is assumed to have been subjected to the biogenic sulphide cycle through the metabolic process of sulphate reducing or dissimilatory bacteria. In order to explain the sedimentary sulphide development, Thode, Harrison and Monster (1960), in a study of recent sediments, reveal that isotope fractionation continues after burial of the sedimentary sulphide species (i.e.,  $\text{SO}_4^{2-}$ ,  $\text{S}^0$ ,  $\text{S}^{2-}$ ). The sulphur, therefore, will tend toward total fractionation or depletion of the heavy isotope. The study found that more consistent isotopic fractionation with respect to sea water exists at depths in excess of 20 feet. This progressive fractionation, leading to isotopic stability through time and burial, is likely due to bacterial reduction, and may explain the discrepancy that exists between the  $\delta^{34}\text{S}$  values of sedimentary pyrite and those of ore minerals.

#### B. SOURCE OF SULPHUR (THEORY)

Thode and Monster (1965) examined the sulphur of petroleum and evaporites, the latter representing the sulphur of ancient seas. This compari-

Table 2.

 $\delta^{34}\text{S}$  per mil Values in the Wrigley Deposit

Sample No.	Mineral	$\delta^{34}\text{S}\%$	Temperature (after Czamanske & Rye, 1974)
48-1 (61)	sp gn	+ 5.5 + 1.9	163°C
48-1 (94)	sp gn	+ 5.1 + 1.6	170°C
48-1 (375)	sp gn	+ 5.2 + 1.5	162°C
48-1 (383)	sp gn	+ 5.3 + 2.0	181°C
48-1 (445)	py	+ 5.6	
48-1 (460)	py	+15.0	
36-5 (311)	sp gn	+15.1 + 9.8	90°C
36-5 (312)	sp gn	+16.3 +10.1	65°C
12-2 (119.5)	py	-15.7	
12-4 (255)	sp gn	+ 5.0 + 2.4	240°C
12-4 (349)	sp gn	+ 8.1 + 4.5	164°C
76-1 (19)	sp gn	+ 5.4 + 2.6	232°C
B-73-5 (648)	sp gn	+ 4.2 + 2.0	293°C

Mean Values:

Galena and Sphalerite	+ 5.7 $\pm$ 4.3%
Sphalerite	+ 7.5 $\pm$ 4.4%
Galena	+ 3.8 $\pm$ 3.3%
Pyrite (excluding sed. py,gn,sp)	+10.3%
Sedimentary Pyrite	-15.7%
Temperature	176°C
$\Delta\text{sl-gn}$	3.7 $\pm$ 1.2%

Mean Values (excluding 36-5 (311 and 312)):

Sphalerite	5.5 $\pm$ 1.1%
Galena	2.3 $\pm$ 1.0%
$\Delta\text{sl-gn}$	3.2 $\pm$ 0.6%

son is valid on the basis that sulphur precipitated as gypsum from sea water will exhibit insignificant fractionation. Therefore a direct relation may be drawn between evaporites and the ancient seas with respect to geological time (Sangster, 1968). The study points to sea water sulphate of sedimentary basins as being the source of the petroleum sulphur, because of a consistent depletion of  $\delta^{34}\text{S}$  value in the amount of 15‰, which equilibrates to the expected degree of isotopic fractionation of bacterial reduction of evaporites.

Holser and Kaplan (1966) extended a part of the work of Thode and Monster (1965) by extensive examination of the sulphate of evaporites within the geological time context. The curve so developed has been substantiated by subsequent work, the most recent being Davies and Krouse (1975). The plots of the sulphur isotope composition of the Devonian seas are presented in Fig. 17.

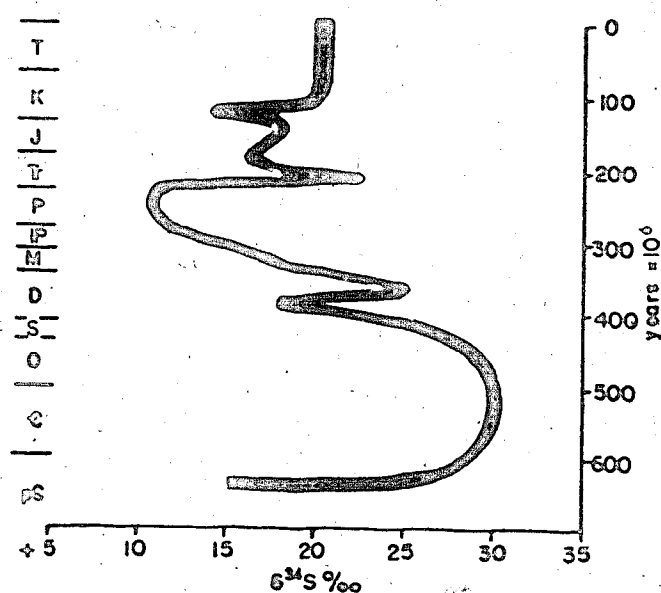


Fig. 17. The sulphur isotope age curve of Holser and Kaplan (1966).

Sangster (1968, 1971) and Sasaki and Kajiwara (1971) have (stratabound and syngenetic sulphide deposits in an attempt to prove a relationship exists between base metal sulphur and ancient sea water sulphate, through bacterial reduction of the sulphate of evaporites, as Thode and Monster (1965) illustrated with regard to petroleum sulphur. Sangster (1971) has presented his findings, which illustrate the fractionation factor through time, and this factor may be defined as  $\Delta\delta^{34}\text{S} = \delta^{34}\text{S}_{(\text{sea water})} - \delta^{34}\text{S}_{(\text{avg. sulphide deposit})}$ . Within the consideration of stratabound sulphide deposits, the volcanic type ores have an average  $\Delta\delta^{34}\text{S}$  value of 17.3%, whereas the stratiform sedimentary type ores average  $\Delta\delta^{34}\text{S}$  value of 13.6%. Sasaki and Kajiwara (1971) tested the average values determined by Sangster (1968) with respect to Kuroko type ores by relating the  $\Delta\delta^{34}\text{S}$  value to the isotopic equilibrium temperatures. Temperature discrepancy motivated the examination of frequency diagrams and employment of the 'minimum'  $\delta^{34}\text{S}$  sulphide average value was found to provide greater accuracy. The significance of the 'minimum' value is related to the lack of sulphur equilibrium attainment within the deposit, which in turn is related to the generally slow rate of the isotopic exchange reaction relative to mineral crystallization (Sasaki and Kajiwara, 1971).

Both Sangster (1968, 1971) and Sasaki and Kajiwara (1971) agree that the relation of the sulphide of the two classes of deposits and sulphates of sea water, considered in the geological context, indicate that the sulphur of the sulphide ores originated from bacterially reduced sea water sulphate.

Ohmoto (1972) and Rye and Ohmoto (1974) consider that minerals from hydrothermal systems of 'low temperature', such as Mississippi Valley type



deposits which may reveal considerable variation in  $\delta^{34}\text{S}$ , are not easily categorized within the realms of magmatic hydrothermal or sedimentary, nor do they completely equate to what is considered sulphur of true anaerobic bacterial origin. Consideration of the variations of  $\delta^{34}\text{S}$ , therefore, is developed in the context of control of the chemistry of the ore solutions on sulphur isotope composition of sulphide minerals. This approach varies from Jensen and Dessau (1967) who define magmatic hydrothermal deposits as those having a narrow  $\delta^{34}\text{S}$  value distribution very close to 0, and deposits of bacteriogenic origin as exhibiting a wide spread in  $\delta^{34}\text{S}$  values that indicate increased concentration in the lighter isotope with reference to sea water sulphate.

From the above discussion it is apparent that there are various approaches to analyzing sulphur isotope data in an attempt to determine the source of the sulphur of an ore deposit. In the following sections of this chapter, the Wrigley deposit sulphur will be considered relative to sea water sulphate and to the chemical control of ore solutions.

#### C. CONSIDERATION OF THE WRIGLEY SULPHIDE SULPHUR AND THE DEVONIAN SEA WATER SULPHATE

The northern Camsell Range is primarily Devonian in age. Stratigraphically equivalent to the Landry, Manetoe, Arnica and Funeral formations complex is the Bear Rock Formation, which, in the Interior Plains, is equivalent to the Lower Chinchaga evaporites (Law, 1971). The Bear Rock Formation, comprised of anhydrite, dolomite (with some silicification), minor limestone and shale, represents a probable source for the Wrigley sulphide sulphur.

In order to compare Middle Devonian sea water sulphate with the sulphides of the Wrigley deposit it is necessary to ascertain the  $\delta^{34}\text{S}$  value of the Bear Rock evaporites. No samples of the evaporites were experimentally run by the writer; however, extensive work has been done on evaporites of Middle Devonian age (Fig. 17) which permits relatively accurate estimation of the  $\delta^{34}\text{S}$  value. Middle Devonian evaporites of the Elk Point Basin of the Pine Point area, N.W.T., range from 18.5‰ to 19.8‰ with an average of 19.1‰ (Sasaki and Krouse, 1969). Holsen and Kaplan (1966) indicate that the Middle Devonian evaporites range from 16‰ to 22‰, while the Lower-Middle Devonian is within the area of 19.5‰. In the Arctic Archipelago, Davies and Krouse (1975) have noted the  $\delta^{34}\text{S}$  value of Middle Devonian evaporites of the Blue Fiord Formation to be 19.0‰ while Early Devonian sulphate is recorded as 19.2‰. From these sulphate  $\delta^{34}\text{S}$  values it is within reason to consider the Middle Devonian evaporite sulphate of the Bear Rock Formation would have a  $\delta^{34}\text{S}$  value of approximately 19.0‰.

Following the approach of Sangster (1968, 1971) and Sasaki and Kajiwara (1971), using the minimum average  $\delta^{34}\text{S}$  value of the Wrigley deposit (3.6‰) (see Fig. 18) with the estimated Middle Devonian sea water sulphate (19.0‰), the  $\Delta\delta^{34}\text{S}$  value is 15.4‰. This value is slightly lower than the average volcanic stratabound sulphide deposit  $\Delta\delta^{34}\text{S}$  value of 17.3‰ determined by Sangster (1971) and slightly higher than his sedimentary sulphide ore average of 13.6‰.

In order to explain the variance in fractionation (larger fractionation revealed in larger  $\Delta\delta^{34}\text{S}$ ), consideration must be given to the bacterial metabolic rate in sulphate reduction. Within a volcanic stratabound sulphide environment bacterial metabolism would be reduced resulting in a

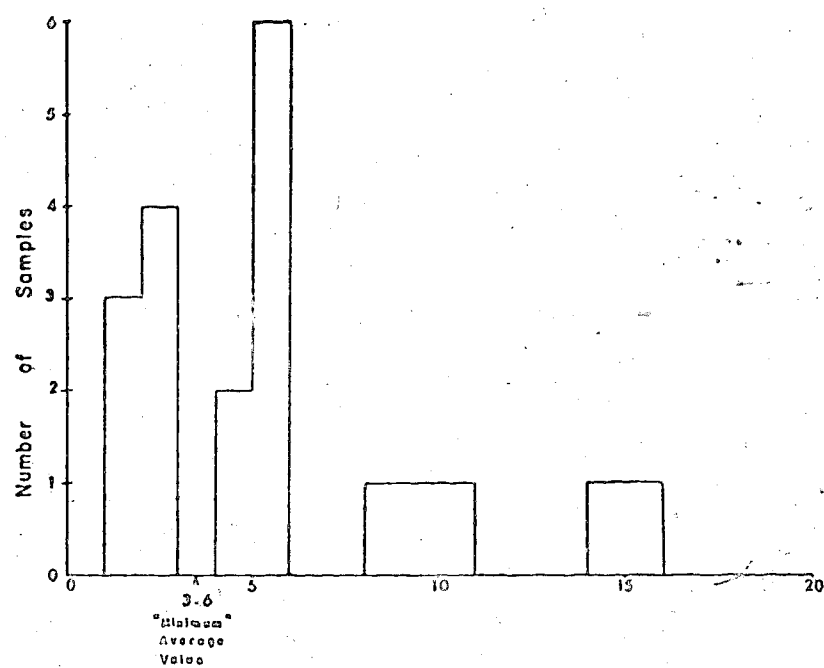


Fig. 18. Histogram of the sphalerite-galena  $\delta^{34}\text{S}$  values, Wrigley property.

higher  $\Delta\delta^{34}\text{S}$  value, while the reverse would occur in a sedimentary environment because of an increase in organic nutrient. On this basis, the degree of bacterial nutrition and thus the degree of fractionation within the Wrigley area is equivalent to neither the volcanic environment nor to the sedimentary environment. Considered within the concept of 'open and closed' environments (Schwartz and Burnie, 1973) the Wrigley deposit may be designated 'closed'. As sulphur reduction proceeds due to bacterial processes, the  $\delta^{34}\text{S}$  value of the residual sulphate in the environment increases, and each successive aliquot is heavier than the previous one. The resultant  $\delta^{34}\text{S}$  distribution, developed over a range, would center around zero and range up to  $\delta^{34}\text{S}_{\text{sw}}$ . In this way the fractionation pattern may in part be explained. Sasaki and Kajiwara (1971) consider that isotopic variation may be explained by non-direct isotopic exchange between sulphate and sulphide. It represents the exchange equilibrium between  $\text{SO}_4^{2-}$  and some intermediate form from which sulphides might have formed with little isotopic fractionation. Alternatively, a more plausible explanation is that 'the observed fractionation is the relic of the equilibrium at higher temperatures' (Sasaki and Kajiwara (1971)).

#### D. TO TEST THE VALIDITY OF $\Delta\delta^{34}\text{S}$

Should chemical and isotopic equilibrium among sulphur species in solutions and in precipitating mineral phases be attained, then the isotopic difference ( $\Delta$ ) should be closely related to the isotopic equilibrium temperature. Sasaki and Kajiwara (1971) used this basis to consider the findings of Sangster (1968) with respect to Kuroko-type deposits. In a similar fashion the Wrigley deposit may be considered. Using the

value ( $\Delta\delta^{34}\text{S}$ ) of 15.4%, based upon the assumption that this value represents the isotopic exchange equilibrium reaction between  $\text{SO}_4^{2-}$  and  $\text{H}_2\text{S}$  (or pyrite), a temperature slightly greater than  $400^\circ\text{C}$  is attained (Rye and Ohmoto, 1974). This temperature does not agree with the temperatures determined by way of sulphur geothermometry or by fluid inclusion filling temperatures. Therefore, equilibrium conditions with respect to isotopic exchange ( $\text{SO}_4^{2-} - \text{H}_2\text{S}$ ) was not attained.

The Hare Indian pyrite considered in this manner reveals that chemical and isotopic equilibrium was attained for the sedimentary pyrite. The Early Givetian pyrite  $\delta^{34}\text{S}$  value is -15.7% and the sea water sulphate value, as chosen for the Eifelian Bear Rock evaporites, is 19.0%. Therefore, the  $\delta^{34}\text{S}$  value is 34.7%, and the inferred temperature (Rye and Ohmoto, 1974) is approximately  $170^\circ\text{C}$ . This temperature is in line with the average  $\delta^{34}\text{S}_{(\text{sl-gn})}$  temperature of  $176^\circ\text{C}$ , and is slightly higher than the range of temperatures determined from fluid inclusions ( $80\text{--}156^\circ\text{C}$ ).

Consequently, the lack of isotopic equilibrium of the ore sulphides might be attributed to retarded isotopic exchange with respect to the mineralization process, which involves the rates of deposition and cooling of sulphides in the ore forming process. The previously considered possible causes of variance in fractionation, however, cannot be disregarded.

#### E. CONSIDERATION OF THE CONTROL OF THE CHEMISTRY OF THE ORE SOLUTIONS

Rye and Ohmoto (1974) consider the variations of  $\delta^{34}\text{S}$  values in the context of control of the chemistry of the ore solutions on sulphur isotopic composition of sulphide minerals. The sulphur isotopic composition of precipitating sulphide mineral phases from ore solution is controlled by the following conditions:

- (1) the total sulphur isotopic composition ( $\delta^{34}\text{S}_{\Sigma\text{S}}$ ) of the fluids, which directly relates to the origin of the sulphur;
- (2) the relative abundance of the oxidized and reduced sulphur species in solution, ( $\text{H}_2\text{S}$ ,  $\text{HS}^-$ ,  $\text{S}^{2-}$ ,  $\text{SO}_4^{2-}$ ,  $\text{HSO}_4^-$ , and  $\text{NaSO}_4^-$ );
- (3) the relative amount of isotopic equilibrium;
- (4) the isotopic fractionation factors relative to the aqueous sulphur species and the precipitating mineral phase (Ohmoto, 1972).

Therefore, the proportion of sulphur species in ore fluids may be evaluated in terms of  $T^\circ$ , pH, and  $f_{\text{O}_2}$  of hydrothermal fluids, which in turn permits evaluation of  $\delta^{34}\text{S}$  values of minerals in the same terms, based upon the assumption that the sulphur species in solutions and precipitating mineral phases are in chemical and isotopic equilibrium (Rye and Ohmoto, 1974). This therefore implies that the  $\delta^{34}\text{S}$  values respond to changes in the chemical environment of ore deposition. This may not be the case, however, in bacteriogenic deposits which are identified by way of sulphur isotope disequilibrium. The probability of sulphur isotope disequilibrium with respect to sulphur species in solution and the precipitating mineral phases in the Wrigley deposit has been implied in the previous section, by reason of the large difference in  $\delta^{34}\text{S}$  values of ore pyrite and of sedimentary pyrite (see Table 2). Rye and Ohmoto (1974) consider that 'in surficial, low temperature environments the only known means of reducing sulphate to  $\text{H}_2\text{S}$  and precipitating sulphides is by the life processes of sulphur reducing bacteria'. They add that deep circulation of sea water or saline brines into high temperature regions may result in inorganic reduction of the sulphate. In order to evade speculation, consideration of the chemical nature of ore-forming solutions and the sulphur isotopic composition of hydrothermal minerals, based upon the assumption that isotopic equilibrium is established between the sulphur species  $\text{H}_2\text{S} - \text{SO}_4^{2-}$ , will follow.

Consider a hypothetical ore-forming fluid composed of two sulphur species,  $\text{H}_2\text{S}$  (aq) and  $\text{SO}_4^{2-}$ , in which  $\delta^{34}\text{S}_{\Sigma\text{S}} = 20\%$ , and in which the sphalerite precipitates from the fluid at  $175^\circ\text{C}$ . The temperature chosen is the Wrigley mean, and remains constant since it controls the differences in the  $\delta^{34}\text{S}$  value among the sulphur species. Under these conditions, when isotopic equilibrium is established  $\Delta\delta^{34}\text{S}_{\text{SO}_4^{2-} - \text{H}_2\text{S}} = 35\%$ , and  $\Delta\delta^{34}\text{S}_{\text{H}_2\text{S} - \text{ZnS}} = 1.5\%$ , at  $175^\circ\text{C}$ . Should the two sulphur species be equally abundant, then the  $\delta^{34}\text{S}$  values are  $\delta^{34}\text{S}_{\text{H}_2\text{S}} = -7.5\%$  and  $\delta^{34}\text{S}_{\text{SO}_4^{2-}} = +27.5\%$  (see Fig. 19). However, should the  $\text{H}_2\text{S}$  species predominate in the fluid, then the  $\delta^{34}\text{S}_{\text{H}_2\text{S}}$  will approach  $0\%$ , and  $\delta^{34}\text{S}_{\text{SO}_4^{2-}}$  will approach  $+35\%$ . It is only in the case where  $\text{H}_2\text{S}$  predominates in the fluid that  $\delta^{34}\text{S}_{\text{ZnS}}$  approaches a positive value.

PbS	ZnS	$\text{H}_2\text{S}$	$\text{SO}_4^{2-}$	$\delta^{34}\text{S}$			
3.7	1.5	35					
Ratio							
$\text{H}_2\text{S} : \text{SO}_4^{2-}$				$\text{H}_2\text{S}$	$\text{SO}_4^{2-}$	ZnS	PbS
.1 : .9				-31.5	+ 3.5	-32.0	-36.7
$\Sigma\text{S} = 20\%$ .5 : .5				- 7.5	+27.5	- 9.0	-12.7
.9 : .1				- 3.5	+31.5	- 5.0	- 8.7

Fig. 19. Variation of  $\delta^{34}\text{S}$  of sulphate (iron or mineral),  $\text{H}_2\text{S}$ , and sulphide minerals with variation in  $\text{H}_2\text{S}/\text{SO}_4^{2-}$  of the hydrothermal solution at  $T = 175^\circ\text{C}$ ,  $\delta^{34}\text{S}_{\Sigma\text{S}} = 20\%$ , (varied after Rye and Ohmoto, 1974).

Considered in the realm of the Wrigley hydrothermal fluids, to obtain a mean  $\delta^{34}\text{S}_{\text{ZnS}}$  of  $+7.5 \pm 4.4\%$ , and  $\delta^{34}\text{S}_{\text{PbS}}$  of  $+3.8 \pm 3.3\%$ , the ratio of  $\delta^{34}\text{S}_{\text{H}_2\text{S}}$  to  $\delta^{34}\text{S}_{\text{SO}_4^{2-}}$  must have been very high or sulphur isotope disequilibrium must have existed due to bacteriogenic reduction of sulphate, or both.

In actual situations the aqueous sulphur species present in the ore solutions include such species as  $\text{HS}^-$ ,  $\text{S}^{2-}$ ,  $\text{SO}_4^{2-}$ ,  $\text{HSO}_4^-$ , and  $\text{NaSO}_4^-$ , and they also must be considered. Ohmoto (1972) has shown that the various species of sulphur may be determined as functions of  $f_{\text{O}_2}$  and pH along with alkali concentration. Similarly changes in the  $\delta^{34}\text{S}$  values of the sulphide species may be determined.

Figure 20 reveals the changes in  $\delta^{34}\text{S}_{\text{ZnS}}$  along with stability boundaries of Fe-S-O minerals at  $\Sigma\text{S} = 0.001$  moles/kg  $\text{H}_2\text{O}$  and of calcite and graphite at  $\Sigma\text{C} = 0.1$  moles/kg  $\text{H}_2\text{O}$ . Sphalerite of various  $\delta^{34}\text{S}$  values would precipitate in chemical and isotopic equilibrium with solutions of ionic strength 1,  $\delta^{34}\text{S}_{\Sigma\text{S}}$  value of 20‰ and temperature of  $150^\circ\text{C}$ . It should be noted that the ore-forming fluid ionic strength of 1 has been adopted, although  $I = 3$  would be correct, because the variation in shape and position of the iso- $\delta^{34}\text{S}$  line is minor ( $< 0.3 \log f_{\text{O}_2}$  units) within the ionic strength range of .5-3 (Ohmoto, 1972).

Due to the fact that the  $\delta^{34}\text{S}$  values of minerals depends primarily upon  $\delta^{34}\text{S}_{\Sigma\text{S}}$ , pH,  $f_{\text{O}_2}$  and  $T^\circ$ , knowledge of the paragenetic sequence of the deposit (see Fig. 7) and the position of the stability boundaries (Fig. 20) of Fe-S-O minerals, calcite and carbon permits estimation of the maximum pH which prevailed at the time of ore deposition. From the pH and the experimentally determined  $\delta^{34}\text{S}_{\text{ZnS}}$  the approximate range in  $f_{\text{O}_2}$  that prevailed at the time of ore deposition may be ascertained. Consequently, the fugacity of oxygen in the mineralizing fluids at the time of deposition of sulphides in the Nahanni limestone was -44.8 to -46.9, which corresponds to  $f_{\text{CO}_2}$  of about 5 atmospheres (Robinson, 1971), at  $150^\circ\text{C}$ . The fluid pH was likely held in the vicinity of pH 5.8 due to the buffer effect of the carbonates (Robinson, 1971).



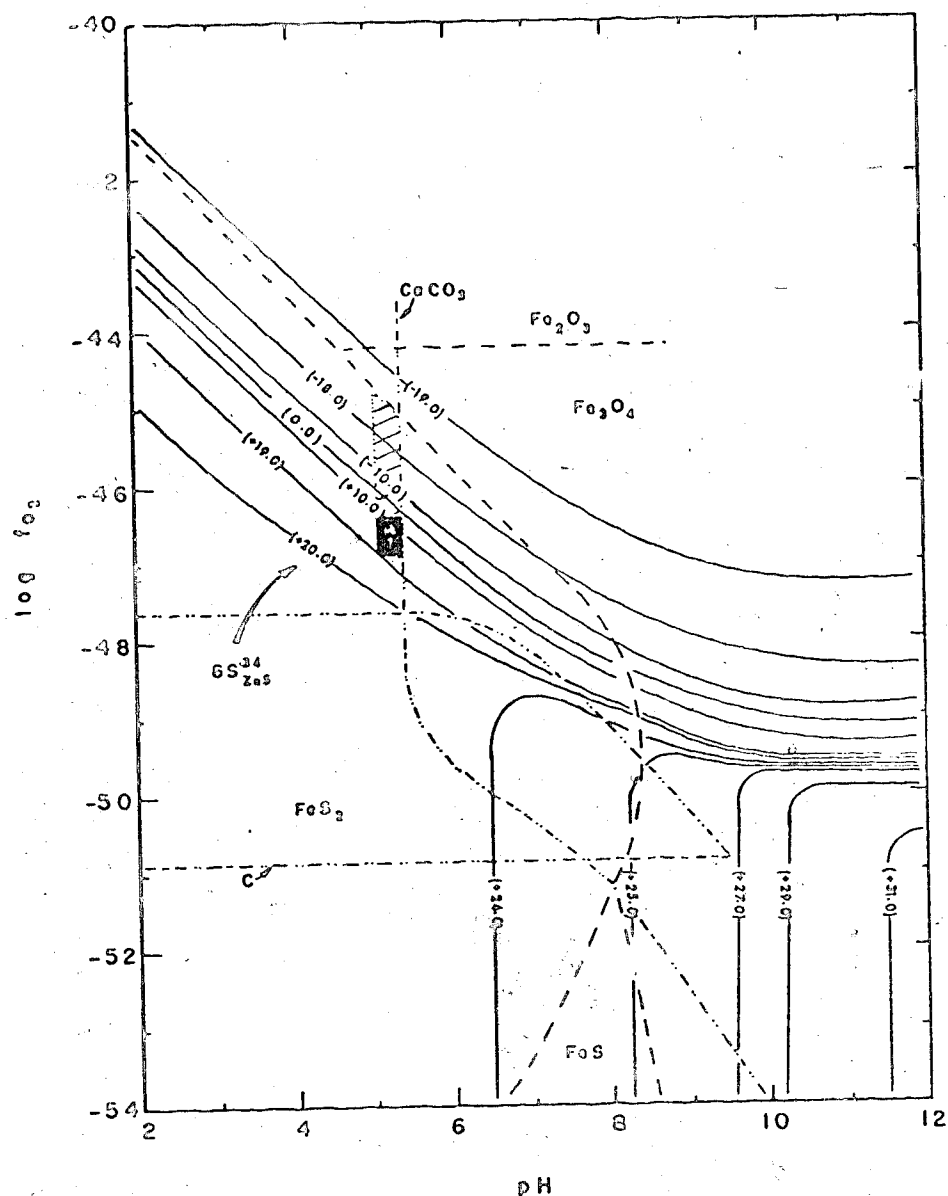


Fig. 20. Comparison of the positions of  $\delta^{34}\text{S}$  contours with the stability fields of Fe-S-O minerals, calcite and graphite.  $T = 150^\circ\text{C}$  and  $I = 1.0$ .

—:  $\delta^{34}\text{S}$  contours.      in ( ) are for ZnS at  $\delta^{34}\text{S}_{\text{Fe}} = 20\%$ .  
 - - - - -: Fe-S-O mineral stability fields at  $x_s = 0.001$  moles/kg  $\text{H}_2\text{O}$ .  
 . . . . .: Stability boundaries for calcite and graphite at  $x_c = 0.1$  moles/kg  $\text{H}_2\text{O}$ .  
 Dark shaded areas =  $\delta^{34}\text{S}$  sulphur range for Wrigley sulphides.  
 (adapted from Ohmoto, Figs. 6 and 12, 1972).

The indicated chemical environment of the ore fluids (shaded area, Fig. 20) signifies that the sulphides precipitated over the  $f_{O_2}$  range of -44.8 to -46.9 at pH of about 5.5, with a  $\delta^{34}S$  value range of about -18.5 to +16%. This, however, is not the case. The Wrigley  $\delta^{34}S$  values (dark shade, Fig. 20) show a relatively narrow range, with an average of  $5.7 \pm 4.3\%$ . This signifies that the  $\delta^{34}S$  values of the Wrigley deposit did not respond to changes in the chemical environment of deposition. This situation finds parallels in that of the Creede deposit, Colorado (Rye and Ohmoto, 1974). This expression of disequilibrium with respect to isotopic exchange ( $H_2S-SO_4^{2-}$ ), indicative of a bacteriogenic derivation of reduced sulphur, corroborates the previous illustration of how sulphur isotopic compositions of precipitating mineral phases are affected by the chemistry of ore fluids.

Due to the apparent disequilibrium and to the lack of sulphate (i.e. barite, gypsum) it is not possible to determine the total sulphur composition or the relative abundance of the sulphur species. Rye and Ohmoto (1974) state that "the  $\delta^{34}S$  values of bacteriogenic deposits should not be amenable to the type of approach we have discussed for the hydrothermal deposits because kinetic factors are always involved in the bacteriogenic reduction of sea water sulphate".

#### F. CONCLUSION

The Wrigley sulphur is chemically and isotopically in disequilibrium, and appears to indicate a sulphur derived bacteriogenically from reduced sea water (evaporite) sulphate. The derived hydrogen sulphide was transported by meteoric or connate waters, and represents an independent source to that of the heavy metals (Jackson and Beales, 1967).

The Wrigley sulphides are very similar to sulphides from Mississippi Valley type deposits. The variations in the  $\delta$  sulphur values for the deposits within this class are thought to be due to isotopic disequilibrium brought about by variation in the bacterial metabolic rate and by slow isotopic exchange reaction rates during ore deposition in a 'closed' system.

#### G. SULPHUR GEOTHERMOMETRY

Czamanske and Rye (1974) experimentally determined sulphur isotope fractionation between sphalerite and galena, the results were subsequently checked by Rye (1974) by comparison with filling temperatures of sphalerite fluid inclusions. Since this cross-check was positive, the experimental linear function ( $1000 \ln_{\alpha_{\text{S1-gn}}} = 7.0 \times 10^5 T^{-2}$ ) has been adopted for temperature determination of Wrigley sphalerite-galena pairs, in preference to similar functions proposed by Kajiwara and Krouse (1971) and Grootenboer and Schwarcz (1969).

The calculated temperatures of equilibration determined from  $\delta^{34}\text{S}$  values are listed in Table 2. The temperatures range from a low of 65°C to a high of 293°C. However, the majority of temperatures lie within the range of 162-240°C. The large spread in temperature may be explained by the isotopic state of disequilibrium assumed for the deposit.

## Chapter VI

### LEAD ISOTOPE STUDIES

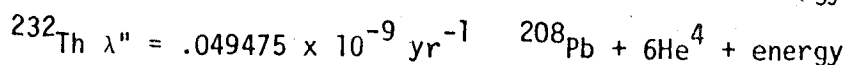
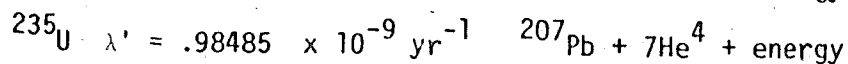
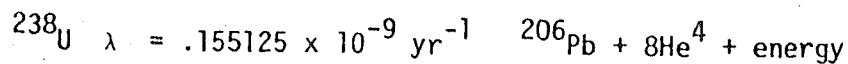
Lead isotope theory is concerned with the physical and chemical properties of the earth's mantle-crust system, with respect to isotopic variations of the elements uranium, thorium and lead. The lead isotopes,  $^{206}\text{Pb}$ ,  $^{207}\text{Pb}$ ,  $^{208}\text{Pb}$ , are radioactive daughter products of  $^{238}\text{U}$ ,  $^{235}\text{U}$  and  $^{232}\text{Th}$ , respectively. Due to the relationship of the parent to the daughter nuclide, dates may be arrived at from the following ratios:  $^{238}\text{U}/^{206}\text{Pb}$ ,  $^{235}\text{U}/^{207}\text{Pb}$ ,  $^{232}\text{Th}/^{208}\text{Pb}$  and/or  $^{207}\text{Pb}/^{206}\text{Pb}$  for a U-Th mineral. These methods, which have been considered by Baadsgaard (1964), are not applicable to sulphide ores (i.e. galena, etc.) because ore-lead seldom contains more than trace amounts of uranium and thorium. Consequently, the dating of ore-lead depends upon a definite model, based upon assumptions to explain the genesis of the lead-bearing ore and the variations in lead isotopic composition over geological time. The  $^{207}\text{Pb}/^{204}\text{Pb}$  vs  $^{206}\text{Pb}/^{204}\text{Pb}$  compositional diagram is used and the validity of the 'age' depends upon the degree to which the sample satisfies the assumptions of the model.

The theory and models of common lead dating will be considered briefly and the experimental data can be made to yield data on the age and source of the metals.

#### A. THEORY OF LEAD DATING

The calculation of model lead dates depends upon the mathematical model which considers the isotopic composition of the lead. The isotopes

(except  $^{204}\text{Pb}$ ) have changed over geologic time due to the radioactive decay of uranium and thorium. Therefore the model lead interpretive theory centers on the lead isotopes  $^{206}\text{Pb}$ ,  $^{207}\text{Pb}$ , and  $^{208}\text{Pb}$  which have evolved by the radioactive breakdown of the parent nuclei to produce the daughter stable isotopes. The system may be portrayed as follows:



The non-radiogenic ( $^{204}\text{Pb}$ ) lead isotope has an absolute abundance which does not vary with time due to radioactive processes.

At time  $t_0$  when the earth formed, the terrestrial lead was homogeneous, the isotopic ratios throughout being  $a_0$ ,  $b_0$ ,  $c_0$ . Within the homogeneous closed system the alteration of ratios is through the addition of radiogenic lead from uranium and thorium. At some time  $t_1$  an event transpired which released lead from the original U-Th-Pb system. Subsequent to time  $t_1$  the lead is free of U and Th, so the isotopic composition of the lead remains constant until the present ( $t=0$ ). Therefore, the isotopic composition of the lead ( $t=0$ ) reflects that of the lead source at time ( $t_1$ ). Chemically the isotopes are identical.

From these assumptions of a single stage model a mathematical derivation of the model age is possible. Because radiogenic lead was formed from time ( $t_0$ ) until time ( $t_1$ ), then the growth equation may be expressed in the form

$$N = N_0 \exp \lambda t \quad (1)$$

where  $N$  is the number of atoms of the isotope present at time  $t_1$ .  $N_0$  represents the number of atoms at the present time  $t=0$  (time is measured positively into the past).

From this expression the number of atoms of a particular isotope may be derived for time  $t_1$ , such as  $\text{Pb}^{206}$ :

$$N(^{206}\text{Pb})_{t_1} = N(^{206}\text{Pb})_{t_0} + N(^{238}\text{U})_{t_0} - N(^{238}\text{U})_{t_1} \quad (2)$$

Placed in the context of  $^{204}\text{Pb}$ , and adopting the symbols defined in Table 3, the equation becomes:

$$x_1 = a_0 + u_1(\exp \lambda t_0 - \exp \lambda t_1) \quad (3)$$

Similar equations for  $^{207}\text{Pb}$  and  $^{208}\text{Pb}$  may be generated:

$$y_1 = b_0 + \frac{u_1}{\alpha} (\exp \lambda' t_0 - \exp \lambda' t_1) \quad (4)$$

$$z_1 = c_0 + w_1 (\exp \lambda'' t_0 - \exp \lambda'' t_1) \quad (5)$$

These equations define the growth curve for ordinary leads.

The definition of the various classifications of lead follows.

Common lead is comprised of primeval lead (which represents the isotopic composition of the lead at the time the earth was formed) and radiogenic lead (which has formed since the origin of the earth from the decay of uranium and thorium). From this basis two general categories of lead have been defined, namely 'ordinary' and 'anomalous' lead.

(1) 'Ordinary' lead is considered to have developed in a unique U-Th-Pb system subsequent to the formation of the earth and prior to the time of mineralization. The isotopic data when plotted  $^{207}\text{Pb}/^{204}\text{Pb}$  against  $^{206}\text{Pb}/^{204}\text{Pb}$  fit the growth curve (Cooper *et al.*, 1969; Stacey and Kramers, 1975; Cumming and Richards, 1975).

(2) 'Anomalous' lead is considered to have developed in more than one U-Th-Pb system (Kanasewich, 1968a) thereby representing multi-stage lead. These leads commonly show a linear trend when plotted on the  $^{207}\text{Pb}/^{204}\text{Pb}$  vs  $^{206}\text{Pb}/^{204}\text{Pb}$  ratio diagram.

Table 3.  
Lead Isotope Symbols and Constants

Isotope Ratios	Present $t=0$	Time $t_1$	Primeval $t_0$
$^{206}\text{Pb}/^{204}\text{Pb}$	$a$	$x$	$a_0$
$^{207}\text{Pb}/^{204}\text{Pb}$	$b$	$y$	$b_0$
$^{208}\text{Pb}/^{204}\text{Pb}$	$c$	$z$	$c_0$
$^{238}\text{U}/^{235}\text{U}$	$\alpha$		
$^{238}\text{U}/^{204}\text{Pb}$	$\mu$	$\mu e^{\lambda t_1}$	$\mu e^{\lambda t_0}$
$^{235}\text{U}/^{204}\text{Pb}$	$v$	$v \lambda' t$	$v e^{\lambda' t_0}$
$^{232}\text{Th}/^{204}\text{Pb}$	$\omega$	$\omega e^{\lambda'' t}$	$\omega e^{\lambda'' t_0}$

Parameters used in this paper (taken from Cumming and Richards, 1975):

Decay Constants	Nuclide	Symbol
$0.155125 \times 10^{-9} \text{ yr}^{-1}$	$^{238}\text{U}$	$\lambda$
$0.98485 \times 10^{-9} \text{ yr}^{-1}$	$^{235}\text{U}$	$\lambda'$
$0.049475 \times 10^{-9} \text{ yr}^{-1}$	$^{232}\text{Th}$	$\lambda''$

$$\alpha = 137.88$$

### B. AGE OF THE EARTH

In lead-lead model age dating, the age of the earth is significant although not all models demand the age be known. From the age of the earth and the theory of the growth curve, it is possible to ascertain the parameters  $a_0$ ,  $b_0$ ,  $c_0$ .

Lord Rayleigh made preliminary age estimations of the earth from U-Pb and He-U ages, determining a figure of 2.0 b.y. It was not until the work of Gerling (1942), Holmes (1946) and Houtermans (1946) that the age of the earth was determined using lead isotopes of lead-bearing minerals. The relationship of the age to the mineralization of time  $t_1$  was the slope of the isochron on which the measured isotopic ratios fell. The validity of this approach has been questioned. Subsequent work related meteorite isotope results to terrestrial determinations. This approach is based upon the partition at a single instant of a chemical system into isolated parts with different U/Pb ratios which would result in the production of a series of leads whose isotope ratios would be linearly related. Therefore, a  $^{207}\text{Pb}/^{204}\text{Pb}$  vs  $^{206}\text{Pb}/^{204}\text{Pb}$  ratio plot would yield a straight line of slope determined by the isotope values of the time of separation of the respective closed systems, and thereby be related to the age of the earth. Meteorites, which are assumed to represent developmental stages of our solar system, provide the necessary linear array (meteoritic isochron) from which to calculate the age. It should be noted that the meteorite lead isotope ratios are considered to have developed from time  $t_0$ , in a closed system, and are therefore related to the parameters  $a_0$ ,  $b_0$ ,  $c_0$ .



From this basis Patterson (1955, 1956) estimated the age of the earth to be 4.55 b.y. He considers the Canyon Diablo meteorite lead to be of primeval composition, due to the minor amount of uranium present and thus negligible radiogenic lead production. The lead ratios of the primeval lead are:

$$^{206}\text{Pb}/^{204}\text{Pb} = 9.46 = a_0$$

$$^{207}\text{Pb}/^{204}\text{Pb} = 10.34 = b_0$$

$$^{208}\text{Pb}/^{204}\text{Pb} = 20.44 = c_0$$

as determined by Patterson.

Subsequent workers have varied the values of  $a_0$ ,  $b_0$ ,  $c_0$  and  $t_0$  but the method of derivation has remained consistent. Cooper et al. (1969) proposed a time  $t_0$  of 4.578 b.y., using more accurately defined growth curve parameters (Oversby, 1970).

Further accuracy in the determination of the isotopic composition of Canyon Diablo triolite lead (Tatsumoto et al., 1973) provide new values which are:  $a_0 = 9.307$ ,  $b_0 = 10.294$ ,  $c_0 = 29.476$  and  $t_0 = 4.57$  b.y. These parameters have been adopted by Stacey and Kramers (1975) and by Cumming and Richards (1975) in their respective models for terrestrial lead isotope evolution.

### C. CONSIDERATION OF THEORETICAL MODELS

Within the above context various theoretical lead models have been proposed. The change in ideas has centered around the interpretation of the U-Pb system, with respect to the amount of radiogenic parent in the system at some time  $t$  in the past. The value  $\mu$ , which corresponds to  $^{238}\text{U}/^{204}\text{Pb}$  ratio reduced to the present, may be defined by:

$$(^{238}\text{U}/^{204}\text{Pb})_t = \mu \exp \lambda t \quad (6)$$

based upon the assumption that the lead developed in a single lead-uranium system, unlike that for anomalous lead.

The concept of a 'closed system' evolved from the work of Gerling (1942), Holmes (1946) and Houtermans (1946). They consider that within locally closed systems the uranium, thorium and lead-204 remain constant, and the radiogenic lead isotope ratios evolve with time according to the growth curve, the curvature of which is dependant upon the particular  $^{238}\text{U}/^{204}\text{Pb}$  ratio. The ratio  $^{238}\text{U}/^{204}\text{Pb}$  therefore changes only by radioactive decay, due to insignificant fractionation of uranium. From this basis, the equations 3, 4, and 5 are valid. So for mineralization of time  $t_1$  derived from locally closed systems the isotopic ratios of the mineralization will plot on an isochron defined by:

$$\frac{y_1 - b_0}{x_1 - a_0} = R = \frac{(\exp \lambda' t_0 - \exp \lambda' t_1)}{137.88 (\exp \lambda t_0 - \exp \lambda t_1)} \quad (7)$$

the slope of which relates the age of the earth and the time of mineralization. This equation is only applicable for leads of a single uranium-thorium-lead closed system, which developed between  $t_0$  and  $t_1$  (Kanasewich, 1968a), and is referred to as Houtermans' "isochron equation".

Subsequent consideration of isotopic data of greater precision indicates that the basis of this model is an over simplification of geological history (Kanasewich, 1968a). Data spread along the isochron is actually due to experimental error, lack of standardization or the inclusion of anomalous leads. Because lead evolution in discrete systems, each with unique U/Pb and Th/Pb ratios, as proposed by Houtermans, is not justified by greater precision data, additional models have been proposed.

Russell and Farquhar (1960), Stanton and Russell (1959) consider that at the time of formation of the earth all lead therein had the same isotopic proportions, referred to as primeval lead ( $t_0$ ). Evolution of the primeval lead transpired in a single closed system, with a constant amount of uranium, thorium and lead (Houtermans' model has discrete systems with variable U/Pb and Th/Pb ratios). From this evolving lead, ore bodies form representing samples of lead of the homogeneous source, the upper mantle, which is isotopically related to the primeval lead. Vein lead is found to be more radiogenic and this is considered to be due to migration of lead through surface rocks, where assimilation of additional radiogenic lead results in formation of anomalous leads.

From this model it is possible to determine the uranium-lead and the thorium-lead values from the best fit of the data to the growth curve. Should the assumed homogeneous source evolve through to time  $t=0$  or the present, then the equations 3, 4, and 5 may be written:

$$a = a_0 + \mu_1 (\exp \lambda t_0 - 1) \quad (8)$$

$$b = b_0 + \frac{\mu_1}{137.88} (\exp \lambda' t_0 - 1) \quad (9)$$

$$c = c_0 + W_1 (\exp \lambda'' t_0 - 1) \quad (10)$$

which with resubstitution into the equations 3, 4, and 5 will yield:

$$x = a - \mu_1 (\exp \lambda t - 1) \quad (11)$$

$$y = b - \frac{\mu_1}{137.88} (\exp \lambda' t - 1) \quad (12)$$

$$z = c - W_1 (\exp \lambda'' t - 1) \quad (13)$$

Consequently, from this model the age of formation (model age) may be determined from the experimentally derived  $a$ ,  $b$ ,  $c$  and  $\mu$ ,  $W$  without having to rely upon the highly debated age of the earth designated by  $a_0$  and  $b_0$ .

Patterson and Tatsumoto (1964) deviated from the closed system evolutionary model of Russell and Farquhar (1960) through the study of lead in potassium feldspar. The isotopic variation noted, namely radiogenic lead increase in the feldspar as the age decreases, was assessed to indicate that since the formation of the earth there has been some kind of mechanism that controlled diffusion and differentiation of U, Th and Pb in the earth. Uranium and thorium transport initially is from the inner mantle to the outer mantle layer. The outer mantle gives rise to continental crust formation at various times. The rates of transport of the respective elements is considered to have decreased after the first 100 m.y. following formation of the earth, after which lead transport is essentially nil, while that of U-Th is decreased, but does not cease.

Consequently the continental segments at the time of formation contain U-Th-Pb values equivalent to those of the outer mantle. The crustal formation event would segregate lead, as in a closed system, until the time of freezing out of the feldspar by orogenic events. As test of this model, calculated values for lead give an almost perfect fit with observed isotopic ratios.

In assessing the closed system model of Russell and Farquhar (1960) and of Stanton and Russell (1959), which was developed from the study of ore leads of volcanic derivation, Patterson and Tatsumoto (1964) consider the leads 'have isotopic compositions that appear to conform approximately with closed system evolution, yet such leads have, in fact, evolved in complexities of open systems'. Consequently, the Patterson and Tatsumoto model is termed 'continuous diffusion'.

Subsequent workers were not content with the above-mentioned models, Sinha and Tilton (1973) consider lead from galenas and from feldspars of

granitic rocks isotopically and determined that stratiform ore lead, considered in the context of terrestrial lead evolution, does not fit a 'closed system' interpretation. The state "the data are best fitted to evolution models in which the value of  $\mu$  ( $^{238}\text{U}/^{204}\text{Pb}$  normalized to the present day) in the source has increased either over approximately the past 3.6 b.y. or since the time of formation of the earth". To account for the change in  $\mu$  the authors propose either mantle differentiation or crustal contamination; however, preference is given to the former due to the evidence derived from volcanic rock lead-strontium studies.

The work of Tilton and Tilton (1973) has provided the mathematical basis (although correction had to be made for the work of Cumming and Richards (1975) and therefore indicates the 'conventional' closed system interpretation of lead is greatly in question.

In further substantiation that U/Pb and Th/Pb uniformity, indicative of stratiform leads, does not necessarily imply a homogeneous source, Chow and Patterson (1962) suggest that homogenization could result from heterogeneous crustal lead by way of complete mixing of the lead. In this way the U/Pb and Th/U would represent a source comparable to that of the homogeneous upper mantle as envisaged by Stanton and Russell (1959). Kanasewich (1968a) suggests that seismic and heat flow studies indicate potential heterogeneities of  $^{238}\text{U}/^{204}\text{Pb}$  and  $^{232}\text{Th}/^{204}\text{Pb}$  ratios within the mantle, which raises the question of whether there is any truly homogeneous source of lead. Should heterogeneity with respect to the U-Th-Pb system exist, possibly to varying degrees, in both the mantle and the crust, the degree of mixing in either model will determine the eventual homogeneity of the  $^{238}\text{U}/^{204}\text{Pb}$  and  $^{232}\text{Th}/^{204}\text{Pb}$  ratios.

Richards (1971) considers the weight of ideas has directed thought away, from the significance of crustal averaging as presented by Cannon et al. (1961), and therefore the scientific examination has been biased. Studies pertaining to the Mississippi Valley type mineralization, of late, have tended to favour crustal averaging (Doe and Delevaux, 1972; Gerdmann and Myers, 1972) to explain the anomalous radiogenic character of the lead, which is indicative of incomplete mixing.

LeCouter (1973) equates the crustal mixing by natural environments to the observed characteristics of homogeneity of sulphur isotopes of oil fields, as related in the work of Monster (1972) and Thode et al. (1958). Lead-zinc-rich oil field brines (Carpenter et al., 1974) of central Mississippi reveal isotopic values that are very similar to the lead isotopes of the Red Sea brine (Delevaux et al., 1967) and the Salton Sea (Doe et al., 1966) all of which fall near the growth curve. For the latter two geothermal deposits, White (1968) has proposed that Na-Ca-Cl-rich brines are the mineral transport fluid which leached the base metals from the sediments. Thus it becomes evident that through the crustal mixing by convecting brines near uniformity of the  $^{238}\text{U}/^{204}\text{Pb}$  and  $^{232}\text{Th}/^{204}\text{Pb}$  ratios may be attained, such that the mathematical single stage model based upon a homogeneous source of constant U/Pb appears to be valid.

Richards (1971) has stated on the basis of more precise isotopic measurements that there are three basic fallacies evident with respect to the single stage model. These are: (1) Cenozoic basalts, most likely representative of mantle rock, should reveal uniform isotopic ratios. As more data is provided it is apparent the isotopic composition of the

basalt is very unlike that of the assumed mantle rock. They lack uniformity (Russell, 1972) and they do not fall on the growth curve of Cooper *et al.* (1969). This implies that the assumed mantle conditions are not valid. (2) The U/Pb ( $\mu$ ) for the source of the basalts is not constant, and therefore the ore source may have a variable U/Pb, a quality drawn upon to varying degrees by Stacey and Kramers (1975) and by Cumming and Richards (1975) in the construction of alternative growth curves. (3) The model ages do not always agree with the stratigraphically derived age.

Other fields of study have cast doubt upon the single stage lead model, as in the area of fluid inclusions (Roedder, 1967b) and of sulphur isotopes (Sangster, 1971). The studies have corroborated, to a degree, the ideas of Jackson and Beales (1967) and Kesler, Stoiber and Billings (1972), that the Na-Ca-Cl-rich brines are significant in the acquisition and transport of the lead and zinc metals, and that they are likely leached from the sediments.

Highly saline brines appear to be a common entity with regard to sulphide deposits (Roedder, 1967b), and may be viewed in the process of transport in the Salton Sea geotherm (White, 1968) and the Cheleken Peninsula geotherm (Lebedev, 1972). The Red Sea deposit of stratiform sulphides (Ross, 1972) is within a highly saline environment, and shows similarity to deposits such as Mount Isa and MacArthur River, Australia. These cases directly question the homogeneous upper mantle theory of lead evolution; however, the suggested similarity does not imply identical origins (White, 1968).

#### D. CONSIDERATION OF 'NEW' GROWTH CURVES

The 'single stage' growth curve (Cooper et al., 1969), developed on the basis of the mantle origin of lead model, has proven to be inadequate (Cumming and Richards, 1975). This became apparent with the use of improved uranium and thorium decay constants and accurate measurement of the isotopic composition of lead. Consequently, at least two 'new' growth curve models have been proposed.

Stacey and Kramers (1975) developed a two stage model, which considers that lead evolved from primeval lead 4.57 b.y. ago, of specific  $^{238}\text{U}/^{204}\text{Pb}$  and  $^{232}\text{Th}/^{204}\text{Pb}$  ratios. A catastrophic event transpired at 3.7 b.y. ago, initiating a second stage in which the  $^{238}\text{U}/^{204}\text{Pb}$  and  $^{232}\text{Th}/^{204}\text{Pb}$  ratios increased and it is this second stage that gave rise to the ore leads.

Cumming and Richards (1975) approach the growth curve by examining three models, adopting the best of the three. The model of Russell and Reynolds (1969) deals with ratios, not with ages, and thereby evades the meteoritic age problem. Using the latest U and Th constants and a restricted class of ore leads (excluding anomalous lead), the best fitting curve to the data (considered of equal weight) is developed. Whether the Canyon Diablo meteorite data is included or excluded does not alter the derived parameters and examination reveals that the value  $V$  is not constant for all the data. The model permits the best-fitting curve to pass through the meteoritic value, but thereby assigns a younger than accepted age for the Canyon Diablo lead. The second model approach is to 'force' the single stage growth curve through the Canyon Diablo meteorite data (Tatsumoto et al., 1973) since the first model revealed that



the data fits the growth curve. The results of this model are essentially the same as for model one with respect to the parameters. However, for both models the model ages lack in agreement with the known geologic ages of specific ore deposits. The third model is based on a 'steady linear change of U/Pb and Th/Pb' (U/Pb steadily increases while Th/Pb does not increase as rapidly). The age of 429 m.y. for Captains Flat, N.S.W., is adopted as a fixed point through which the growth curve passes, because the age 430 m.y. is considered geologically correct and the lead of the deposit is considered to be homogeneous, as shown by repeated isotopic measurements. From this approach the age of the earth is determined to be 4.509 b.y., which is less than many reported age determinations of meteorites and moon rocks. Even so, the growth curve does provide good geological fit and thereby is comparable to that of Stacey and Kramers (1975).

The implication of the two growth curve models is that the U/Pb and Th/Pb ratios of the earth have not been constant (i.e., existing in a closed system) throughout geological time. Either the change is episodic or gradual. Therefore the origin of the ore lead may not be the mantle, but may be a combination of the mantle and the crust or be totally of crustal origin.

#### E. ANOMALOUS LEADS

Leads which form in more than one U-Th-Pb system are called anomalous leads (Kanasewich, 1968a). Relative to the growth curve the anomalous leads are usually noted by the linear relation of the isotopic data when plotting  $^{207}\text{Pb}/^{204}\text{Pb}$  against  $^{206}\text{Pb}/^{204}\text{Pb}$ , caused by a second stage initiated by an event which altered the  $^{238}\text{U}/^{204}\text{Pb}$  ratio. In certain cases of vein deposits this is attributed to radiogenic lead contamination

derived from crustal rocks. The developed linear array is termed a secondary isochron or anomalous lead line. The equation defining the secondary isochron is similar to the Houtermans' isochron equation, the difference being the substitution of primeval lead with the evolved lead values at the start of the second stage and the age of the earth is replaced by the age at the commencement of the second stage. Examples of this category of lead are many. Doe and Delevaux (1972) determined the age and source of the southeast Missouri lead by the study of the secondary isochrons of crystalline basement lead and of Lamotte sandstone lead.

The equations used in interpreting secondary isochrons are as follows:

$$x_2 = x_1 + \mu_2 (\exp \lambda t_1 - \exp \lambda t_2) \quad (14)$$

$$y_2 = y_1 + \frac{\mu_2}{137.88} (\exp \lambda' t_1 - \exp \lambda' t_2) \quad (15)$$

$$z_2 = z_1 + W_2 (\exp \lambda'' t_1 - \exp \lambda'' t_2) \quad (16)$$

and by elimination of  $\mu$ , equations 14 and 15 may be combined so that the time of mineralization is related to the slope of the isochron. The secondary isochron equation is:

$$R = \frac{y_2 - y_1}{x_2 - x_1} = \frac{(\exp \lambda' t_1 - \exp \lambda' t_2)}{137.88 (\exp \lambda t_1 - \exp \lambda t_2)} \quad (17)$$

where  $x_1$ ,  $y_1$  and  $z_1$  represent the isotopic ratios at time  $t_1$ . The slope of the lead line is dependent upon the time of uranium introduction ( $t_1$ ) and the time of uranium and radiogenic lead separation due to mineralization ( $t_2$ ) (Kanasewich, 1968a).

Kanasewich (1968a) considers the simplest anomalous lead is achieved by mixing two ordinary leads to produce a series of plots in linear array which lie within the curvature of the growth curve, where  $\mu_1 = \mu_2$  and  $W_1 = W_2$ . Gale and Mussett (1973) consider the two-stage model with sub-

systems and have developed general multi-stage model equations which reduce for the  $i$ th sub-system in a two-stage model to:

$$i(^{206}\text{Pb}/^{204}\text{Pb})_0 = a_p + \mu_1 (\exp \lambda t_0 - \exp \lambda t_1) + \mu_2 i (\exp \lambda t_1 - 1) \quad (18)$$

$$\left\{ \begin{aligned} i(^{207}\text{Pb}/^{204}\text{Pb})_0 &= b_p + \frac{\mu_1}{137.88} (\exp \lambda t_0 - \exp \lambda t_1) + \frac{\mu_2 i}{137.88} (\exp \lambda t_1 - 1) \end{aligned} \right. \quad (19)$$

where  $a_p$  and  $b_p$  represent the primeval isotopic abundance ratios of the source,  $i(^{206}\text{Pb}/^{204}\text{Pb})_0$  is the present-day isotopic ratio in the  $i$ th sub-system, and the other symbols are as previously defined.

Similarly, multi-stage lead in theory has been considered by Kanase-wich (1962, 1968a), Russell et al. (1966). Based upon the assumption that the U/Pb ratio is variable from place to place and that orogenic events may cause a mixing of the U/Pb environments, their model is referred to as 'frequent mixing'. The approximate lead isotope ratios may be calculated after  $n$  stages using the following formulae, providing a history of the rocks is known.

$$\begin{aligned} (^{206}\text{Pb}/^{204}\text{Pb})_{t=0} &= (^{206}\text{Pb}/^{204}\text{Pb})_{t_0} + 1(^{238}\text{U}/^{204}\text{Pb})_{t=0} (\exp \lambda t_0 - \exp \lambda t_1) + \\ &2(^{238}\text{U}/^{204}\text{Pb})_{t=0} (\exp \lambda t_1 - \exp \lambda t_2) + \dots n(^{238}\text{U}/^{204}\text{Pb})_{t=0} \\ &(\exp \lambda t_{n-1} - \exp \lambda t_n) \end{aligned} \quad (20)$$

$$\begin{aligned} (^{207}\text{Pb}/^{204}\text{Pb})_{t=0} &= (^{207}\text{Pb}/^{204}\text{Pb})_{t_0} + 1(^{238}\text{U}/^{204}\text{Pb} \cdot 137.88)_{t=0} (\exp \lambda t_0 - \\ &\exp \lambda t_1) + 2(^{238}\text{U}/^{204}\text{Pb} \cdot 137.88)_{t=0} (\exp \lambda t_1 - \exp \lambda t_2) \\ &+ \dots n(^{238}\text{U}/^{204}\text{Pb} \cdot 137.88)_{t=0} (\exp \lambda t_{n-1} - \exp \lambda t_n) \end{aligned} \quad (21)$$

where time ( $t_1, t_2, \dots, t_n$ ) are the ages of mixing of leads into new U/Pb systems, and  $1, 2, \dots, n(^{238}\text{U}/^{204}\text{Pb})_{t=0}$  represent the values of various localities, and the other symbols are as earlier defined.

## F. RESULTS AND DISCUSSION

Lead isotopes were determined for 16 galena and 4 sedimentary pyrite samples of the Wrigley and Lou properties. The sample preparation, analytical method, instrumentation, and standard determination will be found in Appendix III.

The lead isotope data are tabulated in Table 4, and the data have been graphically presented in the  $^{207}\text{Pb}/^{204}\text{Pb}$  vs  $^{206}\text{Pb}/^{204}\text{Pb}$  ratio diagrams, Fig. 21. Consideration of the data will not include  $^{208}\text{Pb}/^{204}\text{Pb}$  ratio because it does not yield an independent estimate of time  $t_2$  (Kasevich, 1962).

The lead isotope data have been considered within the classification of two-stage anomalous leads. The best fitting straight line has been calculated for the data using the formulation of Cumming *et al.* (1972). Fig. 21 reveals the galena-lead line which has a slope of  $0.139 \pm 0.018$ . The line intersects the growth curve at  $^{207}\text{Pb}/^{204}\text{Pb}$  ratios of 15.667 and  $^{206}\text{Pb}/^{204}\text{Pb}$  of 18.728, which represents time  $t_2$ , and the time  $t_1$  intersection is at  $^{207}\text{Pb}/^{204}\text{Pb}$  of 15.105 and  $^{206}\text{Pb}/^{204}\text{Pb}$  of 14.679. Respectively, the model ages are:  $58 \pm 142$  m.y. and  $2.213 \pm 0.260$  b.y. The isotope ratios have a  $^{206}\text{Pb}/^{204}\text{Pb}$  range of 19.422 to 20.236.

The pyrite-lead line (Fig. 21) has a slope of  $0.050 \pm 0.007$ . It intersects the growth curve at  $^{207}\text{Pb}/^{204}\text{Pb}$  of 15.599 and  $^{206}\text{Pb}/^{204}\text{Pb}$  of 17.660, which represents 674 m.y. The pyrite-lead isotopes have a  $^{206}\text{Pb}/^{204}\text{Pb}$  ratio spread of 17.516 to 19.764.

The galena and pyrite lines intersect at about  $^{207}\text{Pb}/^{204}\text{Pb}$  of 15.64 and  $^{206}\text{Pb}/^{204}\text{Pb}$  of 18.53. The intersection lies below the growth curve.

Table 4.

## Wrigley-Lou Galena-Lead and Pyrite-Lead Isotopic Data

Sample Number		$^{206}\text{Pb}/^{204}\text{Pb}$	$^{207}\text{Pb}/^{204}\text{Pb}$	$^{208}\text{Pb}/^{204}\text{Pb}$
Galena:	Bourne	19.533(.004)	15.745(.007)	39.389(.034)
	B-73-5(195)	19.755(.026)	15.795(.019)	39.728(.033)
	B-73-5(537)	19.454(.009)	15.771(.010)	39.409(.034)
	B-73-5(648)	19.625(.001)	15.781(.006)	39.546(.025)
	12-4 (255)	19.490(.004)	15.774(.005)	39.410(.021)
	12-4 (349)	19.565(.001)	15.785(.010)	39.502(.001)
	48-1 (61)	19.715(.016)	15.777(.036)	39.303(.254)
	48-1 (94)	19.723(.001)	15.803(.013)	39.722(.002)
	48-1 (291)	19.633(.016)	15.807(.010)	39.607(.020)
	48-1 (375)	19.489(.006)	15.771(.021)	39.404(.070)
	48-1 (445)	19.513(.013)	15.782(.005)	39.429(.017)
	36-4 (28.5)	19.516(.030)	15.785(.039)	39.475(.058)
	36-4 (82.5)	19.512(.009)	15.792(.018)	39.467(.057)
	76-1 (25)	19.422(.009)	15.763(.006)	39.292(.028)
	12N-2+50E	20.236(.029)	15.871(.032)	40.212(.088)
	Hammer	20.089(.011)	15.860(.011)	40.067(.029)
Sedimentary Pyrite:	12-2 (119.5)	19.123(.021)	15.668(.024)	38.625(.093)
	12-2 (130.5)	19.034(.011)	15.670(.006)	38.789(.067)
	B-73-5(678)	19.764(.021)	15.701(.016)	39.383(.034)
	36-4 (259)	17.516(.014)	15.591(.013)	37.400(.013)

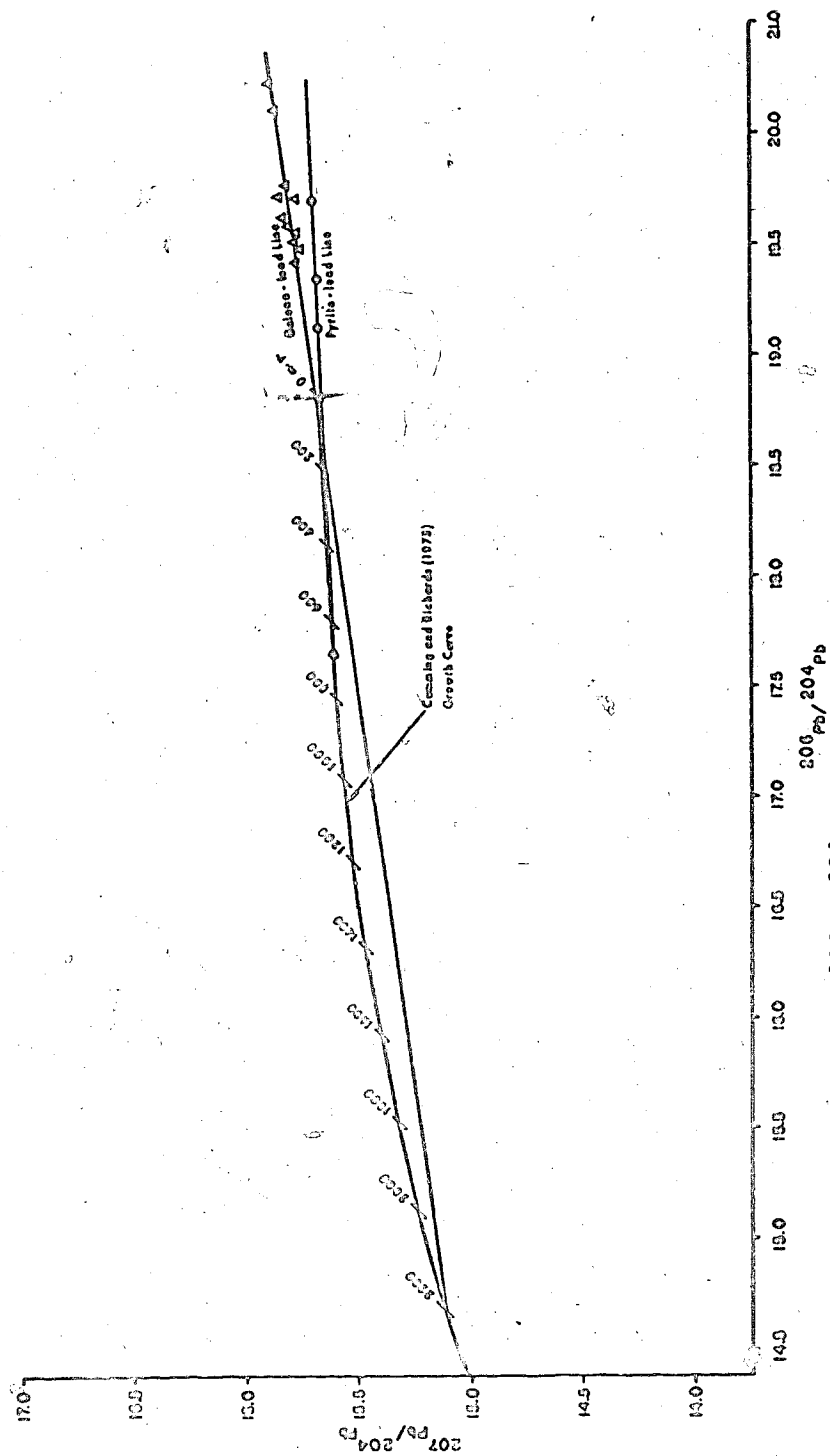


Fig. 21.  $^{207}\text{Pb}/^{204}\text{Pb}$  vs  $^{206}\text{Pb}/^{204}\text{Pb}$  ratio plot of galena-lead and pyrite-lead isotope data of Wrigley-Lou properties.

## 1. Possible Source of Lead

There are three possible sources of lead, namely the upper mantle, the Precambrian crystalline basement, or the host sediments. Consideration of the respective source areas follows:

(a) The upper mantle source of lead was considered previously. Cenozoic basalts, 'the mantle rock representative', are variable in U/Pb, as are the isotopic ratios (Richards, 1971). As such, the theory of mantle derivation of lead is in question.

(b) The Precambrian crystalline basement is a potential source of lead, and according to Zartman (1974) has a  $^{206}\text{Pb}/^{204}\text{Pb}$  ratio in the range of 16.2 and 18.8, determined from a study of western United States deposits. The feldspars are the primary lead carriers of the crystalline terrain and feldspar lead isotopic studies (Doe, 1970) have revealed that the ratios do not depart significantly from the growth curve. Perthite and quartz lead is also similar ( $^{206}\text{Pb}/^{204}\text{Pb} = 18.6$ , Tilton et al., 1955). Variations in isotopic ratios of this lead could be achieved by the addition of varying amounts of more radiogenic lead, contained within sphene, zircon and apatite ( $^{206}\text{Pb}/^{204}\text{Pb} = 39.1, 1000 (?), 31.9$ , respectively) (Tilton et al., 1955). The ore-lead isotopic composition would therefore depend upon the leaching efficiency of the brine, which in turn would be dependent on the physio-chemical conditions prevailing and the degree of homogeneity of the lead would be dependent on the efficiency of the mixing process.

Zartman (1974) considers characteristic patterns in lead isotope compositions of Mesozoic and Cenozoic igneous rock types and hydrothermal ore deposits, from which he defines discrete mineral provinces. He asserts that the lead derived primarily from Precambrian basement normally

produces a linear array when plotted  $^{207}\text{Pb}/^{204}\text{Pb}$  vs  $^{206}\text{Pb}/^{204}\text{Pb}$  and the array has a 'slope determined by the age of the local basement rocks'. Also, the isotopic ratios of the ore-lead derived from the basement crystalline rock are more radiogenic, possibly due to leaching of more radiogenic lead from such minerals as sphene and apatite. This radiogenic lead addition is more critical for small or peripheral deposits than for large deposits.

(c) Examination of Mississippi Valley type deposits of southeast Missouri (Doe and Delevaux, 1972) indicates the source rock of the ore-lead is the Paleozoic Lamotte Formation. This study therefore reveals that the sediments may, through a leaching process by brines, provide the lead or part of the lead that comprises an ore deposit.

Zartman (1974) considers lead derived from sediments eroded from the Precambrian basement. This class of ore-lead is distinctly radiogenic ( $^{206}\text{Pb}/^{204}\text{Pb} = 19.1 - 19.7$ ), very similar to that of the Wrigley deposit. The lead is quite homogeneous, likely due to chemical and isotopic mixing that took place during the sedimentary process. To set into perspective the sedimentary derived lead, Zartman states that "lead in modern sediments from lakes and restricted seaways predominantly draining Precambrian Shield areas is characteristically heterogeneous and highly enriched in radiogenic isotopes ( $^{206}\text{Pb}/^{204}\text{Pb} = 20.1 - 25.0$  and  $^{208}\text{Pb}/^{204}\text{Pb} = 40.3 - 49.3$ ) (Chow, 1965; Hart and Tilton, 1966). On the other hand, lead in open marine environments of the major ocean basins has a more uniform and less radiogenic isotopic composition ( $^{206}\text{Pb}/^{204}\text{Pb} = 18.8 - 19.2$  and  $^{208}\text{Pb}/^{204}\text{Pb} = 39.1 - 39.9$ ) (Chow and Patterson, 1959, 1962; Reynolds and Dasch, 1971)".



From this sedimentary model it is conceivable that the Wrigley-Lou ore-lead derived from both basement rock and sediments of basement origin deposited in an open marine environment. Circulating connate brines, as postulated by White (1968) for heavy metal geotherms, likely completed the chemical and isotopic evolution of the lead following the major folding and faulting of the Laramide orogeny. The structural deformation disrupted the fluid circulation system, opening faults for fluid movement up-dip into the younger formations. Block faulting of the basement prepared the Paleozoic sediments, so that the brine flow was channeled to the depository areas. Location of deposition of the sulphide ores is possibly dependent upon the base metal-bearing brines intercepting brines carrying reduced sulphur, in the style conceived by Jackson and Beales (1967).

## 2. Age of Source Rocks

Due to the linear relationship of the  $^{207}\text{Pb}/^{204}\text{Pb}$  and  $^{206}\text{Pb}/^{204}\text{Pb}$  ratios on a compositional diagram, anomalous leads can be used to indicate the approximate age of primary orogenesis (see Fig. 21). This time is designated  $t_1$  and for the Wrigley and Lou galena lead is  $2.213 \pm .260$  b.y. This age compares with post-Kenoran events of the Slave Province. Leech (1966) reported a period of diabase dike intrusion in the Slave Province of 2.2 to 2.4 b.y., while the Yellowknife differentiated intrusion gave dates ranging from 1.925 to 2.09 b.y. Stockwell *et al.* (1970) indicate the ages of 2.1 and 2.15 b.y. These ages relate to the calculated event of Ozard *et al.* (1973) of 2.25 b.y. Consequently, there appears to be a relationship between post-Kenoran Slave Province event(s) and the Wrigley-Lou ore-lead time  $t_1$ . Within experimental error, however, the time  $t_1$  relates with Kenoran and/or Hudsonian orogenic event(s).

It should be noted that ore-lead derived from Precambrian basement rock and from Precambrian derived sediments will theoretically increase the complexity of the isotopic interpretation. Adoption of the multi-stage lead interpretation, such as the 'frequent mixing model' (see equations 20 and 21), would probably be mathematically more correct. Hart and Tilton (1966) used this model approach to study Lake Superior sediment lead extract and found that the ages obtained correspond with those of the Superior Province, the probable source of the sediments. Kanasewich (1962) and Russell (1963), however, showed that the slope of the anomalous lead line about which the lead compositions of each stage scatter is dependent upon the time of commencement of the first stage and the time at the end of the last stage, and the intervening stages of differing U/Pb have essentially no effect. Consequently, the multi-stage lead history may be mathematically simplified to a two-stage evolutionary history.

Upon this basis the above interpretation of the history of Wrigley-Lou ore-lead is thought to be approximately correct, although greatly simplified. The scatter of points along the anomalous lead line according to Kanasewich (1968a) is indicative of incomplete mixing of the crustal lead\*. The more compact the values, and the closer they lie to the growth curve, the greater the degree of homogeneity. Richards (1971), by this approach, relates anomalous leads and ordinary leads.

### 3. Age of Sulphide Mineralization

The age of the mineralization has been considered from the structural point of view. The Laramide orogenic event is considered to have been the

---

\*Gale and Mussett (1973) examine in greater detail the linear relationship in multi-stage lead and the implication of the scatter of data points.

event which led to the mineralization of the northern Camell Range Palaeozoic sediments at time  $t_2$ . The lead model age has supported this consideration with the age of 58 m.y.; however; the large intersection deviation implies a certain degree of uncertainty.

#### 4. Consideration of the Lead Isotopes of Sedimentary Pyrite

The samples of pyrite were extracted from shale beds of the Headless, Nahanni and Hare Indian Formations. Consequently, the sedimentary pyrite-lead isotope data represent the lead contained within the argillaceous sediments of these formations. The pyrite-lead data, considered earlier, is listed in Table 4.

The pyrite-lead isotope values represent a U-Pb system which developed through the evolution of  $^{238}\text{U}/^{204}\text{Pb}$  much unlike that of the galena-lead. According to Rye, Doe and Delevaux (1974), 'a mechanism to produce the nearly constant  $^{232}\text{Th}/^{204}\text{Pb}$  and variable Th/U ratios necessary in the source materials has been observed in recent sediments. K.K. Turekian (oral communication) finds that the lead and thorium concentrations in anoxic sediments tend to follow each other while uranium concentrations vary independently. This relationship perhaps is not surprising, because uranium is extremely soluble in the hexavalent state, and the uranium concentration in the sediments will vary considerably with the oxidation state in the sediments and the overlying water at the time of sedimentation, while the lead and thorium will not be affected by the oxidation state of the depositional environment'. For this reason variation in the pyrite  $^{206}\text{Pb}/^{204}\text{Pb}$  ratio is observed.

From petrographic studies the sedimentary pyrite was formed either before or during diagenesis in which case the pyrites likely contain lead of three types: (1) 'ordinary' lead incorporated at the time of pyrite

formation; (2) lead comparable to the two-stage ore-lead; (3) lead that resulted from uranium that entered the pyrite lattice at the time of formation (Koeppel and Saager, 1974), or a combination of them. Consequently, the lead in pyrite emulates the sedimentary environment of formation.

Depending upon the degree of leaching and the contained amounts of the respective lead types, the isotopic composition of the pyrite-lead will reflect the relative abundance of the respective lead types in the pyrite. The lead types in turn will reflect the stratigraphy in which the particular pyrite formed. The shale formations have a greater percentage per volume of radiogenic lead. Ramdohr (1966) states that sedimentary occurrences of uranium result from solution of  $U^{+6}$ , which originates from granites and volcanics. Consequently, sedimentary pyrite formed within extensive shale units will have, at the time of formation, incorporated more  $U^{+6}$  than will pyrite formed within a predominantly calcareous unit. This is represented in Fig. 21 where the pyrite sample number 36-4 from the Nahanni Limestone Formation is not radiogenic and essentially lies on the growth curve.

The pyrite-lead line intersects the growth curve at  $^{206}\text{Pb}/^{204}\text{Pb} = 17.660$  and  $^{207}\text{Pb}/^{204}\text{Pb} = 15.599$ , which indicates an age of  $674 \pm 198$  m.y. This date relates well with K-Ar determinations of sills in the Shaler Group along the Minto Arch. The dates are 635 and 640 m.y., while dates from sills cutting Coppermine sediments range from 445 to 718 m.y. (Stockwell *et al.*, 1970). Wanless *et al.* (1966) have recorded dates in the Minto Arch, Coppermine Arch and northern Bear Province which range from 440 to 863 m.y. These dates represent the age of the Neohelikian, Hadrynian and/or pre-Middle Cambrian sediments. It is possible the re-

lation of the pyrite-lead model age and those of the sediments to the north indicates the source of the Middle Devonian sediments in the northern Camosell Range.

#### G. CONCLUSION

The lead isotope composition of the galena from the Wrigley and Lou properties indicates that mineralization probably occurred during the Laramide orogeny, the determined model age being  $58 \pm 142$  m.y. The lead comprising the deposits appears to derive predominantly from (1) the Precambrian basement rock, (2) the Paleozoic sediments which possibly derive from the Slave Province and/or the Minto Arch, Coppermine Arch and northern Bear Province, the latter indicated by the lead isotopes of the sedimentary pyrite. The primary event determination (time  $t_1$ ) is  $2.213 \pm .260$  b.y., which relates to events in the Slave Province of Kenoran, post-Kenoran or Hudsonian age.

## Chapter VII

### SUMMARY - WRIGLEY-LOU LEAD-ZINC MINERALIZATION

The Wrigley-Lou deposit gives some insight into ore genesis. The deposit type has been defined by Sangster (1976) as a 'stratabound deposit emplaced post-lithification of host rocks and which appear to be controlled by pre-ore, post-host structures', which is also typical of the Mississippi Valley type deposits. The characteristics of the Mississippi Valley type deposits have been reviewed by Jensen and Dessau (1967) and Heyl et al. (1974).

In recent studies consideration of the source of the Mississippi Valley type ore has been undertaken through the study of isotopes and fluid inclusions (Jackson and Beales, 1967; Skinner, 1967; White, 1968; Roedder, 1968, 1971; and Heyl et al., 1974). The general consensus is that a Na-Ca-Cl connate brine transported the base metal ions and precipitation of the sulphides resulted from the mixing with a second brine transporting reduced sulphur. Transportation of the base metal ions was most likely as a chloride complex; however, agreement on the source of metals and the sulphur is variable, interpreted differently as the geological environment of the particular deposit varies (Davidson, 1966; Dunham, 1966). The heat source, whether geothermal, igneous or magmatic, is debated. Many of the ideas that are debated have application to the Wrigley-Lou deposit.

The fluid inclusion studies have revealed strong parallels to the Mississippi Valley type deposits as considered in Chapter IV. These parallels relate to salinity, density, temperature and depth of burial

of the forming deposit. The minimum temperature of formation ( $80-156^{\circ}\text{C}$ ) is much greater than expected in terms of the geothermal gradient, unless the metal-bearing brine came from great depths in the crust. The deep circulation model presented by White (1968) to explain the Salton Sea geothermal system may be applicable for the Wrigley-Lou deposit. Release of interstitial formational fluids (LeCouter, 1973) of the Precambrian may also explain the high fluid inclusion temperatures. Irrespective of the model used, the basement structural deformation of the Laramide orogeny is necessary to explain the high temperatures and the brine mobility in the Paleozoic sediments of the northern Camsell Range.

The lead isotopes give a model age of  $58 \pm 142$  m.y. for time  $t_2$ . As Zartman (1974) indicated, the time  $t_1$  should relate to the mineral source rocks. This appears to be the case for the northern Camsell Range deposits. The time  $t_1$  relates to K-Ar dated event(s) in the Precambrian basement (see Chapter VI), thereby revealing a genetic relation between the ore-lead and the basement rock. Work by Gerdemann and Meyers (1972), in consideration of southeast Missouri lead district, proposed Precambrian basement and Paleozoic rocks to be the metal source. In like manner, the northern Camsell Paleozoic stratigraphy (shales and carbonates) cannot be disregarded as having provided some of the metal.

The source of sulphur is considered to be the evaporites of the Bear Rock Formation. Other sulphur sources may have played a nominal role. As in the case of the Salton Sea geothermal system, White (1968) considers the sulphur constituents may be of varied origins, including meteoric water, evaporites, clastic carbonates and silicate minerals.

The model of mineral emplacement for the Wrigley and Lou properties, as determined from this study, is as follows:

(1) Deposition of the Paleozoic stratigraphy from Cambrian to Upper Devonian time with no major deformation involving the Precambrian basement.

(2) The Laramide orogeny mobilized the Precambrian basement and severely deformed the Paleozoic sedimentary sequence. The deformation of the basement released saline interstitial brines and/or permitted circulating brines (White, 1968; Lange and Murray, in press) to penetrate into and to leach metals from the rock. The fault deformation permitted up-dip mobility of the brines, which due to salinity and heat were capable of leaching some metals from the Paleozoic sediments.

(3) The Hare Indian Formation, having a high argillaceous to carbonate content, acted as a pseudo-impermeable barrier preventing further up-dip migration of the metal-bearing brine.

(4) The sulphur, principally derived from reduced sulphate of the Bear Rock Formation, was transported by a second brine. The structural deformation opened the avenues for brine migration.

(5) The two brines intercepted in various localities of the structurally prepared Middle Devonian carbonate formations. Because the respective brines migrated predominantly within the structurally developed fault and fracture systems the sulphide precipitation occurred here. The Nahanni Formation is the best mineralized formation because the Hare Indian Formation, not to mention the Fort Simpson Formation, prevented further migration of the metal and sulphur-bearing brines. Therefore, within the realm of the optimum physico-chemical conditions, the ore minerals were precipitated.



## Chapter VIII

### SULPHUR AND LEAD ISOTOPES FROM LITTLE CORNWALLIS ISLAND, ARCTIC ARCHIPELAGO

The Polaris zinc-lead sulphide deposit on Little Cornwallis Island, in the Canadian Arctic Archipelago, was discovered by the Cominco-Bankeno exploration team in 1971. Through drilling and underground exploration the Polaris deposit has proven 20 million tons of 20% combined zinc-lead (Kerr, 1975). The deposit is the major one of ten showings in the Cornwallis Fold Belt, and the area may be designated the Cornwallis Lead-Zinc Province (Kerr, 1976). The Eclipse is the second largest deposit with one million tons proven to 13% combined sulphides. The ten known showings are indicated on the index map (Fig. 22), and the geology and geological circumstances of the showings are summarized in Table 5 (Kerr, 1975).

Sangster (1974) refers to the Polaris deposit as a karst-controlled Mississippi Valley type deposit. Within this general classification, the Polaris and surrounding deposits are similar to those of the Pine Point district, N.W.T., with respect to mineralogy, texture, environment and isotope results. Fluid inclusion studies are also comparable, the filling temperatures of the Polaris sphalerites lie within the range of +52 to +105°C (Jowett, 1975), and that of Pine Point sphalerite +51 to +97°C (Roedder, 1968).

To reveal greater understanding as to the source of the mineralization, sulphur and lead isotopes were determined on a limited number of Polaris and Truro sulphide samples. The study will also indicate the temperature of formation and the model age of the sulphides.

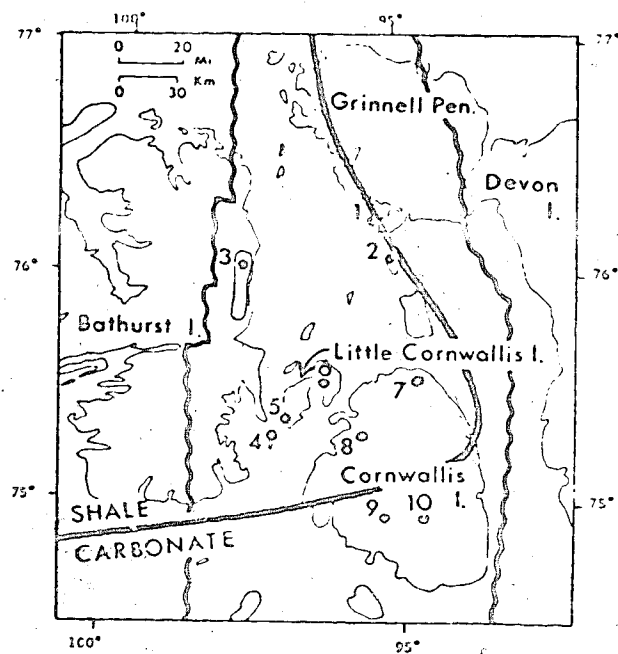


Figure 22. Lead-zinc occurrences of the Canadian Arctic referred to in Table 5. The solid line marks a facies change from the Cape Phillips shale formation to equivalent carbonate units. The wavy lines show the limit of the Cornwallis Fold Belt. (after Kerr, 1975)

### A. GENERAL GEOLOGY

The sedimentary sequence pertinent to this study ranges in age from Ordovician to Devonian (see Fig. 23). The sedimentary deposition took place within the generally east-west trending Franklinian miogeosynclinal trough which became defined in Early Ordovician time. This miogeosynclinal sequence comprises sediments of carbonate shelf and/or bank deposition with associated evaporites and/or shales. The deposition was continuous until the Lower Devonian, at which time emergence and sea water withdrawal allowed development of the angular unconformity which truncates the Read Bay - Cape Philips Formations.

The Thumb Mountain of Ordovician age, is host to all the lead-zinc showings except one, the Allen Bench, which is found within the Allen Bay Formation (Table 5). The Thumb Mountain is predominantly medium to thick, massive bedded lime mud, dolomitized in part, and resistant to weathering. According to Thorsteinsson and Kerr (1968), the dolomitization is primarily restricted to the upper part of the formation, proximal to the angular unconformable surface which separates the overlying Middle Devonian Disappointment Bay Formation. The unconformity also transects the Irene Bay Formation, a shallow water limestone interbedded with green shales, and the Cape Philips Formation, a black shale and argillaceous carbonate unit.

The 1700 foot thick Thumb Mountain Formation is immediately underlain by about 1,000 feet of less resistant carbonate, shale and evaporite of the Bay Fiord Formation. The lower half of this formation is predominantly gypsum and anhydrite. This formation, in turn, is underlain by fine-grained, buff weathering limestone of the Eleanor River Formation, which measures a 2,000 foot thickness. The Lower Ordovician

Table 5.

Summary of the geology of lead-zinc occurrences of the central Canadian Arctic Islands.

Locations are shown by number on Index Map (Fig.22).

Unconformities shown by number in Column 5 are those listed in Table 6.

1	2	3	4	5	
No.	Name of showing	Discoveries to date	Host Formation(s)	Relation to Silurian Facies Change	Relation of Thumb Mountain Formation to unconformities
1	Sheills Peninsula	Good shows from surface and drilling	Thumb Mountain	Below Cape Phillips shale belt	Truncated by Unconformity 3
2	Dundas Island	Spectacular surface showing	Thumb Mountain	Below Cape Phillips shale belt	Truncated by Unconformity 3
3	E. Bathurst Island	Minor surface showings	Thumb Mountain	Below Cape Phillips shale belt	Truncated by Unconformity 3
4	Truro Island	Spectacular surface showing	Thumb Mountain	Below Cape Phillips shale belt	Truncated by Unconformity 3
5	Polaris	20 million tons 20% combined Pb-Zn proven by drill and shaft	Thumb Mountain	Below Cape Phillips shale belt	Truncated by Unconformity 3
6	Eclipse	1 million tons 13% combined Pb-Zn proven by drilling	Thumb Mountain	Below Cape Phillips shale belt	Truncated by Unconformity 2
7	Stuart River	Small showings in cores	Thumb Mountain (and Disappointment Bay)	Below Cape Phillips shale belt	Truncated by Unconformity 3
8	Rookery Creek	Small showings in cores	Thumb Mountain, Disappointment Bay and Griper Bay	Below Cape Phillips shale belt	Truncated by Unconformities 3 and 4
9	Taylor River	Small surface showings	Thumb Mountain	Below carbonate belt	Unknown
10	Allen Branch	Small surface showing	Allen Bay	In carbonate belt	Unknown

(after Karr, 1975)

Table 6.

Unconformities Affecting the Cornwallis Fold Belt and  
Referred to in Column 5 of Table 5

Unconformity No. (Table 5, Col. 5)	Age	Formation Succeeding Unconformity
4	Late Devonian	Griper Bay (quartz sandstone)
3	Early Devonian	Disappointment Bay (dolomite)
2	Early Devonian	Stuart Bay (limestone) or Snowblind Bay (dolomite)
1	Early Silurian	Cape Storm (limestone; Kerr, in press)

(after Kerr, 1975)

Lithology	Formation and thickness in feet	Epoch	Period	Era
Glacial gravels, morainal debris, silt, clay, stream sediments, marine beach deposits		Pleistocene and Recent	Quaternary	Cenozoic
Angular Unconformity			Tertiary	
			Cretaceous	Mesozoic
Sandstone, minor siltstone, shale (marine)	Griper Bay 800 ±	Famennian Frasnian	Devonian	Paleozoic
Angular Unconformity				
Limestone, sandstone, siltstone (marine)	Bird Flord 500 ±	Givetian Eiffelian		
Limestone (marine)	Blue Flord 100-150	Eiffelian		
Dolomite; minor conglomerate (marine)	Disappointment Bay 400-830	Eiffelian		
Angular Unconformity				
Limestone; minor dolomite and conglomerate	Stuart Bay 350 +	Emesian Siegenian Gedinnian		
Angular Unconformity - locally conformable				
Shale, limestone, cherty limestone, chert, dolomitic limestone	Cape Phillips 9,800 ±	Gedinnian Ludlovian Wenlockian Llandoveryian Ashgillian	Silurian	
Shale, limestone (marine)	Irene Bay 30 - 150	Cornwallis Group	Caradocian	
Limestone, dolomite (marine)	Thumb Mountain 1,700 ±		Caradocian	
Gypsum, anhydrite limestone; minor shale, siltstone (marine)	Bay Flord 1,000 ±		Caradocian (?) Llandeilian (?)	
Limestone, minor dolomite (marine)	Eleanor River 2,000 ±		Llanvirnian Arenigian	
Gypsum, anhydrite; minor limestone, limestone pebble conglomerate (marine)	Baumann Flord 2,400 +	Arenigian		

Figure 23. Table showing formations north of the Cape Airy - Snowblind Bay line of facies change.  
(after Thorsteinsson & Kerr, 1967)

Baumann Fiord Formation, measuring 2,400 feet, may be divided into three units: a middle limestone member, sandwiched between two anhydritic members.

This Paleozoic sedimentary sequence, which developed in the deepening Franklinian miogeosyncline, was subjected to unstable conditions in Late Silurian to Early Devonian time. The Middle Paleozoic epeirogeny (Drummond, 1973) caused north-south trending areas of uplift resulting in emergence and erosion. The Boothia uplift, representing activated Precambrian basement, formed the northward extending Cornwallis Fold Belt, under which Boothia Arch plunges. The Lower Devonian erosional surface developed subsequent to the epeirogeny, and transgression by the sea in Middle Devonian time resulted in the deposition of carbonates and marine conglomerates of the Disappointment Bay Formation.

The Ellesmerian orogeny (Late Devonian to Early Mississippian) caused folding within the Franklinian geosyncline conformable with its trend, the final result being the Franklinian Fold Complex (Drummond, 1973). The final orogenic event to affect the Cornwallis Fold Belt, the Eureka disturbance of Middle Tertiary age, rejuvenated older structures to affect later sedimentation and to cause north-south and east-west breakage of the Belt (Kerr, 1976).

#### B. MINERALIZATION

The Little Cornwallis - Cornwallis Island mineralization consists of galena, sphalerite, pyrite, with minor silver and marcasite. The mineralization is stratabound within the Thumb Mountain Formation on the whole. The disseminated and massive mineralization is found within vugs, host carbonate and interstices of solution-collapse breccia developed

under an unconformity which may be a factor in mineral concentration. Fractures in calcite may also be mineralized (Jowett, 1975).

The ore in many respects is comparable to that of Pine Point Mines. The sphalerite may be developed as large crystals, of variable brown shades, measured in millimeters; more often the sphalerite is micro-crystalline, of a crusting, colloform banded texture, or is interbanded with massive galena which periodically forms thread-like spines. The galena in vuggy areas reveals masses of cubic crystals and peripheral to the vugs the galena may be disseminated in the host dolomite. In minor instances galena is disseminated in calcite veins, probably indicative of the final stage of mineralization. Pyrite occurs in association with both sphalerite and galena in vugs and in massive replacement ore. In vugs the pyrite forms as crystalline encrustations on both cubic galena and colloform sphalerite, while in the massive replacement ore the pyrite is disseminated. This probably represents two stages of pyrite development, a late and early stage, respectively. The iron sulphide may also appear as breccia fragments within collapsed or structurally deformed areas.

Bituminous matter is present within the deposits, however, no bitumens are evident in sphalerite fluid inclusions (Jowett, 1975).

Dolomite and white spar dolomite are closely associated with the base metal mineralization, but the association is not mandatory. Solution collapse breccia, containing dolomite blocks of various sizes, is the principal host structure for the mineralization. The development of the karst solution caverns in the Mountain Formation may be related to the overlying sub-surface unconformity (Thorsteinsson and Kerr, 1968). Alternative development could have developed



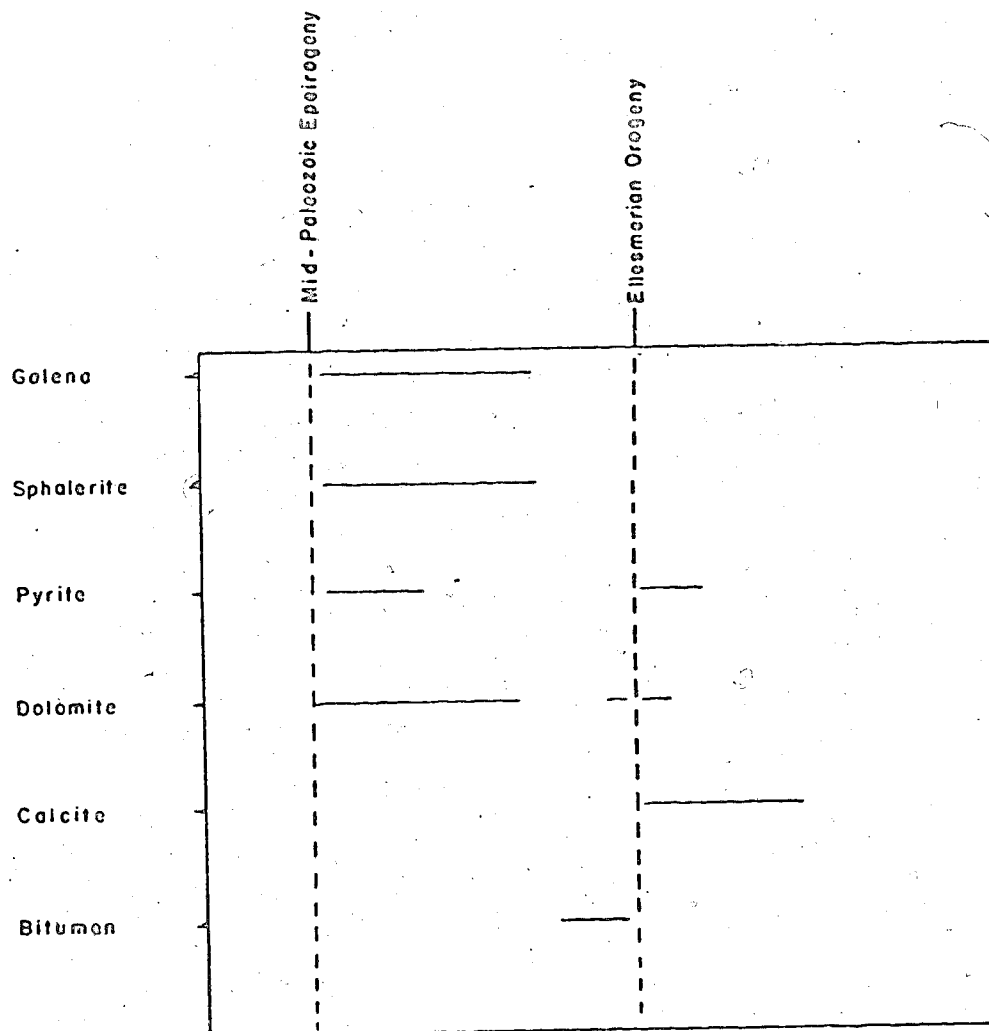


Fig. 24. Paragenesis: Polaris and Truro deposits.

prior to exhumation of the Thumb Mountain carbonates. The shales, subjected to periods of subaerial exposure and weathering, could release sulphuric acid due to the oxidation of the diagenetic iron sulphides. These acidic groundwaters would thereby acquire an increased power to dissolve the underlying carbonates. Because the Cape Philip Shales were first subjected to erosion during the Caledonian orogeny, this would delineate the maximum age of karst development. Should this be the case then the control of circulating ore-fluids would not be the unconformity, rather it would be the shales.

Silver is a trace element which follows lead. High silver values have not been reported, and it may be assumed that the silver values do not exceed a few ounces per ton.

According to Jowett (1975) little barite and no fluorite has been recognized at the Polaris deposit. The relation of the barite to the ore is unknown to the writer.

Fig. 24 indicates a probable paragenetic sequence for the deposits.

### C. SULPHUR ISOTOPES

Samples of three galena-sphalerite sulphur pairs and one pyrite were prepared for sulphur isotope study to provide preliminary indication of equilibrium-disequilibrium conditions within the deposit (Ohmoto, 1972; Rye and Ohmoto, 1974; Sasaki and Kajiwarra, 1971) and to indicate the probable source of the sulphur.

The isotopic sulphur data (sl-gn) indicate the  $\delta^{34}\text{S}$  value range to be +2.3% to +8.9%, the mean being  $3.8 \pm 0.14\%$ . The mean galena  $\delta^{34}\text{S}$  value is  $+4.0 \pm 1.5\%$  and the mean sphalerite value is  $+7.8 \pm 1.7\%$ . The one pyrite value is +8.9% (see Table 7).

Table 7.  
Polaris-Truro - Sulphur Data (%)

Sample Number	$\delta^{34}\text{S}$ sphalerite	$\delta^{34}\text{S}$ galena	$\Delta\text{sl-gn}$	Temperature (Czamanski & Rye, 1974)
7894	5.8	2.3	3.6	170°C
7897	8.7	4.8	3.8	154°C
7899	8.9	4.9	4.0	143°C
7899(py)	8.9			

Mean  $\delta^{34}\text{S}$  values:

Sphalerite	$7.8 \pm 1.7$
Galena	$4.0 \pm 1.5$
$\Delta\text{sl-gn}$	$3.8 \pm 0.14$
Avg T°C	156°C

From the tentatively proposed paragenetic sequence (Fig. 24) it may be considered that the galena-sphalerite mineralization was preceded by pyrite development and ended with calcite vein development. Upon this basis the pH- $f_{O_2}$  diagram used for the Wrigley deposit is applicable to the Little Cornwallis mineralization (see Fig. 20). From the diagram it is apparent the general area of the  $\delta^{34}S_{ZnS}$  value for the deposit should lie within the range of about +16 to -18.5‰ whereas the range of the  $\delta^{34}S$  value is +8.9‰ to +2.3‰. This narrow  $\delta^{34}S$  value spread indicates the Polaris-Truro deposits did not respond to changes in the chemical environment of deposition, and are therefore similar to the Wrigley-Lou and Creede, Colorado deposits. Consequently, it is probable that bacterial reduction was involved in the evolution of the sulphide sulphur (Rye and Ohmoto, 1974). The sulphur likely came from the sea water sulphate, which is geologically possible due to the proximity of the Bay Fiord and Baumann evaporites.

Considering sea water sulphate relative to the ore sulphides (Sangster, 1968, 1971; Sasaki and Kajiwar, 1971), it is necessary to compare the  $\delta^{34}S$  values of the sulphides to those of the Early and Middle Ordovician evaporites. Work by Davies and Krouse (1975) has provided the  $\delta^{34}S$  values of Paleozoic sulphates of the Arctic Archipelago. The Middle Ordovician Bay Fiord and the Baumann Fiord evaporites  $\delta^{34}S$  per mil values are indicated to be 29.3‰ and  $27.9 \pm 1.8$ ‰, respectively. Adopting the  $\delta^{34}S$  average value of 6.3‰ for the Polaris-Truro mineralization, the  $\Delta\delta^{34}S$  value is 23.0‰ and  $21.6 \pm 1.8$ ‰, respectively, where  $\Delta\delta^{34}S\text{‰} = \delta^{34}S_{\text{(sea water)}} - \delta^{34}S_{\text{(sulphide)}}$ .

These  $\Delta\delta^{34}S$  values represent equilibrium conditions in isotope exchange reaction between  $SO_4^{2-}$  and  $H_2S$  (or pyrite) and give a temperature

of above 300°C (Rye and Ohmoto, 1974). This temperature is abnormally high as a formation temperature for this type of deposit. In particular, the fluid inclusion homogenization temperatures are 52-105°C (Jowett, 1975) and the sphalerite-galena sulphur isotope temperatures are 143-170°C (Table 7). The discrepancy between the  $\Delta\delta^{34}\text{S}$  value derived temperature and the experimentally determined temperature, which represents lack of equilibrium attainment, may be the result of the comparatively slow rate of isotopic exchange reaction as compared to the rates of deposition and cooling of the sulphides in the ore-forming process (Sasaki and Kajiwara, 1971), or lack of sufficient samples.

This, therefore, exemplifies a state of disequilibrium, and is in agreement with the previous examination using the pH- $f_{\text{O}_2}$  diagram. In comparison, it should be noted that Pine Point mineralization has an average  $\delta^{34}\text{S}$  value of 20.8‰, while the average evaporitic sulphate value (Elk Point Basin) is 18.9‰ (Sasaki and Krouse, 1969). The  $\Delta\delta^{34}\text{S}$  value is 1.9‰, which represents an isotopic equilibrium temperature of 600°C (Rye and Ohmoto, 1974). This signifies considerable disequilibrium within the Pine Point sulphur system and implies bacterial derivation. Sasaki and Krouse (1969) attribute the origin of the sulphide sulphur to the evaporites of the Elk Point Basin.

Therefore, the relationship drawn between the Polaris-Truro sulphides and the stratigraphically lower sulphates (of the Bay Fiord and Baumann Fiord Formations) appears plausible. Consequently, the sulphur of the stratabound deposits is believed to be biogenic in origin and the source of the sulphur is Ordovician evaporite.

#### D. SULPHUR GEOTHERMOMETRY

The sulphur isotope  $\Delta_{\text{sl-gn}}$  average for the three galena-sphalerite pairs is  $3.8 \pm 0.14\%$  (see Table 7). Using the Czamanski and Rye (1974) formula,  $T^{\circ}\text{C} = \frac{7.0 \times 10^5}{\Delta_{\text{sl-gn}}} - 273^{\circ}$ , the temperature range of sulphide deposition is  $143\text{--}170^{\circ}\text{C}$  and the mean is  $156^{\circ}\text{C}$ . These temperatures are higher than those ascertained by fluid inclusion studies (Jowett, 1975), which have a normal distribution of  $52\text{--}105^{\circ}\text{C}$ , with a mean of  $75.5^{\circ}\text{C}$ . One anomalously high filling temperature of  $131^{\circ}\text{C}$  was found and considered to be valid.

#### E. LEAD ISOTOPES

Galena ore lead from the Polaris and Truro deposits, seven samples in total, were isotopically analyzed and the data are recorded in Table 8 and plotted on Fig. 25. Although the number of samples are few, it is felt the results indicate the model age and throw light on the probable source of the lead.

##### Consideration of the Data

The lead isotope ratios permit a basis of comparison with lead of geologically similar deposits. The Mississippi Valley mineral districts of the United States reveal enrichment in radiogenic isotopes and are termed anomalous (Kanasewich, 1968a). Heyl et al. (1974) have listed the average isotope ratios from the various districts and the  $^{206}\text{Pb}/^{204}\text{Pb}$  ratio range is 20.36 to 22.54 (taken from the work of Brown, 1967; Heyl et al., 1966; Russell and Farquhar, 1960). Within a particular district a relatively wide distribution of values may be obtained. The radiogenic character of these leads has been interpreted as having been derived from a shallow

Table 8.  
Polaris-Truro Lead Isotope Data

Sample Number	$^{206}\text{Pb}/^{204}\text{Pb}$	$^{207}\text{Pb}/^{204}\text{Pb}$	$^{208}\text{Pb}/^{204}\text{Pb}$
7894	17.846(.012)	15.558(.008)	38.156(.024)
7895	17.780(.034)	15.503(.028)	37.958(.058)
7896	17.837(.012)	15.540(.011)	38.089(.027)
7897	17.833(.007)	15.556(.008)	38.121(.023)
7898	18.149(.038)	15.592(.033)	38.198(.085)
7899	17.801(.015)	15.498(.017)	37.959(.038)
7903-A	17.826(.002)	15.517(.006)	38.014(.037)
Average except 7989	17.821(.025)	15.525(.026)	38.050(.085)

crustal source, either of Precambrian rock or the overlying Paleozoic sediments (Heyl *et al.*, 1974). In comparison the Pine Point isotope ratios lie near but above the growth curve (Cumming and Richards, 1975) with the  $^{206}\text{Pb}/^{204}\text{Pb}$  ratios ranging between 18.25 and 18.36; when the ratios are plotted  $^{206}\text{Pb}/^{204}\text{Pb}$  vs  $^{207}\text{Pb}/^{204}\text{Pb}$ , the variation appears to lie along the 204-error line (Fig. 26) (Cumming and Robertson, 1969). The lead data are interpreted as indicative of a homogeneous source since they are adequately explained by the single-stage growth curve model within experimental error. Cumming and Robertson therefore indicate a possible deep-seated lead source, such as the Upper Mantle. Because two geologically similar mineral districts are considered to have radically different metal source regions, it is necessary to consider the lead isotope data of the Polaris and Truro deposits in a broad light. This implies the consideration of the ideas of Richards (1971) among others, that lead isotopes can be thoroughly mixed in crustal environments by natural processes.

The lead isotope data of the Polaris and Truro deposits show remarkable similarity to that of the Pine Point deposit when the respective isotope values are compositionally plotted  $^{206}\text{Pb}/^{204}\text{Pb}$  vs  $^{207}\text{Pb}/^{204}\text{Pb}$  (see Fig. 25, 26). In both cases most of the isotope ratio variation lies along the 204-error line, signifying the major experimental error source centers on the lack of precision in measuring the small 204 peak.

Anomalous lead isotope ratios are not indicated on either of the compositional plots; however, one isotope ratio from the Truro deposit (No. 7898, Table 8) reveals a  $^{206}\text{Pb}/^{204}\text{Pb}$  ratio of 18.149 (see Fig. 25), indicative of increased radiogenic lead. More comprehensive sampling of the deposits might reveal a trend indicative of inhomogeneity with respect to the lead, or a mineral zonation within the district as found by Kuo and Folinsbee (1974) in the Selwyn Basin, Yukon Territory.



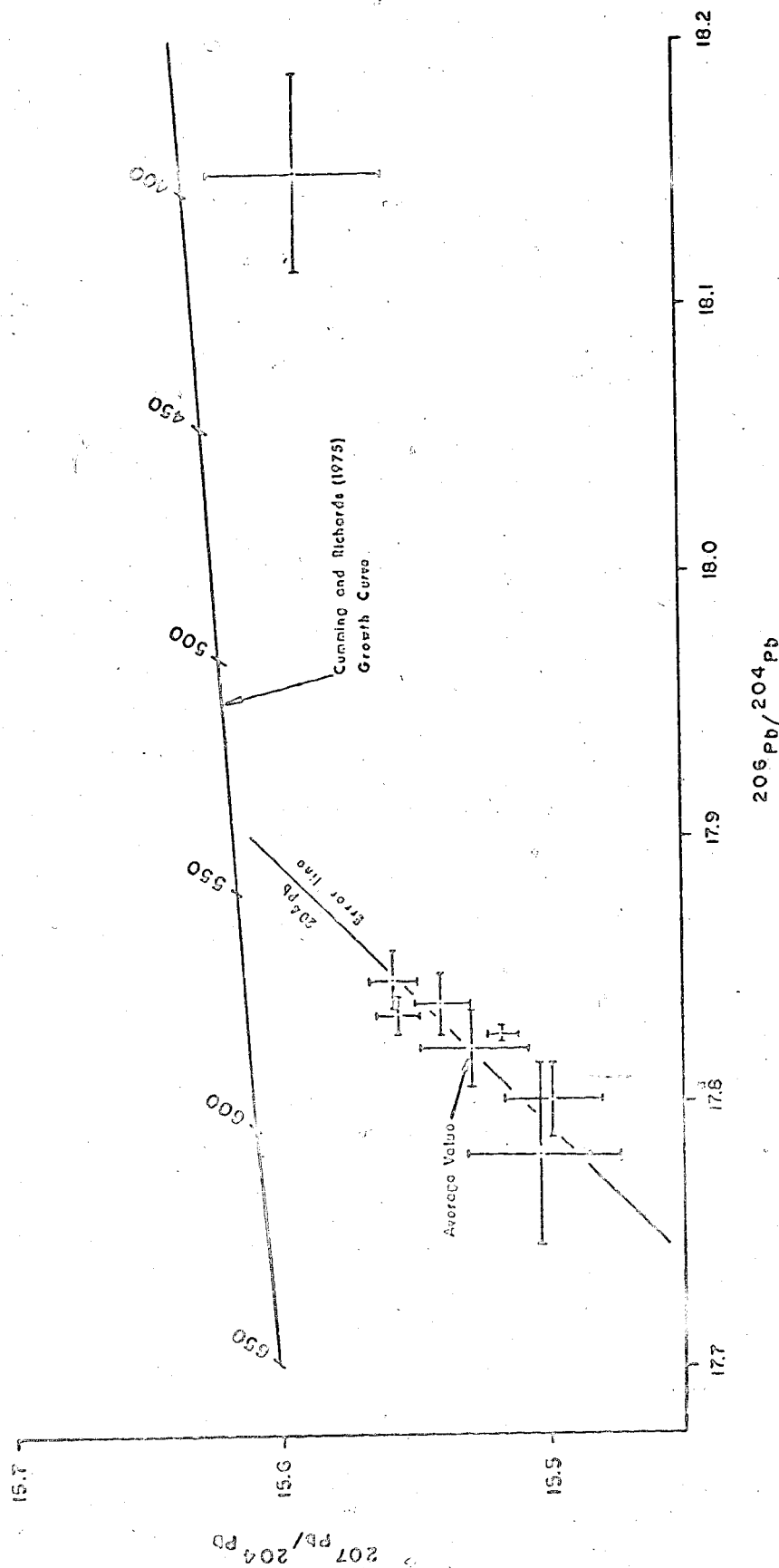


Fig. 25.  $^{207}\text{Pb}/^{204}\text{Pb}$  vs  $^{206}\text{Pb}/^{204}\text{Pb}$  ratio plot of the lead isotope data of the Polaris-Truro deposits, Canadian Arctic.

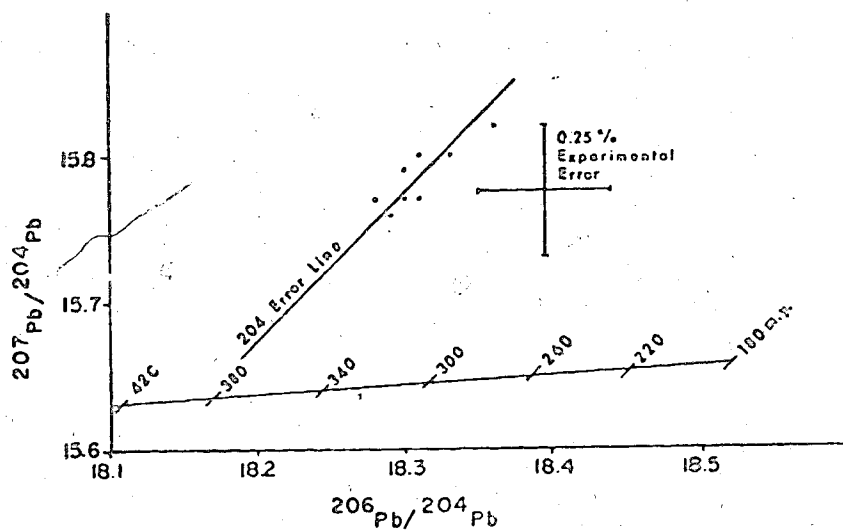


Fig. 26.  $^{207}\text{Pb}/^{204}\text{Pb}$  vs  $^{206}\text{Pb}/^{204}\text{Pb}$  ratio plot of the lead isotope data of Pine Point, N.W.T.

Alternatively, the sample may be from Pine Point Mines. The ratios are very similar to those determined by Cumming *et al.* (1971).

The present isotopic data would indicate the ore lead to be ordinary as it fits the growth curve relatively well. This therefore implies the leads come from a homogeneous source. Stanton and Russell (1959) would consider such uniformity to be derived from 'homogeneous materials within the earth's upper mantle'. Ostic *et al.* (1967) would also attribute the lead to a deep-seated source, which, during the process of emplacement, had limited contact with crustal rocks, thereby decreasing the possibility of incorporation of crustal radiogenic lead.

Within this area of consideration it is worthwhile to compare the isotope ratios of the Red Sea, a stratiform sulphide deposit presently in the process of formation (Cooper and Richards, 1969), to those of Polaris and Truro. The Red Sea  $^{206}\text{Pb}/^{204}\text{Pb}$  average ratio is 18.72 and the  $^{207}\text{Pb}/^{204}\text{Pb}$  average ratio is 15.68 (Delevaux *et al.*, 1967) which lies close to the growth curve. Heyl *et al.* (1974) indicate that a slight radiogenic character is revealed, and some workers attribute the data spread to 'contamination of brine lead with lead from pelagic sediments'. A mantle source of lead, however, is not proposed.

The comparison of the Polaris and Truro lead isotope ratios to those of Pine Point, Red Sea, Wrigley-Lou and Mississippi Valley type deposits, as revealed in Fig. 27, appears to indicate a relationship. In the context of Richards (1971), the aspect in common is the source of lead, namely a crustal origin. Richards (1971) states, "... if a solution circulates (White, 1968) in a particular environment for any appreciable time before conditions force deposition, there should be ample opportunity to yield by

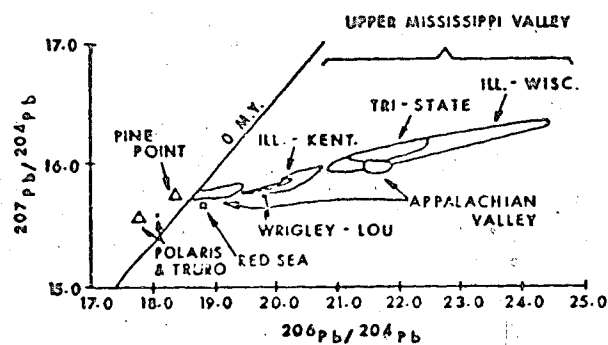


Fig. 27. Range of uranium derived lead isotope compositions observed for the Polaris-Truro and Wrigley-Lou deposits. Pine Point values after Cumming and Robertson (1969), Red Sea values from Delevaux *et al.* (1967) and other Mississippi Valley deposit data from Heyl *et al.* (1966). Adapted from Fig. 7, Kesler and Ascarrunz-K (1973).

mixing the isotopic homogeneity observed in so many lead deposits (Kollar et al., 1960; Cooper and Richards, 1969). The resulting ratios should be close to average lead for at least that portion of the crust affected by the circulating solution". From this, it would appear that the Mississippi Valley type deposits, which are noted for 'J' type lead, were precipitated from brine solutions (Roedder, 1971; Heyl et al., 1974) before complete mixing and homogeneity were attained. Within this context the Polaris and Truro lead isotope data will be considered.

Fluid inclusion studies of Polaris sphalerite crystals (Jowett, 1975) indicate that the mineral-bearing fluids were Na-Ca-Cl-rich brines. Saline brines are common carriers in sulphide deposits (Roedder, 1967b) and White (1968) considers brines to be capable of leaching the base metals from sediments. Helgeson (1967) proposed that hydrothermal fluids could liberate lead from altered potash feldspars and White (1968) considered fine-grained clastic micas and other clay minerals in arkose as a probable source of lead in geothermal areas. Therefore, it is conceivable that the Polaris and Truro lead was derived from either the Precambrian basement or the sediments that were shed from this basement rock.

Zartman (1974) has considered certain western United States deposits and he found the ore leads derived primarily from the Precambrian basement have model ages that relate to the K-Ar age date of the basement rock. The model age of the Polaris and Truro mineralization is about 525 m.y., based upon the assumption that the data points actually represent one point which lies on the growth curve. Thorsteinsson and Tozer (1970) quote dates for the Cape Columbia Group gneiss of northern Ellesmere Island as  $550 \pm 35$  m.y. and  $535 \pm 35$  m.y. (K-Ar dates) from a schistose sandstone of the

Rens Fiord Complex. Christie (1964) quotes a K-Ar age of 545 m.y. for a biotite gneiss of the Cape Aldrich area, northern Ellesmere Island. This age relationship may indicate that the metals were derived from the Precambrian-Cambrian rock.

The Middle Cambrian orogenic deformation is likely responsible for the age determination, even though the Cambrian rocks may be older than the event(s). The possible events which caused the rock ages were the pre-Late Cambrian (Selwynian) orogeny (Roddick *et al.*, 1967) and/or the pre-Middle Cambrian epeirogeny (Kerr and Christie, 1965). The former produced the Boothia complex of gneiss and schist, while the latter produced movement along the Boothia Arch.

The subsequent Silurian-Devonian Boothia uplift was likely related to the up-dip mobilization of saline metal-bearing fluids. The Boothia uplift, accomplished by near vertical, horst-forming faults (Kerr and Christie, 1965), the surface expression of which is shown in Fig. 22, underwent the most intense pulse of deformation in early-Lower Devonian time (Kerr, 1976). The deformation of the Precambrian rock could have permitted the deep circulation of brines (White, 1968) into and/or release of interstitial fluids from the Precambrian rock. These brines would have leached the metals from the rock and the efficiency of circulation would determine the degree of chemical and isotopic evolution of the lead. The near vertical faults provided avenues of transport for the metal-bearing brine to the place of sulphide deposition.

The sulphide deposition in the Upper Thumb Mountain likely depended upon the interception of the metal-bearing brine with a second sulphur or H<sub>2</sub>S-bearing brine. The buried karst development of the carbonate formation, as earlier considered, along with the tectonic deformation,

produced open areas in the formation which were capable of receiving the sulphide minerals. The up-dip migration of the brines was controlled by the shale formations overlying the carbonate formation.

From the preceding a model for mineral emplacement may be proposed.

#### F. MODEL FOR MINERAL EMPLACEMENT

(1) Deposition of the Paleozoic miogeosynclinal sequence, which includes evaporites (Baumann Fiord and Bay Fiord), carbonate shelf and bank deposits (Thumb Mountain) and shales of Upper Ordovician to Lower Devonian (Irene Bay and Cape Philip), was continuous until tectonic developments of the Mid-Paleozoic epeirogeny and the formation of the Cornwallis Fold Belt.

(2) Karst development of the Thumb Mountain Limestone before erosion exhumed the Thumb Mountain Formation in the development of the Cape Philip-Disappointment Bay angular unconformity. The buried karst development was likely due to weathering of the Cape Philip shales during periods of subaerial exposure that released sulphuric acid from the oxidation of the contained iron sulphides. Thus the acidic groundwaters with ease dissolved the underlying limestone formation.

(3) Major rise of the Boothia uplift and tectonic deformation of the Franklinian miogeosyncline in early Lower Devonian time created structural deformation that released interstitial fluids from or permitted circulation of potential lead-bearing brines in the Precambrian rock. The lead ions were likely transported as a chloride complex (Jackson and Beales, 1967) through the near vertical, horst-forming faults to the younger Ordovician Thumb Mountain Formation, by the mechanism of evaporite brine reflux (Lange and Murray, in press).

(4) The up-dip migration of the lead-bearing saline brine was arrested by the Cape Philip Shale, which acted as a cap rock, within the karst developed terrain.

(5) The second saline brine transported bacterially reduced evaporite sulphate up-dip to be arrested by the Cape Philip Formation.

(6) Precipitation of the sulphide minerals occurred upon the meeting of the two brines below the Cape Philip Formation in the karst developed Thumb Mountain Formation. The precipitation of the sulphide occurred under physico-chemical conditions conducive to sulphide formation. According to Jowett (1975) the deposit was probably formed at a depth of 1/2 km or less and the minimum temperature of mineralization was 52-105°C. The sphalerite-galena sulphur isotope temperatures are 143-170°C (see Table 7).



## Chapter IX

### CONCLUSIONS

The Wrigley-Lou and the Polaris-Truro deposits have many aspects in common, as determined from fluid inclusion studies and sulphur and lead isotope studies. The principal points of comparison are as follows:

(1) The respective deposits are composed predominantly of galena and sphalerite hosted in Paleozoic carbonate formations, and dolomite is the principal carbonate host.

(2) The deposits are localized beneath unconformities and the host formations (i.e., Nahanni and Thumb Mountain Formations) are overlain by argillaceous formations (i.e., Hare Indian and Irene Bay, Cape Philips Formations).

(3) The sulphur of the two mineral districts appears to have been derived from evaporite sequences, the sulphate having been reduced by bacterial action. A brine likely transported the reduced sulphur to the area of mineral deposition.

(4) The respective districts appear to have a metal source in the Precambrian rock. The metals most likely were leached from the crustal rocks by hot saline brines, which acted independently from the sulphur transporting brine. The conformable lead of the Polaris-Truro deposits, however, may signify a deep-seated source and thereby differ from the Wrigley-Lou crustal lead source.

(5) The basement movement in the Franklin Mountains and in the Arctic (Boothia uplift) appears to have aided the preparation of the Paleozoic carbonate formations for mineral deposition, and provided the porous and permeable faults which permitted up-dip migration of the respective brines.

These similarities appear to indicate that the method of formation of the sulphide deposits is comparable. The primary difference between the two districts is the size of the deposits. Presumably the source rocks for the metals in the Franklin Mountains were not as well endowed in metals, or the leaching that extracted the metals was not as efficient, or the preparation of the host rock was not sufficient to permit formation of large tonnage deposits such as those in the Little Cornwallis area. Alternatively, the deposits may have been eroded, or not yet found.

The similar aspects of the two districts indicates that in areas of small deposits there is a potential for large sulphide deposits. The possible control over mineralization may be considered to be the degree of preparation of the host rock for reception of the sulphides. Should karst development of the host rock precede the introduction of sulphur and metal-bearing brines then a large deposit is probable; however, should faulting be the only preparation of the host then large deposits are not likely to form due to the lack of porosity and permeability. Irrespective of the size of the deposit, the grades of mineralization may be comparable.

The Little Cornwallis Island and surrounding district would appear to have greater potential for large tonnage ore deposits than the northern Camell Range area because of the extensive karst development in the Thumb Mountain Formation. But this does not deny the possibility that large tonnage deposits may be found in the Paleozoic carbonates of the northern Cordillera.

PLATE I  
MICROPHOTOGRAPHS

Photograph

Description

1.

The Lou property reverse fault which has brought the basal Landry-Manetoe complex in contact with the base of the Nahanni Formation. The fault is considered to be the result of the Laramide orogeny but is not mineralized.

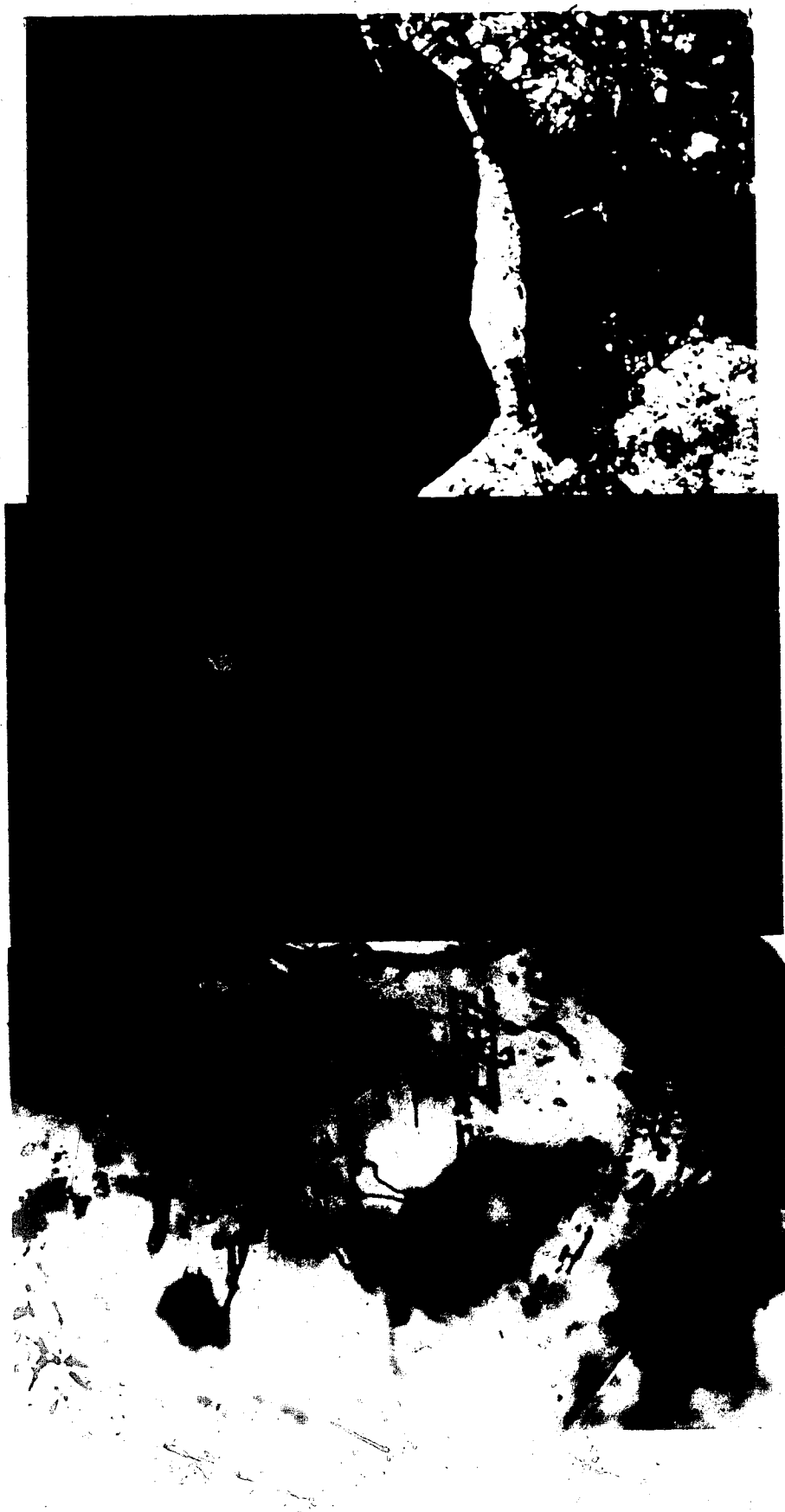
2.

'Crackle' development in the basal Nahanni Formation. A silicified fossil of Favosites limitaris is located bottom center of the picture. Cross-cutting veinlets are welded with white secondary calcite.



PLATE II  
MICROPHOTOGRAPHS

Photograph	Description
3.	A colour-zoned sphalerite crystal fractured due to calcite crystal growth. Note the secondary quartz crystals in the upper right-hand corner. Sample No. B-73-5 (648); magnification 40X.
4.	Dolomite rhomb and pyrite (light grey) contained within. The rhomb probably signifies dolomite post-sulphide stage. Sample No. (379-1); magnification 40X.
5.	Liquid inclusion in orange-red dolomite, 48-1 (345); magnification 400X.



## REFERENCES

- Ault, H.V., 1959: Isotope fractionation of sulphur in geochemical processes. In: *Researches in Geochemistry* (P.H. Abelson, Ed.). Wiley, New York: 241-259.
- Baadsgaard, H., Folinsbee, R.E. and Lipson, J., 1961a: Potassium-argon dates of biotites from Cordilleran granites. *Geol. Soc. Amer., Bull.* 72: 689-702.
- \_\_\_\_\_, 1961b: Caledonian or Acadian granites of the northern Yukon Territory. In: *Geology of the Arctic 1* (G.O. Raasch, Ed.). 458-465.
- Baadsgaard, H., 1964: Geochronology. Paper given at Mineralogisk-Geologisk Institut, Univ. of Copenhagen: 1-47.
- Bachinski, D.J., 1969: Bond strength and sulphur isotopic fractionation in co-existing sulphides. *Econ. Geol.*, 64: 56-65.
- Bassett, H.G., 1961: Devonian stratigraphy, central Mackenzie River region, Northwest Territories, Canada. In: *Geology of the Arctic 1* (G.O. Raasch, Ed.). Alberta Soc. Petrol. Geol. and Univ. of Toronto Press: 481-495.
- Bateman, A.M., 1967: *Economic Mineral Deposits*. Wiley, New York: 916 pp.
- Berry, L.G. and Mason, B., 1959: *Mineralogy - concepts, descriptions, determinations*. W.H. Freeman & Co., San Francisco: 630 pp.
- Billings, G.K., Kesler, S.E. and Jackson, S.A., 1969: Relation to zinc-rich formation waters, northern Alberta, to the Pine Point ore deposit. *Econ. Geol.*, 64: 385-391.
- Bostock, H.S., 1948: Physiography of the Canadian Cordillera with special reference to the area north of the fifty-fifth parallel. *Geol. Soc. Can., Mem.* 247.
- Caldwell, W.G.E., 1971: The biostratigraphy of some Middle and Upper Devonian rocks in the Northwest Territories: a historical review. *The Musk-ox, Publ.* 9: 15-34.
- Cameron, A.E., 1917: Explorations in the vicinity of Great Slave Lake. *Geol. Surv. Can., Summ. Rept.* 1917, Part C: 21-27; fide J. Law, 1971: Regional Devonian geology and oil and gas possibilities, upper Mackenzie River area. *Can. Soc. Petrol. Geol., Bull.* 19: 437-486.

- Campbell, N., 1950: The Middle Devonian in the Pine Point area, Northwest Territories. *Proc., Geol. Assoc. Can.*, 3: 87-96.
- Cannon, R.S.Jr., Pierce, A.P., Antweiler, J.C. and Buck, K.L., 1961: The data of lead isotope geology related to problems of ore genesis. *Econ. Geol.*, 56: 1-38.
- Carpenter, A.B., Trout, M.L. and Pickett, E.E., 1974: Preliminary report on the origin and chemical evolution of lead- and zinc-rich oil field brines in central Mississippi. *Econ. Geol.*, 69: 1191-1206.
- Chatterton, B.D.E., 1976: Aspects of the Lower and Middle Devonian conodont biostratigraphy of western Canada. *Geol. Assoc. Can. and Mineral. Assoc. Can., Programs with Abstracts*, 1: 40.
- Chauhan, D.S., 1974: Diagenetic pyrite from the lead-zinc deposits of Zawar, India. *Mineral. Deposita*, 9: 69-73.
- Christie, R.L., 1964: Geological reconnaissance of northeastern Ellesmere Island, District of Franklin (120, 340, parts of). *Geol. Surv. Can., Mem.* 331.
- Chow, T.J. and Patterson, C.C., 1959: Lead isotopes in manganese nodules. *Geochim. et Cosmochim. Acta*, 17: 21-31.
- 
- 1962: The occurrence and significance of lead isotopes in pelagic sediments. *Geochim. et Cosmochim. Acta*, 26: 263-308.
- Chow, T.J., 1965: Radiogenic leads of the Canadian and Baltic Shield regions. In: *Symposium on Marine Geochemistry*, Rhode Island Univ. Narragansett Marine Lab. Occasional Publ., 3: 169-184.
- Cooper, J.A. and Richards, J.R., 1969: Lead isotope measurements on volcanics and associated galenas from the Coromandel-TeAroha region, New Zealand. *Geochem. Jour.*, 3: 1-14; fide J.R. Richards, 1971: Major lead orebodies - mantle origin?. *Econ. Geol.*, 66: 425-434.
- Cooper, J.A., Reynolds, P.H. and Richards, J.R., 1969: Double spike calibration of the Broken Hill standard lead. *Earth Planet. Sci. Lett.*, 6: 467-478.
- Craig, B.G., 1965: Glacial Lake McConnell and the surficial geology of parts of Slave River and Redstone River map area, District of Mackenzie. *Geol. Soc. Can., Bull.* 122.
- Craig, H., 1966: Isotopic composition and origin of the Red Sea and Salton Sea geothermal brines. *Science*, 154: 1544-1548.
- Crickmay, C.H., 1960: The older Devonian faunas of the Northwest Territories. Evelyn de Mille Books, Calgary: 19 pp.
- Cumming, G.L., 1969: A recalculation of the age of the solar system. *Can. Jour. Earth Sci.*, 6: 719-735.



- Cumming, G.L. and Robertson, D.K., 1969: Isotopic composition of lead from the Pine Point deposit. *Econ. Geol.*, 64: 731-732.
- Cumming, G.L., Burke, M.D., Tsong, F. and McCullough, H., 1971: A digital mass spectrometer. *Can. Jour. Phys.*, 49: 956-965.
- Cumming, G.L., Rollett, J.S., Rossotti, F.J.C. and Whewell, R.J., 1972: Statistical methods for the computation of stability constants, Part I: straight-line fitting of points with correlated errors. *Dalton Trans., Jour. Chem. Soc. Lond.*: 2652-2658.
- Cumming, G.L. and Richards, J.R., 1975: Ore lead isotope ratios in a continuously changing earth. *Earth Planet. Sci. Lett.*, 28: 155-171.
- Czamanske, G.K. and Rye, R.O., 1974: Experimentally determined sulphur isotope fractionations between sphalerite and galena in the temperature range 600° to 275°C. *Econ. Geol.*, 69: 17-25.
- Dahlstrom, C.D.A., 1976: The Snake River iron deposit. 12th Annual Western Inter-University Geological Conf., Edmonton.
- Davidson, C.F., 1966: Some genetic relationships between ore deposits and evaporites. *Trans., Can. Inst. Min. Metall., Sec. B*, 75: B216-B225.
- Davies, G.R. and Krouse, H.R., 1975: Sulphur isotope distribution in Paleozoic sulphate evaporites, Canadian Arctic Archipelago. *Geol. Surv. Can.*, Paper 75-1, Part B: 221-225.
- Delevaux, M.H., Doe, B.R. and Brown, G.F., 1967: Preliminary lead isotope investigations of brine from the Red Sea, galena from the Kingdom of Saudi Arabia and galena from United Arab Republic (Egypt). *Earth Planet. Sci. Lett.*, 3: 139-144.
- de Wit, R., Gronberg, E.C., Richards, W.B. and Richmond, W.O., 1973: Tathlina area, southern District of Mackenzie. In: *The Future Petroleum Provinces of Canada - their Geology and Potential* (R.G. McCrossan, Ed.). *Can. Soc. Petrol. Geol., Mem.* 1: 187-212.
- Doe, B.R., Hedge, C.E. and White, D.E., 1966: Preliminary investigation of the source of lead and strontium in deep geothermal brines underlying the Salton Sea geothermal area. *Econ. Geol.*, 61: 462-483.
- Doe, B.R., 1970: Lead isotopes. In: *Minerals, Rocks and Inorganic Materials Monograph Series of Theoretical and Experimental Studies 3* (H. Von Engelhardt et al., Eds.). Springer-Verlag, New York: 137 pp.
- Doe, B.R. and Delevaux, M.H., 1972: Source of lead in southeast Missouri galena ores. *Econ. Geol.*, 67: 409-425.
- Douglas, R.J.W. and Norris, A.W., 1959: Horn River map area, Northwest Territories. *Geol. Surv. Can.*, Paper 59-11.
- Douglas, R.J.W. and Norris, D.K., 1960: Virginia Falls and Sibbeston Lake map areas, Northwest Territories. *Geol. Surv. Can.*, Paper 60-19.

---

1961: Camsell Bend and Root River map areas, District of Mackenzie, Northwest Territories (95-J and 95-K). Geol. Surv. Can., Paper 61-13.

---

1963: Dahadinni and Wrigley map areas, District of Mackenzie, Northwest Territories (95-N and 95-O). Geol. Surv. Can., Paper 62-33.

Douglas, R.J.W., Gabrielse, H., Wheeler, J.O., Stott, D.F. and Belyea, H.R., 1970: Geology of western Canada. In: Geology and Economic Minerals of Canada (R.J.W. Douglas, Ed.). Geol. Surv. Can., Econ. Geol. Rept. 1, 5th Ed.: 365-488.

Drummond, K.J., 1973: Canadian Arctic Islands. In: The Future Petroleum Provinces of Canada - their Geology and Potential, Mem. 1 (R.G. McCrossan, Ed.). Can. Soc. Petrol. Geol., Publ.: 443-472.

Dunham, K.C., 1966: Role of juvenile solutions, connate waters and evaporitic brines in the genesis of lead-zinc-fluorite-barium deposits. Trans., Can. Inst. Min. Metall., Sec. B, 75: B226-B229.

Eardley, A.J., 1954: Structural geology of North America. (Translation) Izd. Inostr. Lit.; fide T.V. Molchanova, 1968: Zones of resonance-tectonic block structures along the periphery of the circumpacific belt. Geol. Inst. Acad. Sci. USSR, 11: 397-404.

Ellis, A.J. and Golding, R.M., 1963: The solubility of carbon dioxide above 100°C in water and in sodium chloride solutions. Amer. Jour. Sci., 261: 47-60.

Friedman, G.M., 1959: Identification of carbonate minerals by staining methods. Jour. Sed. Petrol., 29: 87-97.

Fritz, P., Drimmie, R.J. and Nowicki, V.K., 1974: Preparation of sulphur dioxide for mass spectrometer analysis by combustion of sulphides with copper oxide. Anal. Chem., 46: 164-166.

Fuerstenau, D.W., Metzger, P.H. and Seele, G.D., 1957: How to use this modified hallimond tube for better flotation testing. Engng. Min. Jour.: 93-95.

Gabrielse, H. and Reesor, J.E., 1964: Geochronology of plutonic rocks in two areas of the Canadian Cordillera. Roy. Soc. Can., Spec. Publ., 8: 96.

Gabrielse, H., 1967: Tectonic evolution of the northern Canadian Cordillera. Can. Jour. Earth Sci., 4: 271-298.

Gabrielse, H., Blusson, S.L. and Roddick, J.A., 1973: Geology of Flat River, Glacier Lake, and Wrigley Lake map areas, District of Mackenzie and Yukon Territory. Geol. Surv. Can., Mem. 366.

Gale, N.H. and Mussett, A.E., 1973: Episodic uranium-lead models and the interpretation of variations in the isotopic composition of lead in rocks. Rev. Geophys. Space Phys., 11: 37-86.

- Gerdemann, P.E. and Myers, H.E., 1972: Relationship of carbonate facies patterns to ore distribution and to ore genesis in the southeast Missouri lead district. *Econ. Geol.*, 67: 426-433.
- Gerling, E.K., 1942: Age of the earth according to radioactivity data. *Doklady Nauk USSR*, 34: 259; 1942: *fide* R.D. Russell and R.M. Farquhar, 1960: Lead isotopes in geology. Interscience, New York: 243 pp.
- Goodman, A.J., 1951: Tectonics of east side of Cordillera in western Canada. *Amer. Assoc. Petrol. Geol., Bull.* 35: 783-796.
- Grootenboer, J. and Schwarcz, H.P., 1969: Experimentally determined sulphur isotope fractionations between sulphide minerals. *Earth Planet. Sci. Lett.*, 7: 162-166.
- Gryc, G., Patton, W.W. and Payne, T.C., 1951: Present Cretaceous stratigraphic nomenclature of northern Alaska. *Jour. Wash. Acad. Sci.*, 41: 159; *fide* H. Gabrielse, 1967: Tectonic evolution of the northern Canadian Cordillera. *Can. Jour. Earth Sci.*, 4: 271-298.
- Haas, J.L.Jr., 1971: The effect of salinity on the maximum thermal gradient of a hydrothermal system at hydrostatic pressure. *Econ. Geol.*, 66: 940-946.
- Hage, C.O., 1945: Geological reconnaissance along lower Liard River, Northwest Territories, Yukon and B.C. *Geol. Surv. Can.*, Paper 45-22.
- Handfield, R.C., 1965: A new lower Cambrian formation in the Mackenzie Mountains. B.Sc. Thesis, Univ. of British Columbia; *fide* H. Gabrielse, 1967: Tectonic evolution of the northern Canadian Cordillera. *Can. Jour. Earth Sci.*, 4: 271-298.
- Harker, P., 1963: Carboniferous and Permian rocks, southwestern District of Mackenzie. *Geol. Soc. Can., Bull.* 95.
- Harrison, A.G. and Thode, G.H., 1958: Sulphur isotope abundances in hydrocarbons and source rocks of Uinta Basin, Utah. *Amer. Assoc. Petrol. Geol., Bull.* 42: 2642-2649.
- Hart, S.R. and Tilton, G.R., 1966: The isotope geochemistry of strontium and lead in Lake Superior waters. In: *The Earth Beneath the Continents* (J.S. Steinhart and J.S. Smith, Eds.): 127-137. *Amer. Geophys. Union Mono.*, 10: 663 pp.
- Helgeson, H.C., 1968: Geologic and thermodynamic characteristics of the Salton Sea geothermal system. *Amer. Jour. Sci.*, 266: 129-166.
- Hewett, D.F., 1928: Dolomitization and ore deposition. *Econ. Geol.*, 23: 821-863.
- Heyl, A.V., 1972: The 38th parallel lineament and its relationship to ore deposits. *Econ. Geol.*, 67: 879-894.

- Hirst, D.M., 1971: Consideration of a sedimentary source for heavy metal content of ore-forming fluids. *Trans., Can. Inst. Min. Metall., Sec. B*, 80: B1-B3.
- Holmes, A., 1946: An estimate of the age of the earth. *Nature*, 157: 680-684.
- Holser, W.T. and Kaplan, I.R., 1966: Isotope geochemistry of sedimentary sulphates. *Chem. Geol.*, 1: 93-135.
- Houtermans, F.G., 1946: The isotope ratios in natural lead and the age of uranium. *Natur Wissenschaften*, 33: 185-186.
- Hume, G.S., 1921: North Nahanni and Root River area and Caribou Island, Mackenzie River District. *Geol. Surv. Can., Summ. Rept. 1921, Part B*: 67-78.
- , 1954: The lower Mackenzie River area, Northwest Territories and Yukon. *Geol. Surv. Can., Mem.* 273.
- Hume, G.S. and Link, T.A., 1945: Canol geological investigations in the Mackenzie River area, Northwest Territories and Yukon. *Geol. Surv. Can., Paper* 45-16.
- Ivanov, V.V., 1961: Geochemistry of cadmium in the deposits of the Deputatskoye Group. *Geochem. Jour.*, 2: 168-217.
- Jackson, S.A. and Beales, F.W., 1967: An aspect of sedimentary basin evolution: the concentration of Mississippi Valley type ores during late stages of diagenesis. *Can. Soc. Petrol. Geol., Bull.* 15: 383-433.
- Jensen, M.L., 1959: Sulphur isotopes and hydrothermal mineral deposits. *Econ. Geol.*, 54: 374-394.
- Jensen, M.L. and Nakai, N., 1962: Sulfur isotope meteorite standards results and recommendations. In: *Biogeochemistry of Sulfur Isotopes* (M.L. Jensen, Ed.). *Proc. of Nat. Sci. Found. Symp., Yale Univ.*: 30-35.
- Jensen, M.L. and Dessau, G., 1967: The bearing of sulfur isotopes on the origin of Mississippi Valley type deposits. In: *Genesis of Stratiform Lead-Zinc-Barite-Fluorite Deposits in Carbonate Rocks - A Symposium* (J.S. Brown, Ed.). *Econ. Geol.*: 400-409.
- Jowett, E.C., 1975: Nature of the ore-forming fluids of the Polaris lead-zinc deposit, Little Cornwallis Island, N.W.T. from fluid inclusion studies. *Can. Inst. Min. Metall., Bull.* 68: 124-129.
- Kajiwarra, Y. and Krouse, H.R., 1971: Sulphur isotope partitioning in metallic sulphide system. *Can. Jour. Earth Sci.*, 8: 1397-1408.
- Kalliokski, J., 1965: Framboids-macrocrystals of colloidal pyrite. *Econ. Geol.*, 60: 1562 (Abstract); *fide* D.S. Chauhan, 1974: Diagenetic pyrite from the lead-zinc deposits of Zawar, India. *Mineral. Deposita*, 9: 69-73.

Kanasewich, E.R., 1962: Approximate age of tectonic activity using anomalous lead isotopes. *Roy. Astron. Soc. Geophys. Jour.*, 7: 158-168.

————— 1968a: The interpretation of lead isotopes and their geological significance. In: *Radiometric Dating for Geologists* (E.I. Hamilton and R.M. Farquhar, Eds.). Interscience, New York: 147-223.

————— 1968b: Precambrian Rift: genesis of stratabound ore deposits. *Science*, 161: 1002-1005.

Kaplan, I.R., Emery, K.O. and Rittenberg, S.C., 1963: The distribution and isotopic abundance of sulphur in recent marine sediments of southern California. *Geochim. et Cosmochim. Acta*, 27: 297-332; *fide* D.S. Chauhan, 1974: Diagenetic pyrite from the lead-zinc deposits of Zawar, India. *Mineral. Deposita*, 9: 69-73.

Kemp, A.W.L. and Thode, H.G., 1968: The mechanism of the bacterial reduction of sulphate and of sulphite from fractionation studies. *Geochim. et Cosmochim. Acta*, 32: 71-91.

Kerr, J.W. and Christie, R.L., 1965: Tectonic history of Boothia uplift and Cornwallis Fold Belt., Arctic Canada. *Amer. Assoc. Petrol. Geol., Bull.* 49: 905-926.

Kerr, J.W., 1975: Summary of stratabound zinc-lead deposits of Little Cornwallis Island and nearby islands, Canadian Arctic. *Geol. Surv. Can., Paper 75-1, Part B*.

————— 1976: A tectonic model for lead-zinc deposition in the Canadian Arctic. 12th Annual Western Inter-University Geological Conf., Edmonton.

Kesler, S.E., Stoiber, R.E. and Billings, G.K., 1972: Direction of flow of mineralizing solutions at Pine Point, N.W.T.. *Econ. Geol.*, 67: 19-24.

Kesler, S.E. and Ascarrunz-k, R., 1973: Lead-zinc mineralization in carbonate rocks, central Guatemala. *Econ. Geol.*, 68: 1263-1274.

Kindle, E.M. and Bosworth, T.O., 1920: Oil-bearing rocks of the lower Mackenzie River valley. *Geol. Surv. Can., Summ. Rept. 1920, Part B*: 37-63.

King, P., 1961: The geological development of North America. (Translation) *Izd. Inostr. Lit.*; *fide* T.V. Molchanova, 1968: Zones of resonance-tectonic block structures along the periphery of the circumpacific-belt. *Geol. Inst. Acad. Sci. USSR*, 11: 397-404.

Koeppel, V.H. and Saager, R.S., 1974: Lead isotope evidence on the detrital origin of Witwatersrand pyrite and its bearing on the provenance of the Witwatersrand gold. *Econ. Geol.*, 69: 318-331.

Kollar, R., Russell, R.D. and Ulrych, T.J., 1960: Precision intercomparisons of lead isotope ratios, Broken Hill and Mount Isa. *Nature*, 187: 754-756.

Kulp, J.L., 1960: The geological time scale. 21st I.G.C., Part III: 18.

- Kuo, S.L. and Folinsbee, R.E., 1974: Lead isotope geology of mineral deposits spatially related to the Tintina Trench, Yukon Territory. *Econ. Geol.*, 69: 806-813.
- Lange, I.M. and Murray, R.C., 1975: Evaporite brine reflux as a mechanism for moving deep warm brines upward in the formation of Mississippi Valley type base metal deposits. *Sci. Comm.*, in press.
- Laporte, L.F., 1969: Recognition of a transgressive carbonate sequence within an epeiric sea: Helderberg Group (Lower Devonian) of New York state. In: *Depositional Environments in Carbonate Rocks* (G.M. Friedman, Ed.). *Soc. Econ. Paleo. Mineral., Spec. Publ.*, 14: 98-119.
- Law, J., 1971: Regional Devonian geology and oil and gas possibilities, upper Mackenzie River area. *Can. Soc. Petrol. Geol., Bull.* 19: 437-486.
- Lebedev, L.M., 1972: Modern growth of sphalerite in Cheleken Peninsula. *Int. Geol. Rev.*, 14: 959-965.
- LeCouteur, P.C., 1973: A study of lead isotopes from mineral deposits in southeastern British Columbia and in the Anvil Range, Yukon Territory. Unpubl. Ph.D. Thesis, Univ. of British Columbia.
- Leech, A.P., 1966: Potassium-argon dates of basic intrusive rocks of the District of Mackenzie, N.W.T. *Can. Jour. Earth Sci.*, 3: 389-412.
- Lemmlein, G.G. and Klevtsov, P.V., 1961: Relations among the principal thermodynamic parameters in a part of the system  $H_2O-NaCl$ . *Geochem. Jour.*, 2: 148-158.
- Levorsen, A.I., 1967: *Geology of Petroleum*. W.H. Freeman & Co., San Francisco: 724 pp.
- Love, W.G., 1967: Early diagenetic iron sulphide in recent sediment of the wash (England). *Sedimentology*, 9: 327-352; *fide* D.S. Chauhan, 1974: Diagenetic pyrite from the lead-zinc deposits of Zawar, India. *Mineral. Deposita*, 9: 69-73.
- Lowell, J.D., 1974: Plate tectonics and foreland basement deformation. *Geology*, 2: 275-278.
- McNamara, J. and Thode, H.G., 1950: Comparison of the isotopic constitution of terrestrial and meteoritic sulphur. *Phys. Rev.*, 78: 307-308; *fide* W.V. Ault, 1950: Isotopic fractionation of sulphur in geochemical processes. In: *Researches in Geochemistry* (P.H. Abelson, Ed.). Wiley, New York: 241-259.
- Martin, L.J., 1959: Stratigraphy and depositional tectonics of north Yukon-lower Mackenzie area. *Amer. Assoc. Petrol. Geol., Bull.* 43: 2399-2455.
- McCrossan, R.G. and Porter, J.W., 1973: The geology and petroleum potential of the Canadian sedimentary basins - a synthesis. In: *The Future Petroleum Provinces of Canada - their Geology and Potential* (R.G. McCrossan, Ed.). *Can. Soc. Petrol. Geol., Mem.* 1: 589-720.

- McCullough, H. and Krouse, H.R., 1965: Application of digital recording to simultaneous collection in mass spectrometry. *Rev. Sci. Instr.*, 36: 1132-1134.
- McLaren, D.J., Norris, A.W. and Cumming, L.M., 1970: Devonian faunas. In: *Geology and Economic Minerals of Canada* (R.J.W. Douglas, Ed.). *Geol. Surv. Can., Econ. Geol. Rept.* 1, 5th Ed.: 614-622.
- Meijer-Drees, N.C., 1974: Geology of the 'Bulmer Lake High', a gravity feature in the southern Great Bear plain, District of Mackenzie. In: *Report of Activities, Part B, November 1973 to March 1974*. *Geol. Surv. Can., Paper* 74-40: 274-276.
- Molchanova, T.V., 1968: Zones of resonance-tectonic block structures along the periphery of the circum-Pacific belt. *Geol. Inst. Acad. Sci. USSR*, 11: 397-404.
- Monster, J., 1972: Homogeneity of sulphur and carbon isotope ratios  $^{34}\text{S}/^{32}\text{S}$  and  $^{13}\text{C}/^{12}\text{C}$  in petroleum. *Amer. Assoc. Petrol. Geol., Bull.* 56: 941-949.
- Newhouse, W.H., 1932: The composition of vein solutions as shown by liquid inclusions in minerals. *Econ. Geol.*, 27: 419-436.
- Noble, J.P.A. and Ferguson, R.D., 1973: Facies relations at edge of early Mid-Devonian carbonate shelf, south Nahanni River area, N.W.T. In: *Arctic Geology* (M.G. Pitcher, Ed.). *Amer. Assoc. Petrol. Geol., Mem.* 19: 83-96.
- Norford, B.S. and Macqueen, R.W., 1975: Lower Paleozoic Franklin Mountain and Mount Kindle Formations, District of Mackenzie: their type sections and regional development. *Geol. Surv. Can., Paper* 74-34.
- Norris, A.W., 1968: Reconnaissance Devonian stratigraphy of northern Yukon Territory and northwestern District of Mackenzie. *Geol. Surv. Can., Paper* 76-53.
- Norris, D.K., 1972: En échelon folding in the northern Cordillera of Canada. *Can. Soc. Petrol. Geol., Bull.* 20: 634-642.
- Ohmoto, H., 1972: Systematics of sulphur and carbon isotopes in hydrothermal ore deposits. *Econ. Geol.*, 67: 551-578.
- Ostic, R.G., Russell, R.D. and Stanton, R.L., 1967: Additional measurements of the isotopic composition of lead from stratiform deposits. *Can. Jour. Earth Sci.*, 4: 245-269.
- Oversby, V.M., 1970: The isotopic composition of lead in iron meteorites. *Geochim. et Cosmochim. Acta*, 34: 65-75.
- Ozard, J.M., Slawson, W.F. and Russell, R.D., 1973: An integrated model for lead isotopic evolution for samples from the Canadian Shield. *Can. Jour. Earth Sci.*, 10: 529-537.

- Patterson, C.C., 1955: The  $^{207}\text{Pb}/^{206}\text{Pb}$  ages of some stone meteorites. *Geochim. et Cosmochim. Acta*, 1: 151.
- 1956: Age of meteorites and the earth. *Geochim. et Cosmochim. Acta*, 10: 230.
- Patterson, C.C. and Tatsumoto, M., 1964: The significance of lead isotopes in detrital feldspar with respect to the chemical differentiation of the earth's mantle. *Geochim. et Cosmochim. Acta*, 28: 1-22.
- Ramdohr, P., 1950: *Der Urmineralien und ihre erwachsungen*. Akademie-Verlag, Berlin: 875 pp; *fide* *Applied Ore Microscopy, Theory and Technique* (H. Freund, Ed.). MacMillan Co., New York: 544, 1966.
- 1966: The microscopical investigation of primary uranium minerals. In: *Applied Ore Microscopy, Theory and Technique* (H. Freund, Ed.). MacMillan Co., New York: 541-554, 1966.
- Reynolds, P.H. and Dasch, E.J., 1971: Lead isotopes in marine manganese nodules and the ore-lead growth curve. *Jour. Geophys. Res.*, 76: 5124-5129; *fide* R.E. Zartman, 1974: Lead isotopic provinces in the Cordillera of the western United States and their geological significance. *Econ. Geol.*, 69: 792-805.
- Richards, J.R., 1971: Major lead orebodies - mantle origin?. *Econ. Geol.*, 66: 425-434.
- Robinson, J., 1971: Studies on the Echo Bay silver deposit, Northwest Territories, Canada. Unpubl. Ph.D. Thesis, Univ. of Alberta.
- Robinson, J. and Ohmoto, H., 1973: Mineralogy, fluid inclusions, and stable isotopes of the Echo Bay Ag-Cu deposits, Northwest Territories, Canada. *Econ. Geol.*, 68: 549-556.
- Roddick, J.A., Wheeler, J.O., Gabrielse, H. and Souther, J.G., 1973: Age and nature of the Canadian part of the circum-Pacific orogenic belt. *Tectonophysics*, 4: 319-337; *fide* R.G. McCrossan and J.W. Porter, 1973: The geology and petroleum potential of the Canadian sedimentary basins. In: *The Future Petroleum Provinces of Canada - their Geology and Potential* (R.G. McCrossan, Ed.). Can. Soc. Petrol. Geol., Mem. 1: 589-720.
- Roedder, E., 1962: Studies of fluid inclusions I: low temperature application of a dual-purpose freezing and heating stage. *Econ. Geol.*, 57: 1045-1061.
- 1963: Studies of fluid inclusions II: freezing data and their interpretation. *Econ. Geol.*, 58: 167-211.
- 1967a: Fluid inclusions as samples of ore fluids. In: *Geochemistry of Hydrothermal Ore Deposits* (H.L. Barnes, Ed.). Holt, Rinehart and Winston Inc., New York: 515-574.
- 1967b: Environment of deposition of stratiform (Mississippi Valley type) ore deposits, from studies of fluid inclusions. In: *Genesis of Stratiform Lead-Zinc-Barite-Fluorite Deposits in Carbonate Rocks - A Symposium* (J.S. Brown, Ed.). *Econ. Geol.*: 349-361.



- \_\_\_\_\_ 1968: Temperature, salinity, and origin of the ore-forming fluids at Pine Point, Northwest Territories, Canada, from fluid inclusion studies. *Econ. Geol.*, 63: 439-450.
- \_\_\_\_\_ 1971: Fluid inclusion evidence on the environment of formation of mineral deposits of the southern Appalachian Valley. *Econ. Geol.*, 66: 777-791.
- \_\_\_\_\_ 1972: Composition of fluid inclusions. In: *Data of Geochemistry* (M. Fleischer, Ed.). U.S. Geol. Surv., Prof. Paper 440-JJ: 1-164.
- Roedder, E. and Skinner, B.J., 1968: Experimental evidence that fluid inclusions do not leak. *Econ. Geol.*, 63: 715-730.
- Ross, D.A., 1972: Red Sea hot brine area. *Rev. Sci. Instru.*, 175: 1455-1456.
- Russell, R.D., 1963: Some recent researches on lead isotope abundances. *Earth Sci. and Meteorites*, North-Holland Publishing Co., Amsterdam: 44-73.
- \_\_\_\_\_ 1972: Evolutionary model for lead isotopes in conformable ores and in ocean volcanics. *Rev. Geophys. Space Phys.*, 10: 529-549.
- Russell, R.D. and Farquhar, R.M., 1960: Lead isotopes in geology. *Interscience*: 243 pp.
- Russell, R.D. and Reynolds, P.H., 1965: The age of the earth. In: *Problems of Geochemistry* (N.I. Khitarov, Ed.). Nauka, Moscow: 37-49, (in Russian). English version, Israel Program for Scientific Translations, Jerusalem: 35-48, 1969; *fide* G.L. Cumming and J.R. Richards, 1975: Ore lead isotope ratios in a continuously changing earth. *Earth Planet. Sci. Lett.*, 28: 155-171.
- Russell, R.D., Kanasewich, E.R. and Ozard, J.M., 1966: Isotopic abundances of lead from a "frequently-mixed" source. *Earth Planet. Sci. Lett.*, 1: 85-88.
- Rye, R.O., 1974: A comparison of sphalerite-galena sulphur isotope temperatures with filling temperatures of fluid inclusions. *Econ. Geol.*, 69: 26-32.
- Rye, R.O. and Ohmoto, O., 1974: Sulphur and carbon isotopes and ore genesis: a review. *Econ. Geol.*, 69: 826-842.
- Rye, R.O., Doe, B.R. and Delevaux, M.H., 1974: Homestake Gold Mine, South Dakota II: Lead isotopes, mineralization ages, and source of lead in ores of the northern Black Hills. *Econ. Geol.*, 69: 814-822.
- Sakai, H., 1957: Fractionation of sulphur isotopes in nature. *Geochim. et Cosmochim. Acta*, 12: 150-169.
- Sangster, D.F., 1968: Relative sulphur isotope abundances of ancient seas and stratabound sulphide deposits. *Proc., Geol. Assoc. C.* 19: 79-91.
- \_\_\_\_\_ 1971: Geological significance of stratabound sulphide deposits. *Proc., Geol. Assoc. Can.*, 23: 69-72.

- 1974: Geology of Canadian lead-zinc deposits. Geol. Surv. Can., Paper 74-1, Part A: 141-142.
- 1975: Canadian carbonate-hosted lead-zinc deposits: a summary. Geol. Soc. Amer., Abstracts with Programs, 7: 848.
- Sangster, D.F. and Lancaster, R.D., 1976: Geology of Canadian lead and zinc deposits. Geol. Surv. Can., Paper 76-1A, Part A: 301-310.
- Sasaki, A. and Krouse, H.R., 1969: Sulphur isotopes and the Pine Point lead-zinc mineralization. Econ. Geol., 64: 718-730.
- Sasaki, A. and Kajiwara, Y., 1971: Evidence of isotopic exchange between sea water sulphate and some syngenetic sulphide ores. In: Proc. IMA-IAGOD Meetings, 1970, IAGOD Volume. Soc. Min. Geol., Japan, Spec. Issue, 3: 289-294.
- Schwarcz, H.P. and Burnie, S.W., 1973: Influence of sedimentary environments on sulphur isotope ratios in clastic rocks: a review. Mineral. Deposita, 8: 264-277.
- Shaw, A.B., 1964: Time in Stratigraphy. McGraw-Hill, Toronto: 385 pp.
- Simpson, R.G., 1975: Stratigraphy and paleoecology of the Hahanni and Headless Formations, north Camell Range, N.W.T. Unpubl. B.Sc. thesis, Univ. of British Columbia.
- Sinha, A.K. and Tilton, G.R., 1973: Isotopic evolution of common lead. Geochim. et Cosmochim. Acta, 37: 1823-1849.
- Skinner, B.J., 1967: Precipitation of Mississippi Valley type ores: a possible mechanism. In: Genesis of Stratiform Lead-Zinc-Barite-Fluorite Deposits in Carbonate Rocks - A Symposium (J.S. Brown, Ed.). Econ. Geol.: 363-369.
- Skinner, B.J., White, D.E., Rose, H.J. and Mays, R.E., 1967: Sulphides associated with the Salton Sea geothermal brine. Econ. Geol., 62: 316-330.
- Smirnov, G.A., Fedorova, G.G. and Pumpyanskii, A.M., 1969: Conditions for the formation of flint in carbonate rocks. Inst. Geol. Geochem., 3: 119-125.
- Sonnenfeld, P., 1963: Dolomites and dolomitization: a review. Can. Soc. Petrol. Geol., Bull. 12: 101-132.
- Stacey, J.S. and Kramers, J.D., 1975: Approximation of terrestrial lead isotope evolution by a two-stage model. Earth Planet. Sci. Lett., 26: 207-221.
- Stanton, R.L. and Russell, R.D., 1959: Anomalous leads and the emplacement of lead sulphide ores. Econ. Geol., 54: 588-607.
- Stockwell, C.H., McGlynn, J.C., Emslie, R.F., Sanford, B.V., Norris, A.W., Donaldson, J.A., Fahrig, W.F. and Currie, K.L., 1970: Geology of the Canadian Shield. In: Geology and Economic Minerals of Canada (R.J.W. Douglas, Ed.). Geol. Surv. Can., Econ. Geol. Rept. 1, 5th Ed.: 43-150.

- Tatsumoto, M., Knight, R.J. and Allegre, C.J., 1973: Time differences in the formation of meteorites as determined from the ratio of lead-207 to lead-206. *Science*, 180: 1279; fide J.S. Stacey and J.D. Kramers, 1975: Approximation of terrestrial lead isotope evolution by a two-stage model. *Earth Planet. Sci. Lett.*, 26: 207-221.
- Thode, H.G. and Monster, J., 1965: Sulphur-isotope geochemistry of petroleum, evaporites, and ancient seas. In: *A Symposium - Fluids in Subsurface Environments* (A. Young and J.E. Galley, Eds.). Amer. Assoc. Petrol. Geol., Publ.: 367-377.
- Thode, H.G., McNamara, J. and Collins, C.B., 1949: Natural variations in the isotopic content of sulphur and their significance. *Can. Jour. Res.*, B27: 361-373; fide W.V. Ault, 1959: Isotopic fractionation of sulphur in geochemical processes. In: *Researches in Geochemistry* (P.H. Abelson, Ed.). Wiley, New York: 241-259.
- Thode, H.G., Wanless, R.K. and Wallouch, R., 1954: The origin of native sulphur deposits from isotope fractionation studies. *Geochim. et Cosmochim. Acta*, 5: 286-298.
- Thode, H.G., Monster, J. and Dunford, H.B., 1958: Sulphur isotope abundances in petroleum and associated materials. *Amer. Assoc. Petrol. Geol., Bull.* 42: 2619-2641.
- Thode, H.G., Harrison, A.G. and Monster, J., 1960: Sulphur isotope fractionation in early diagenesis of recent sediments of northeast Venezuela. *Amer. Assoc. Petrol. Geol., Bull.* 44: 1809-1817.
- Thorsteinsson, R. and Kerr, J.W., 1968: Cornwallis Island and adjacent smaller islands, Canadian Arctic Archipelago. *Geol. Surv. Can.*, Paper 67-64.
- Thorsteinsson, R. and Tozer, E.T., 1970: Geology of the Arctic Archipelago. In: *Geology and Economic Minerals of Canada* (R.J.W. Douglas, Ed.). *Geol. Surv. Can., Econ. Geol. Rep.*, 1, 5th Ed.: 547-590.
- Tilton, G.R., Patterson, C., Brown, H., Inghram, M., Hayden, R., Hess, D. and Larsen, E., 1955: Isotopic composition and distribution of lead, uranium, and thorium in a Precambrian granite. *Geol. Soc. Amer., Bull.* 66: 1113-1148.
- Trudinger, P.A., Lambert, I.B. and Skyring, G.W., 1972: Biogenic sulphide ores: a feasibility study. *Econ. Geol.*, 67: 1114-1127.
- Wanless, R.K., Stevens, R.D., Lachance, G.R. and Rimsaite, R.Y.H., 1964: Age determinations and geological studies, Part I: isotopic ages, report 5. *Geol. Soc. Can., Paper* 64-17, Part 1.
- \_\_\_\_\_ 1966: Age determinations and geological studies, Part II: K-Ar isotopic ages, report 6. *Geol. Soc. Can., Paper* 66-17.
- Warren, P.S. and Steick, C.R., 1962: Western Canadian Givetian. *Alberta Soc. Petrol. Geol.*, 10: 173-291.

Wheeler, J.O., 1959: Mesozoic tectonics of central southern Yukon. Geol. Assoc. Can., 11: 23.

White, D.E., 1967: Outline of thermal and mineral waters as related to origin of Mississippi Valley ore deposits. In: Genesis of Stratiform Lead-Zinc-Sparite-Fluorite Deposits in Carbonate Rocks - A Symposium (J.S. Brown, ed.). Econ. Geol.: 379-381.

——— 1968: Environments of generation of some base-metal ore deposits. Econ. Geol., 63: 301-335.

——— 1974: Diverse origins of hydrothermal ore fluids. Econ. Geol., 69: 945-973.

Yermakov, N.P., et al., 1965: Research on the nature of mineral-forming solutions. (E. Roedder, Ed.). Pergamon Press, Oxford: 743 pp.

Zartman, R.E., 1974: Lead isotopic provinces in the Cordillera of the western United States and their geological significance. Econ. Geol., 69: 792-805.

## APPENDIX I

### Sample Description

- 76-1 (25) Massive sulphides with no associated gangue carbonate. Quartz crystals are disseminated throughout the sulphides (Nahanni Formation).
- 48-1 (61) The sulphide mineralization is contained within grey siliceous dolomite, which is cut by stylolites and calcite healed veins (Nahanni Formation).
- 48-1 (94) Lead-zinc mineralization contained within veinlets is in association with iron-poor dolomite and silica. Disseminated pyrite occurs predominantly in the gangue dolomite, and to a minor degree in the galena. Cross-cutting veins of iron-free white calcite and quartz are not mineralized (Nahanni Formation).
- 48-1 (291) Galena crystals and minor pyrite are localized within shaley stylolites. The host is grey siliceous-limy dolomite which is cross-cut by iron-free calcite healed veinlets (Nahanni Formation).
- 48-1 (375,383) The lead-zinc mineralization is in silicic, grey dolomite, and vug development is filled with iron-poor spar calcite (Headless Formation).
- 48-1 (44) Pyrite mineralization with minor galena localized within light grey, silicified dolomite, which is cut by bituminous/shaley stylolites (Landry Formation).
- 36-4 (28.5) The lead-zinc mineralization is in silicified grey carbonate, cross-cut by stylolites containing shaley bituminous matter. Adjacent to the mineralization is iron-poor to iron-free white spar calcite, apparently post-mineral vein filling (Nahanni Formation).
- 36-4 (82.5) Galena and sphalerite (3-5%) is in grey and white dolomitic calcite which is cut by non-mineralized calcite healed fractures of a fine nature (Nahanni Formation).
- 36-4 (259) Diagenetic pyrite contained within calcareous-argillaceous shale. This represents a bituminous-shaley bed within the Nahanni limestone. Non-mineralized iron-free calcite veinlets cross-cut the sample (Nahanni Formation).
- 36-4 (345) The sulphides are within spar dolomite, and anhedral quartz crystals are present. Post-sulphide secondary calcite and pyrite fill the vuggy areas (Nahanni Formation).

- 36-5 (311) The galena and sphalerite are in intimate contact. The carbonate host is grey quartz needle-rich dolomite which is cross-cut by white spar calcite veins of the post-mineralization period (Nahanni Formation).
- 36-5 (312) Red to honey-coloured sphalerite is intimately associated with galena within grey dolomite host rock. Secondary drusy white calcite development occurs within vugs and this carbonate appears to corrode the sulphides (Nahanni Formation).
- 12-2 (130.5, 119.5) Thinly bedded, fine-grained, black, pyritic, calcareous shale of the Hare Indian Formation. Fenestella texture is revealed which may be of diagenetic derivation. Diagenetic silica is evident, as is fossil material.
- 12-4 (255) Grey siliceous dolomite hosts galena, sphalerite and pyrite. The host is cut by white spar dolomite and calcite healed fractures which lack mineralization (Nahanni Formation).
- 12-4 (349) Galena and sphalerite with very minor pyrite. The mineralization is both disseminated within siliceous dolomite and within cross-cutting stylolites which contain bituminous/shaley matter (Nahanni Formation).
- B-73-5 (195) Galena and sphalerite in grey siliceous dolomite. Some alteration is evident and solution vugs are lined with drusy quartz needles (Nahanni Formation).
- B-73-5 (537) Galena and sphalerite are localized in grey silicified dolomite and are often in close proximity to stylolites. Cross-cutting white vein dolomite is not mineralized (Nahanni Formation).
- B-73-5 (648) Grey siliceous dolomite is the host to sulphide mineralization. Veinlets of iron-free calcite and iron-free dolomite cut the mineralized dolomite, and represent a late stage development. The sulphides are not associated with the late stage veining (Headless Formation).
- 36-1 (54) Large yellow orange sphalerite crystals within a dolomitic host of a fracture system (Nahanni Formation).
- 36-8 (166) Large white-yellow to red sphalerite crystals within a silicified-dolomite host. Galena is a minor constituent. Stylolite development is quite extensive (Nahanni Formation).
- Hammer Massive galena mineralization contained within a vein structure which cross-cuts the Nahanni Formation. Post-mineral tectonic fractures have been healed with secondary spar calcite. Euhedral quartz development is evident in association with the mineralization (Nahanni Formation).

- 12N-2+50E Grey 'quartz needle' dolomite is the principal host to galena and sphalerite mineralization. The host dolomite is cross-cut by white spar dolomite which contains minor galena mineralization and large (to 1 cm) euhedral quartz crystal development (Nahanni Formation).
- Fluorite Mauve and purple crystals (to 3 mm) in silicified, grey dolomite. Minor sphalerite mineralization is associated with the fluorite development. Tectonic deformation has broken the rock permitting a certain degree of oxidation (Nahanni Formation).
- Bourne Massive galena mineralization which is tectonically fractured, healed by spar calcite, is structurally controlled within the Nahanni Formation. 'Viscous' type silicification is present in the galena. Essentially no sphalerite is to be found (Nahanni Formation).

#### Polaris-Truro Samples

- 7894 Massive lead-zinc mineralization from Polaris deposit. The galena is a fine-grained sphalerite crusted with galena cubes.
- 7895 Truro lead-zinc mineralization in dolomite.
- 7896 Colloform sphalerite and galena mineralization, from Truro.
- 7897 Massive galena-sphalerite mineralization in a banded aggregation (Truro deposit).
- 7898 Massive galena-sphalerite mineralization of the Truro deposit.
- 7899 Massive colloform sphalerite with galena as inter-bands and as cubes. Pyrite is both intimately associated with the Zn/Pb and is within open vugs (Polaris deposit).
- 7903-A A massive sphalerite-galena sample from the Polaris deposit.

## APPENDIX II

### Sulphur Isotope Sample Preparation

The samples were chosen following petrographic examination in order to obtain sphalerite-galena pairs which appeared to be 'co-existent'. The samples were washed in an ultrasonic bath, crushed and sieved to 100-140 mesh size. Because contamination was a consideration, all equipment was thoroughly washed, and where possible the ultrasonic bath employed.

Some crushed sulphide samples were separated from the gangue carbonate and silica using methylene iodide; however, separation of the galena and sphalerite was not possible on the Franz Magnetic Separator likely due to the lack of iron in sphalerite. The modified Hallimond tube method (Fuerstenau et al., 1957) was adopted. Although the flotation cell was designed for 65 to 100 mesh feed, the finer grain size would work but with a reduced percentage recovery. The 100-140 mesh size was necessary to evade intergrown gangue minerals with the sulphides. Methylene iodide could not be used before flotation because the heavy liquid alters the mineral surface by coating it and then the flotation or depression of respective minerals does not occur. The size of sample floated was 2-3 grams, the reagents used were K-ethyl-xanthate (25 mg/l) and sodium cyanide (.25 g/l); frother was considered to be unnecessary. The sample was initially conditioned for five minutes in 100 ml solution of the reagents in a stoppered flask, then transferred to the flotation cell. A magnetic stirrer agitated the sample and nitrogen air bubble stream carried the galena to the concentrate stem. The purity of the galena concentrate was about 85-90%. To separate the sphalerite grains from the tailings methylene iodide was used. To gain near 100% purity all samples were hand-picked using a binocular microscope.



### Preparation of Sulphur Dioxide for Mass Spectrometer Analysis

The pure sphalerite and galena samples were individually weighed, and recorded. The sphalerite sample not to exceed 25 mg and galena 60 mg, because larger samples would produce an excessive amount of sulphur gas. The sulphides were combusted with copper oxide, and the copper oxide amount necessary for combustion did not need to exceed 368 mg and 287 mg, respectively. Each sulphide sample was ground with mortar and pestel to a fine powder, as was the copper oxide, and the two were intimately mixed. The mixed sample was then packed in a quartz wool packed open-ended quartz tube. The prepared sample was then combusted in an evacuated chamber at or above 1000°C for 15 minutes. The evolved SO<sub>2</sub> gas was trapped with liquid nitrogen following distillation using dry ice and carbon tetrachloride mixture ( -40°C). The purification of the SO<sub>2</sub> gas (i.e., removal of carbon dioxide) was accomplished with n-pentane and dry ice mixture ( -120°C) through volatilization of the CO<sub>2</sub> gas. The CO<sub>2</sub> gas was collected in a third trap using liquid nitrogen, measured and then pumped out. The sulphur dioxide yield was then determined and transferred to a break-seal. Once sealed in the break-seal the sample was then ready for mass spectrometer analysis. For more detailed explanation of the preparation procedure of the SO<sub>2</sub> gas refer to Fritz et al. (1974).

### Mass Spectrometer

The samples of SO<sub>2</sub> gas were analyzed on a simultaneous ion collection, digital recording mass spectrometer, using a five-figure integrating voltmeter. The mass 64 and 66 ion currents are recorded consecutively for an unknown and standard sample in a <sup>32</sup>S/<sup>34</sup>S analysis (McCullough and Krouse, 1965). The nine recordings are solved consecutively according to (<sup>34</sup>S/<sup>32</sup>S)

sample/ $(^{34}\text{S}/^{32}\text{S})_{\text{line}}$  standard and 8 times average. The standard deviation of a particular run was found to be less than .01% although at times this amount was exceeded slightly.

Standard samples were run at the beginning and end of each operating day. The standard used was NBS Sulphur. At all times the standard analyses were within 0.04% deviation of the previous run. The variation is attributed to fractionation of the gas during freeze-over. This degree of deviation was reached only when the standard gas had been used a number of times.

The machine sulphur line standard was calibrated according to the following standards of known isotopic composition: NBS #120 (Native Sulphur), NBS #200 (Galena, Ivigtut), Peace River Troilite, PbS Line Standard,  $\text{BaSO}_4$  ('Merck'), Pine Creek NW (Sour Gas), and McMaster 'Ag<sub>2</sub>S'. From the developed straight line a correction formula was developed to relate the  $\delta^{34}\text{S}$  of the unknown sample to the known  $\delta^{34}\text{S}$  Canyon Diablo Troilite. The correction formula used in this thesis are:

$$\delta^{34}\text{S}_{\text{CDT-x}}(\%) = \delta^{34}\text{S}_{\text{LS-x}}(\%) \times 1.158 + 4.5 \quad (\text{S. Burnie et al.})$$

$$\delta^{34}\text{S}_{\text{CDT-x}}(\%) = \delta^{34}\text{S}_{\text{LS-x}}(\%) \times 1.1149 + 2.65 \quad (\text{S.L. Kuo})$$

where

$$\delta^{34}\text{S}_{\text{CDT-x}} = \delta^{34}\text{S} \text{ of unknown against } \delta^{34}\text{S} \text{ of Canyon Diablo Troilite}$$

and

$$\delta^{34}\text{S}_{\text{LS-x}} = \delta^{34}\text{S} \text{ of unknown against } \delta^{34}\text{S} \text{ of Line Standard.}$$

Sulphur isotopic data consider the two more abundant species,  $^{32}\text{S}$  and  $^{34}\text{S}$ . The isotopic analytical results are reported as per mil (‰) difference from a primary standard as follows:

$$\delta^{34}\text{S}\% = \frac{(^{34}\text{S}/^{32}\text{S})_{\text{sample}} - (^{34}\text{S}/^{32}\text{S})_{\text{standard}}}{(^{34}\text{S}/^{32}\text{S})_{\text{standard}}}$$

The Canyon Diablo Troilite is the accepted standard ( $^{34}\text{S}/^{32}\text{S} = 0.0450045$ , Jensen and Nakai, 1963), and has a  $\delta^{34}\text{S} = 0\%$ .

The sphalerite-galena sulphur isotope temperatures were determined from the experimentally derived fractionation curve of Czamanske and Rye (1974), and the linear function is described by the equation:

$$1000 \ln_{\infty\text{S}}^{\text{S}} = 7.0 \times 10^5 T^{-2}.$$

### APPENDIX III

Samples of galena and pyrite were prepared for lead isotopic analysis. The following is an itemized list of the procedures adopted to separate the minerals and to purify the lead. The purified lead was used for mass spectrometer analysis.

#### Lead Isotope Sample Preparation

The galena and pyrite samples were physically prepared as follows:

- (1) The selected rock sample was placed in an ultrasonic bath to clean any loose or extraneous rock particles.
- (2) The sample was crushed and sieved to 100-140 mesh size, and each step was executed under conditions of cleanliness.
- (3) The sieved rock sample was suspended in methylene iodide in order to separate the gangue from the sulphides.
- (4) The respective galena and pyrite samples were purified by the Franz Magnetic Separator and by hand-picking so that near 100% purity was attained. At least 20 mg of galena and 250-300 mg of pyrite was purified so that the initial sample was well represented.

#### Chemical Methods

To purify the lead from the galena and the pyrite pure reagents were used. The reagents used are listed below, each having been distilled twice (i.e., lead-free):

- (1) Pure HCl (8 N), (6 N)
- (2) Pure HCl (1.5 N)
- (3) Pure water

The reagents used for silica gel loading of the filament are:

(1) Pure phosphoric acid (0.75 N -- E. Mercks ultrapure diphosphorus pentoxide + pure  $H_2O$ ).

(2) Pure silica gel (B.D.H. iron-free colloidal powder).

In order to avoid lead contamination the glassware (i.e., beakers, columns, etc.) was cleaned in the following manner:

(1) washed in soap,

(2) soaked in chrom-sulphuric acid,

(3) rinsed with double distilled  $H_2O$ ,

(4) soaked overnight in 8 N  $HNO_3$ ,

(5) rinsed with single and double distilled  $H_2O$  and then wrapped in parafilm.

The method of purification adopted was that of ion exchange columns, cation and anion. The ion exchange columns are made of quartz glass of 5 mm diameter, capable of holding 5 cm of resin with 2 cc liquid capacity above the resin. The resin is restrained at the bottom of the column by a quartz frit. The resin is never used twice.

To purify galena-lead the cation exchange column (Dowex 50w x 12,200-400  $H^+$  form) was used. The procedure follows:

(1) Dissolve a few microscopically pure galena cubes in 8 N HCl, and evaporate to dryness.

(2) Dissolve the residue in about 1 ml 1.5 N HCl.

(3) Put the supernatant liquid through the pre-set ion exchange column. The column has been pre-set by rinsing with the following, providing the resin was not in the dry state: (a) 8 N HCl - 10 ml, and (b) 1.5 N HCl - 10 ml.

(4) Rinse the column with the following: (a) 2 ml 1.5 N HCl, (b) 2 ml 1.5 N HCl (collect for Pb analysis), and (c) 2 ml 1.5 N HCl (collect in case some Pb is delayed in passing through the column).

(5) The second 2 ml aliquot is taken to dryness.

(6) Silica gel loading of the button (see below) is the final step before mass spectrometer measurement.

Purification of the pyrite was accomplished by the following procedure:

(1) Decompose approximately 300 mg of microscopically pure pyrite in 1 ml HCl, and take to dryness.

(2) Dissolve the residue in 1-2 ml 1.5 N HCl.

(3) Centrifuge the sample to obtain the supernatant.

(4) Put the supernatant liquid through a pre-set cation exchange column as described above.

The second aliquot collected is then repurified using the anion exchange column (Dowex 1 x 8 reagent grade, 200-400 mesh chloride form).

(1) Put the second aliquot through the pre-set anion exchange column.

(2) Rinse the column with the following: (a) 4 ml 1.5 N HCl, (b) 4 ml 6 N HCl, and (c) 2 ml 6 N HCl (collect for Pb analysis).

(3) Take the 2 ml aliquot to dryness.

The sample (lead chloride) is ready to load onto the filament.

To load the filament:

The lead chloride sample is loaded on a .002 mm refined rhenium ribbon which has been outgassed for 15 minutes at 4 amperes in a vacuum of about  $2 \times 10^{-7}$  Torr. The clean filament is loaded with between 1 and 2  $\mu$ g of purified lead. The silica gel method of loading the filament is as follows:

(1) With a clean capillary tube and pure  $H_2O$  pick up 1 to 2  $\mu g$  of pure lead chloride and place one drop of the sample in the center of the outgassed rhenium filament. Take to dryness by increasing the filament current to 0.8 amperes.

(2) With a second capillary tube add one drop of silica gel-phosphoric acid to the dry lead sample and take to dryness.

(3) Heat the lead-silica gel-phosphoric acid load by increasing the current gradually to 1.2 amperes, and leave it at this amperage for 15 minutes in order to permit the release of bubbles and to allow the silica, lead and phosphoric acid to become evenly distributed.

(4) Increase the current gradually until the load begins to fume (about 2.0-2.1 amperes). Do not alter the current until the fuming has ceased.

(5) Gradually increase the current until the filament glows a dull red (about 2.2 amps). At this point the load has a new white color. The filament is now ready to load in the solid source mass spectrometer.

#### Mass Spectrometer

The analytical results reported in this thesis were derived from a solid source, 12 inch,  $90^\circ$  radius digital mass spectrometer. The mass spectrometer scans by magnetic field sweeping in increments and is synchronized to the data reading function. The data reading function has been modified by addition of a high speed digital voltmeter which allows the data to be recorded on magnetic tape more rapidly. The data are subsequently reduced by an IBM 360 computer, by a method of polynomial fitting (Cumming et al., 1971) which provides a good level of precision.

### Error Considerations and Standardization

The possible sources of error are: (1) lead sample contamination; (2) fractionation; (3)  $^{204}\text{Pb}$ -error; and (4) non-linearity of the electrometer and time constant error.

(1) Lead sample contamination: Contamination may be introduced from reagents, glassware and/or silica gel loading procedure. In order to avoid possible cross-contamination, only pure reagents are used and glassware is washed as described above. The silica gel-phosphoric acid solution is regularly changed, and duplicate runs are made on all samples. The second run is always loaded from a fresh silica gel-phosphoric acid solution. A blank run is used to check the purity of the solution as a final check.

(2) Fractionation error is mass-dependent. Cumming *et al.* (1971) consider fractionation is produced by slow heating to operating temperature, or the positioning of the filament in the mass spectrometer. The former is related to the lead-silica gel-phosphoric acid load composition. The requisite lead load conditions are necessary to insure high temperature stability so that stable ion emission will result without unequal loss of neutral molecules (enriched in  $^{204}\text{Pb}$ ) by evaporation during the heating process.

The fractionation process causes differences between the measured ratios. The  $^{204}\text{Pb}$  isotope, being the lightest isotope, will be released in a greater proportion than the heavier isotopes and this will result in ratio measurements that are lower than the true value (i.e., Cooper *et al.*, 1969, values). To test the relative degree of fractionation of the unknown samples, standards are run and the degree of fractionation



is determined for the standard. This is considered to reflect the conditions of the unknown samples. These calculations will be reviewed subsequently.

(3)  $^{204}\text{Pb}$ -error: Inaccurate measurement of the  $^{204}\text{Pb}$  due to the small peak size may be significant. This error will result in either a larger or smaller  $^{204}\text{Pb}$  peak height measurement. The former would result in ratio measurements approaching the true value while the latter would cause the reverse effect. To test for this error, Broken Hill standard runs were analyzed, as indicated below.

(4) Non-linearity of the electrometer and time constant errors may be a factor, but normally these variations are not weighted in either one direction or another and may be compensated for by averaging a sufficiently large number of values. This area of error is therefore minimized by the computer reduction of data.

To test for the principal errors, namely fractionation and  $^{204}\text{Pb}$ -error:

The Broken Hill standard is run a number of times throughout the period of running the unknown lead samples. The standard ratio values are analyzed in the following manner (Fig. 28).

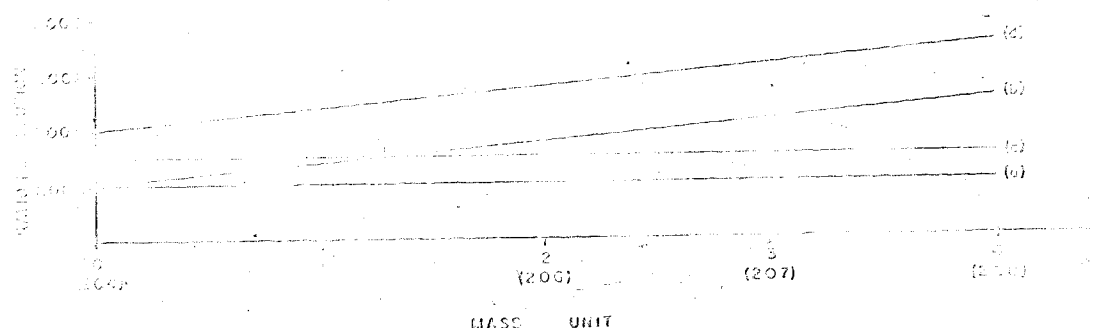


Fig. 28 Method of analysis standard ratio values

The Broken Hill standard ratios experimentally determined are normalized to the known Broken Hill ratios (Cooper et al., 1969), (B.H. true), and these 'measured correction values' are plotted mass unit (B.H. measured) against ratio distribution (Fig. 28). Four conditions may arise:

(1) A straight line plot (a), which passes through 1.000 and is parallel to the x-axis, indicates there is no fractionation and no 204-error.

(2) A line with a slope (b), which intersects the y-axis at 1.000, indicates fractionation error and no 204-error. The degree of slope relates to the amount of fractionation error.

(3) A straight line parallel to x-axis (c), which intersects y-axis at a point other than 1.000, indicates 204-error and no fractionation error. The degree of deviation from 1.000 on the y-axis is related to the amount of 204-error.

(4) A straight line with both slope and intersection of the y-axis (d), other than 1.000, indicates that both fractionation and 204-error have affected the lead isotope ratio values.

When the experimental Broken Hill ratio values are so plotted, usually the line is not straight throughout, as portrayed in line (e), which indicates other errors have had an effect on the ratio values. In such a case, to ascertain the fractionation and 204-error, a best fit straight line is developed according to the equation:

$$y = ax + b$$

where:

$$a = \frac{n\sum xy - \sum x \cdot \sum y}{n\sum x^2 - (\sum x)^2}$$

$$b = \frac{\sum x^2 \cdot \sum y - \sum x \cdot \sum xy}{n\sum x^2 - (\sum x)^2}$$

x represents the respective lead mass units, y represents the respective measured correction factors, a represents the slope of the line, and b is the y-axis intercept. Thus, from fitting the straight line to the standard ratios a fairly accurate assessment of these errors may be determined, which will likely reflect the running conditions of the unknown lead samples.

#### Broken Hill Standard Results:

Six Broken Hill standards were isotopically analyzed and the results are as in Table 9.

The measured correction factors determined from the Cooper et al. (1969) ratio values are:

	Cooper et al. (1969)	B.H.-Measured	Correction Factor
$^{206}\text{Pb}/^{204}\text{Pb}$	16.003	15.966	1.00231
$^{207}\text{Pb}/^{204}\text{Pb}$	15.390	15.311	1.00513
$^{208}\text{Pb}/^{204}\text{Pb}$	35.660	35.441	1.00619

When the measured correction factors are plotted ratio distribution against mass unit, the Fig. 29 plot is attained.

The lack of linearity (Fig. 29) reveals that possible errors other than fractionation and  $^{204}\text{Pb}$  affected the isotope ratios. The other possible errors may include non-linearity of the electrometer and/or time constant error.

To reveal the relation of the standard Broken Hill measured values to the true Broken Hill ratio values in light of  $^{204}\text{Pb}$  and fractionation error, the following plot may be constructed (Fig. 30).

Table 9.  
Broken Hill Lead Isotope Data

$^{206}\text{Pb}/^{204}\text{Pb}$	$^{207}\text{Pb}/^{204}\text{Pb}$	$^{208}\text{Pb}/^{204}\text{Pb}$	
15.9666 .0012	15.3158 .0008	35.4633 .0019	
15.9574 .0049	15.3008 .0078	35.4142 .0085	
15.9630 .0327	15.3083 .0315	35.4552 .0738	
15.9891 .0076	15.3367 0.318	35.4971 0.618	
15.9517 .0160	15.3062 .0155	35.4068 .0366	
15.9690 .0178	15.3008 .0172	35.4063 .0405	
15.9661 .0129	15.3114 .0136	35.4405 .0372	Average Ratios Standard Deviations

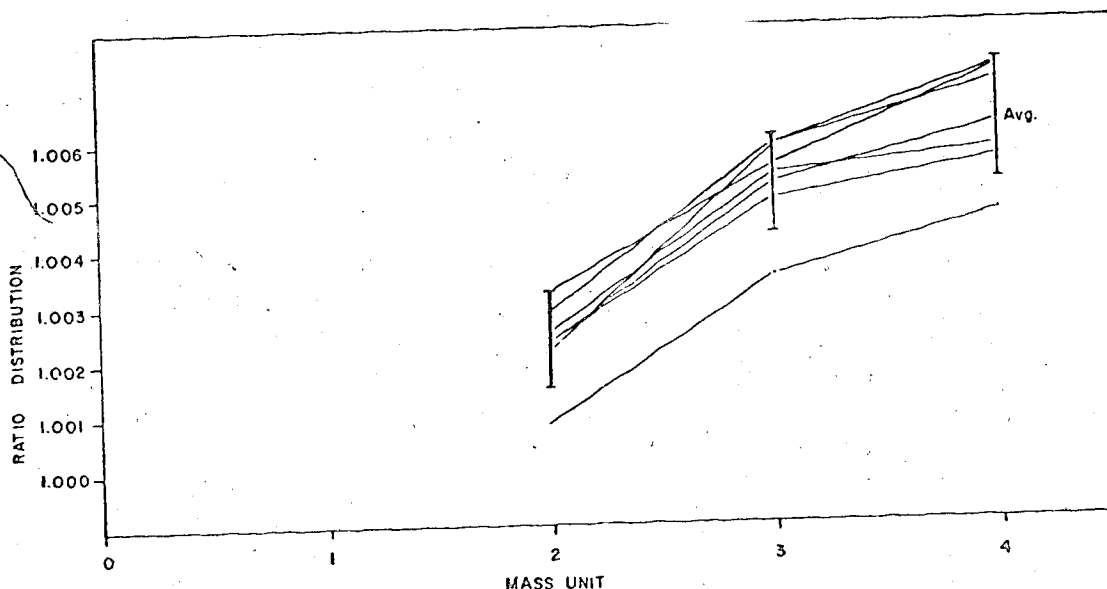


Fig. 29. Measured correction factors, plotted ratio distribution against mass unit.

The slope of the 204-error line is approximately 1 due to the near equal intensity of  $^{206}\text{Pb}$  and  $^{207}\text{Pb}$ . The slope of the fractionation error line is about 1.5 because of the mass unit relationship of  $^{204}\text{Pb}$ ,  $^{206}\text{Pb}$ , and  $^{207}\text{Pb}$ . Should the only errors be 204 and fractionation, then the Broken Hill ratios on the  $^{206}\text{Pb}/^{204}\text{Pb}$  vs  $^{207}\text{Pb}/^{204}\text{Pb}$  plot should lie within the error lines and below the true value (see Fig. 30). In this case the Broken Hill ratios lie close to the 204-error line, but not within the lines thereby indicating that errors other than 204 and fractionation have affected the values.

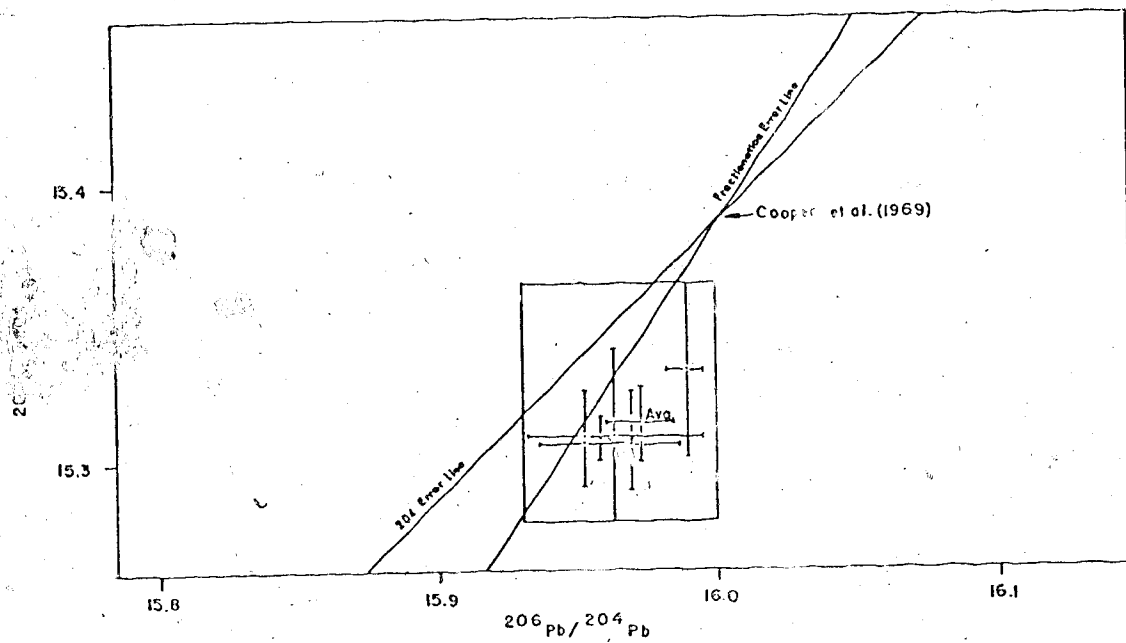
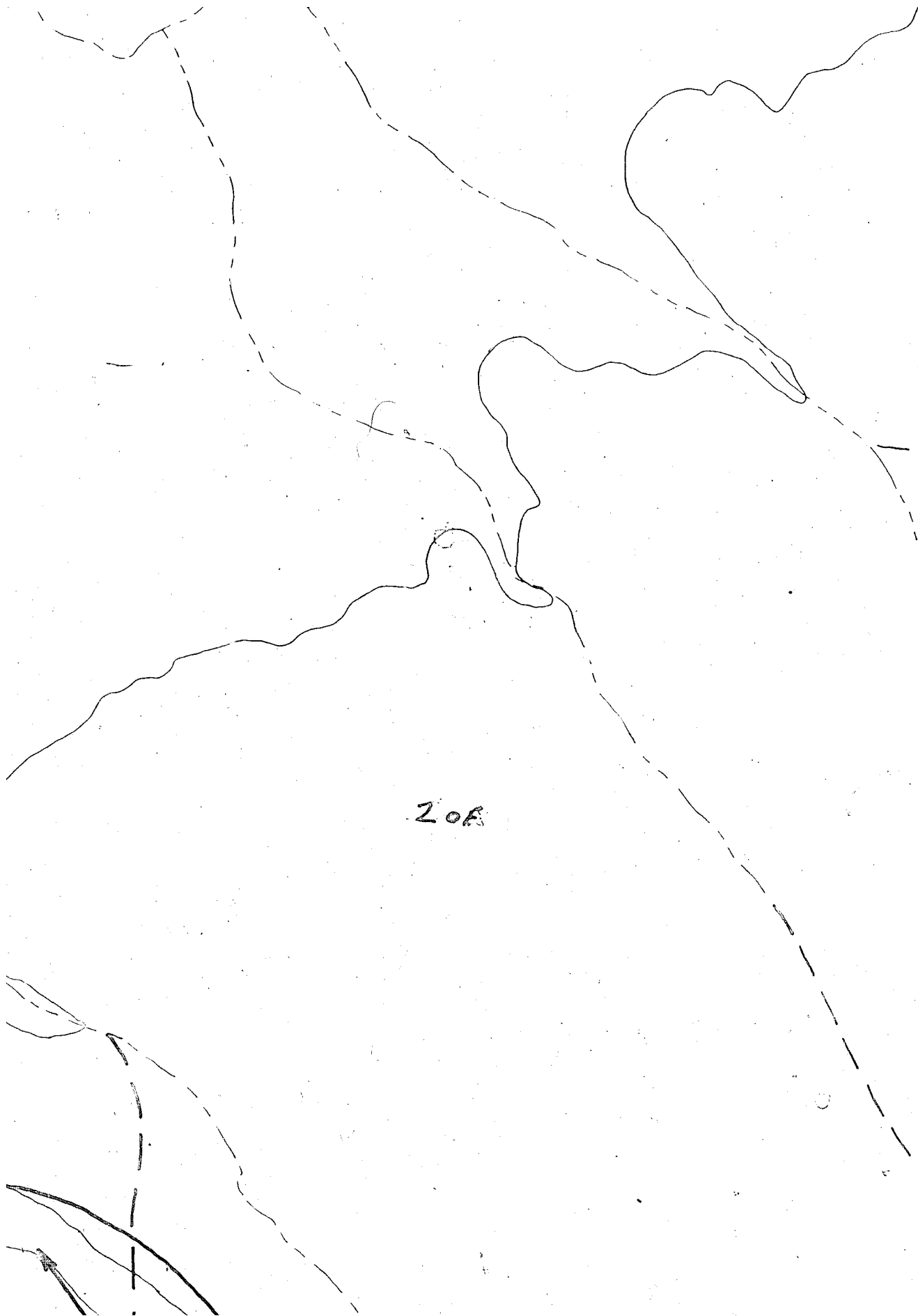


Fig. 30. Standard Broken Hill measured values plotted relative to  $^{204}\text{Pb}$  and fractionation error lines, and the true Broken Hill ratio values (Cooper et al., 1969).

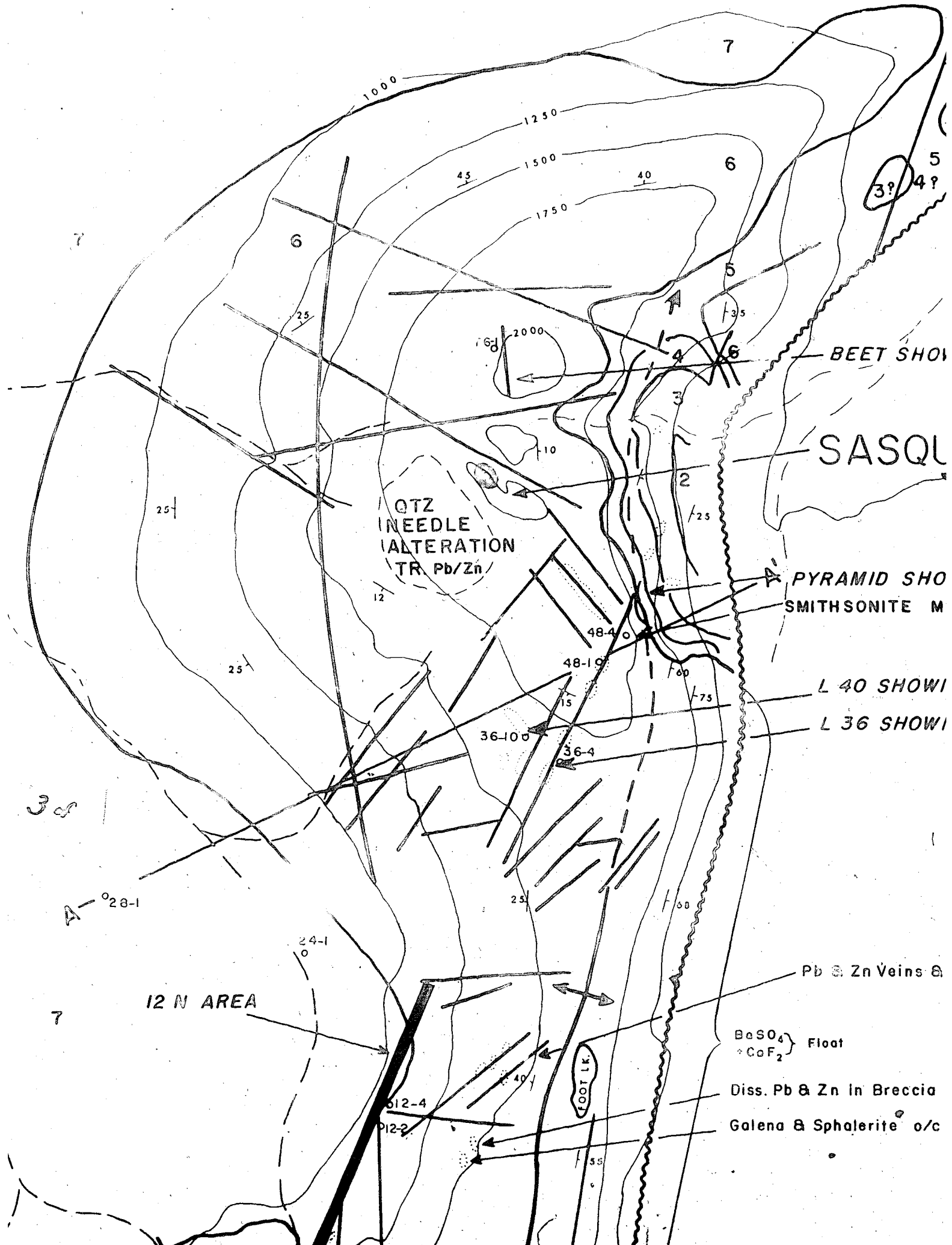
10F





206





QTZ  
NEEDLE  
ALTERATION  
TR. Pb/Zn

SASQL

PYRAMID SHO  
SMITHSONITE M

L 40 SHOWI

L 36 SHOWI

Pb & Zn Veins &

BaSO<sub>4</sub> } Float  
+ CoF<sub>2</sub>

Diss. Pb & Zn in Breccia

Galena & Sphalerite o/c

12 N AREA

FOOT LK

48-4

48-10

36-10

36-4

28-1

24-1

36

45

40

7

6

5

5

4

3

2

1

0

-1

-2

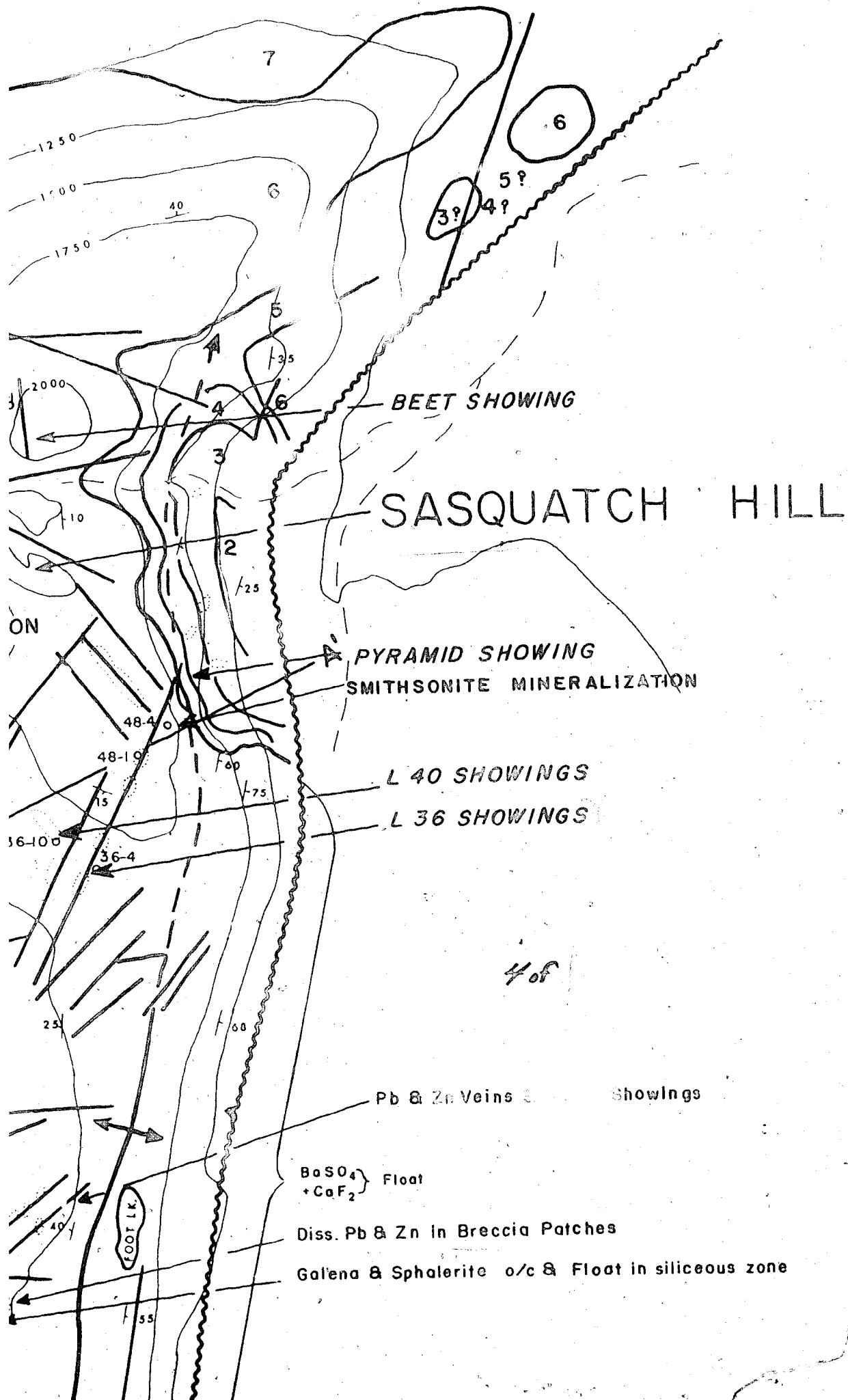
-3

-4

-5

-6

-7



123° 35'  
63° 08'

50F

THUMB MTN.

SOLUTION CAVITIES

750

1000

1250

1500

1750

50

41

60

42

42

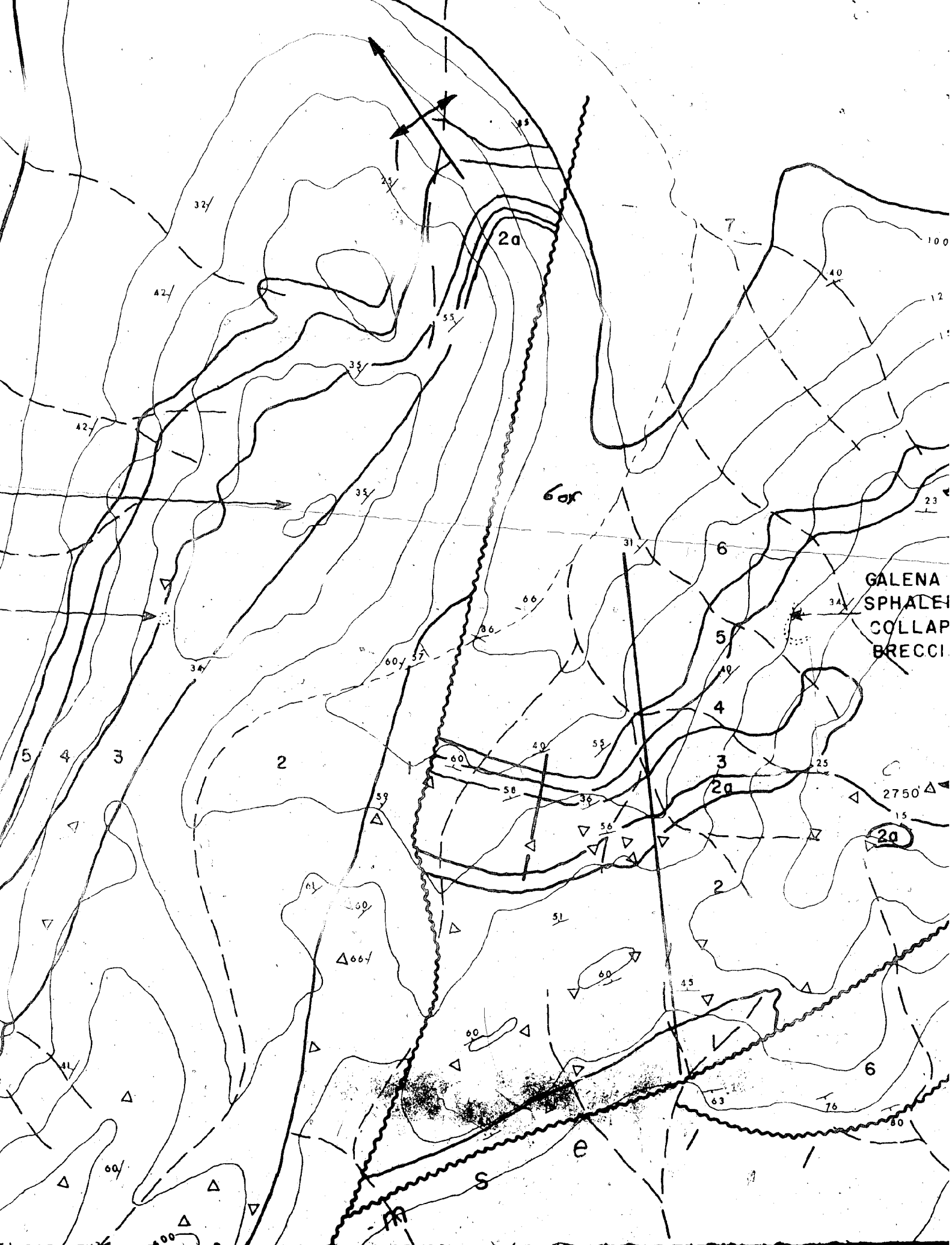
7

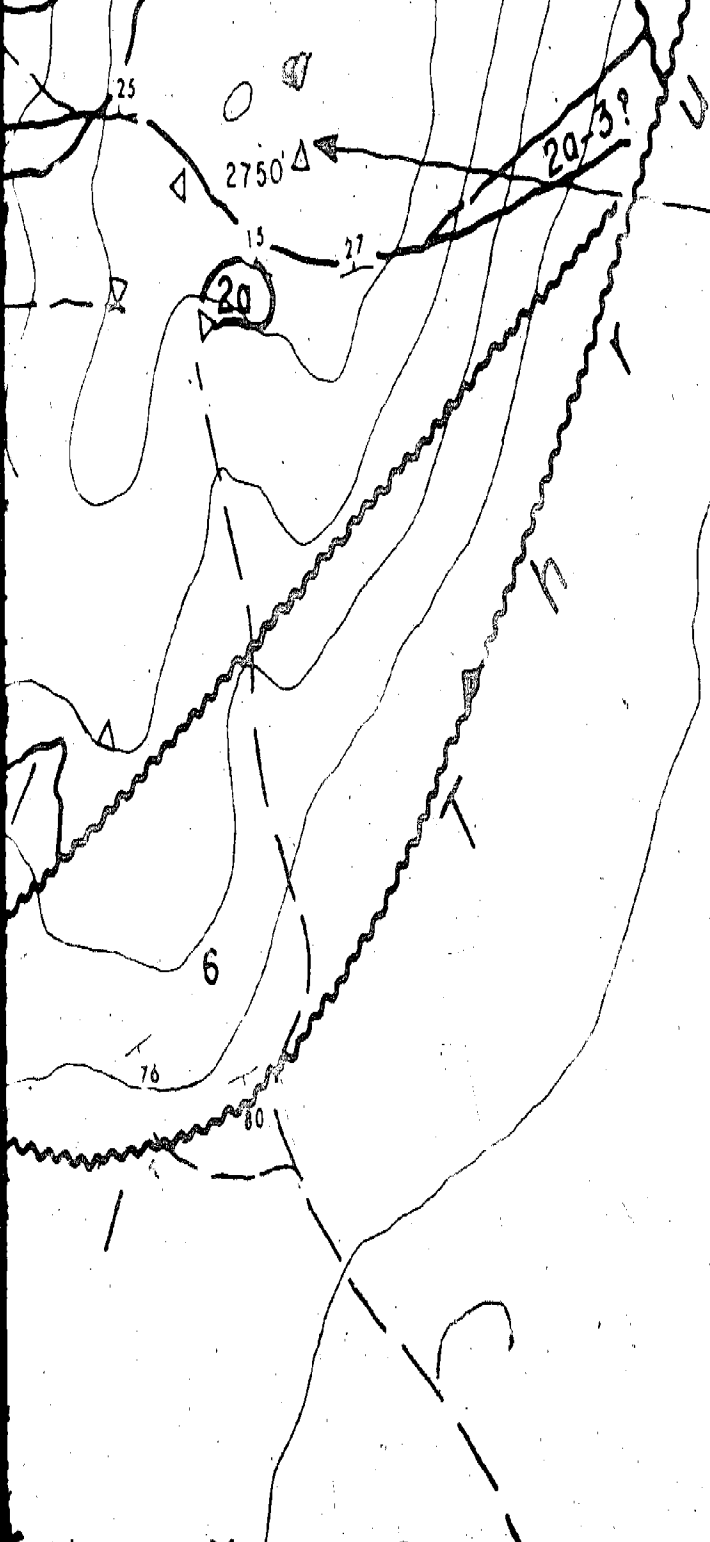
6

5

4

3





GROUCH MTN.

7 of

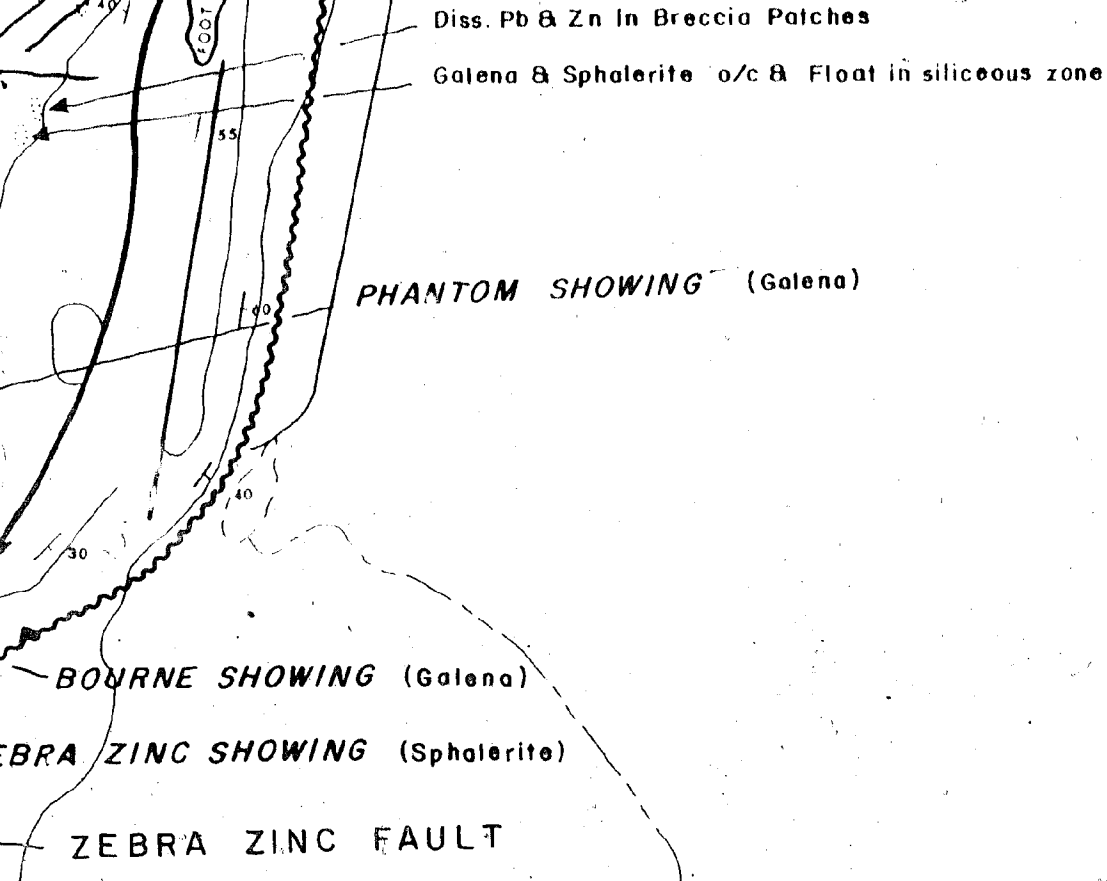


Fig. 1-A

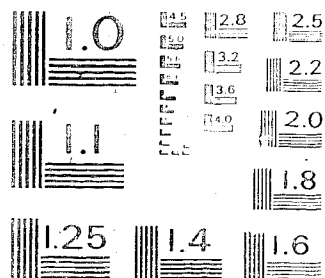
# WRIGLEY PROPERTY

## Legend

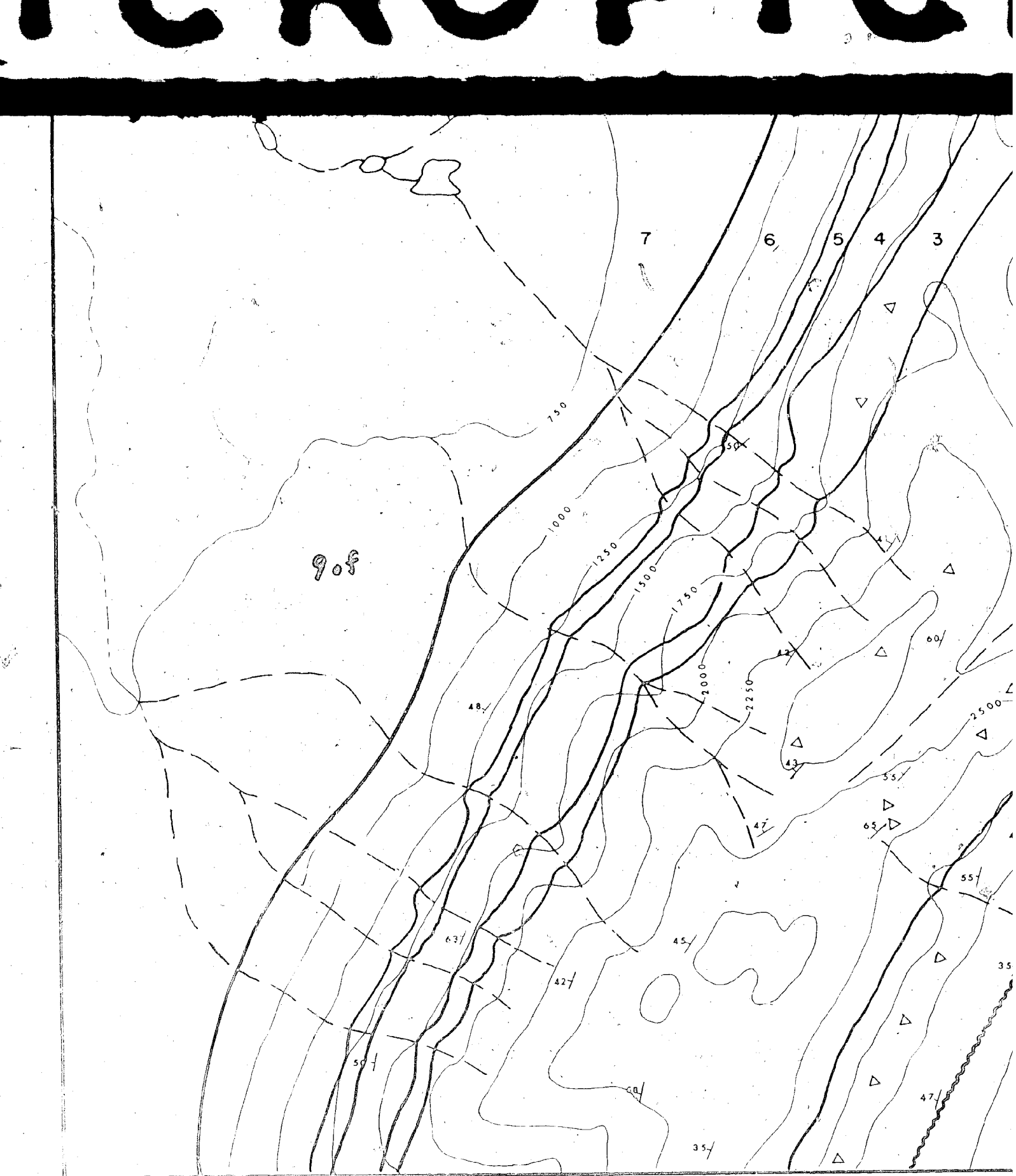
- |      |  |
|------|--|
| 7    | Hare Indian & Fort Simpson Shale               |
| 6    | Nahanni Limestone                              |
| 5    | Headless Shale & Limestone                     |
| 4 4a | Landry Limestone (4) : Transition Zone (4a)    |
| 3    | Manetoe Dolomite                               |
| 2 2a | Arnica Dolomite (2) : Late Stage Dolomite (2a) |
| 1    | Delorme Dolomite & Limestone                   |

3 3

OF/DE

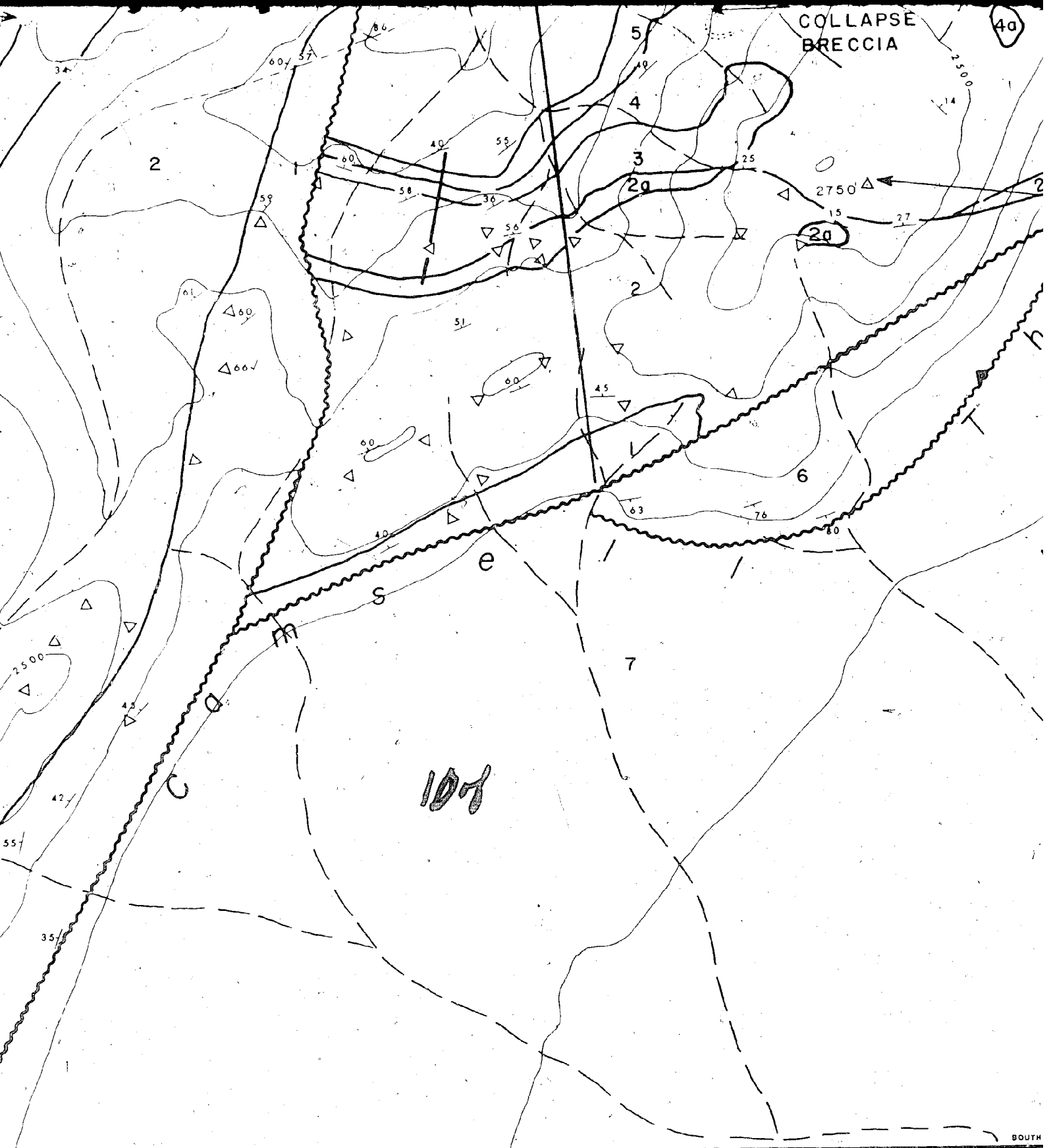


RESOLUTION TEST CHART  
BUREAU OF STANDARDS-1963-A





LE



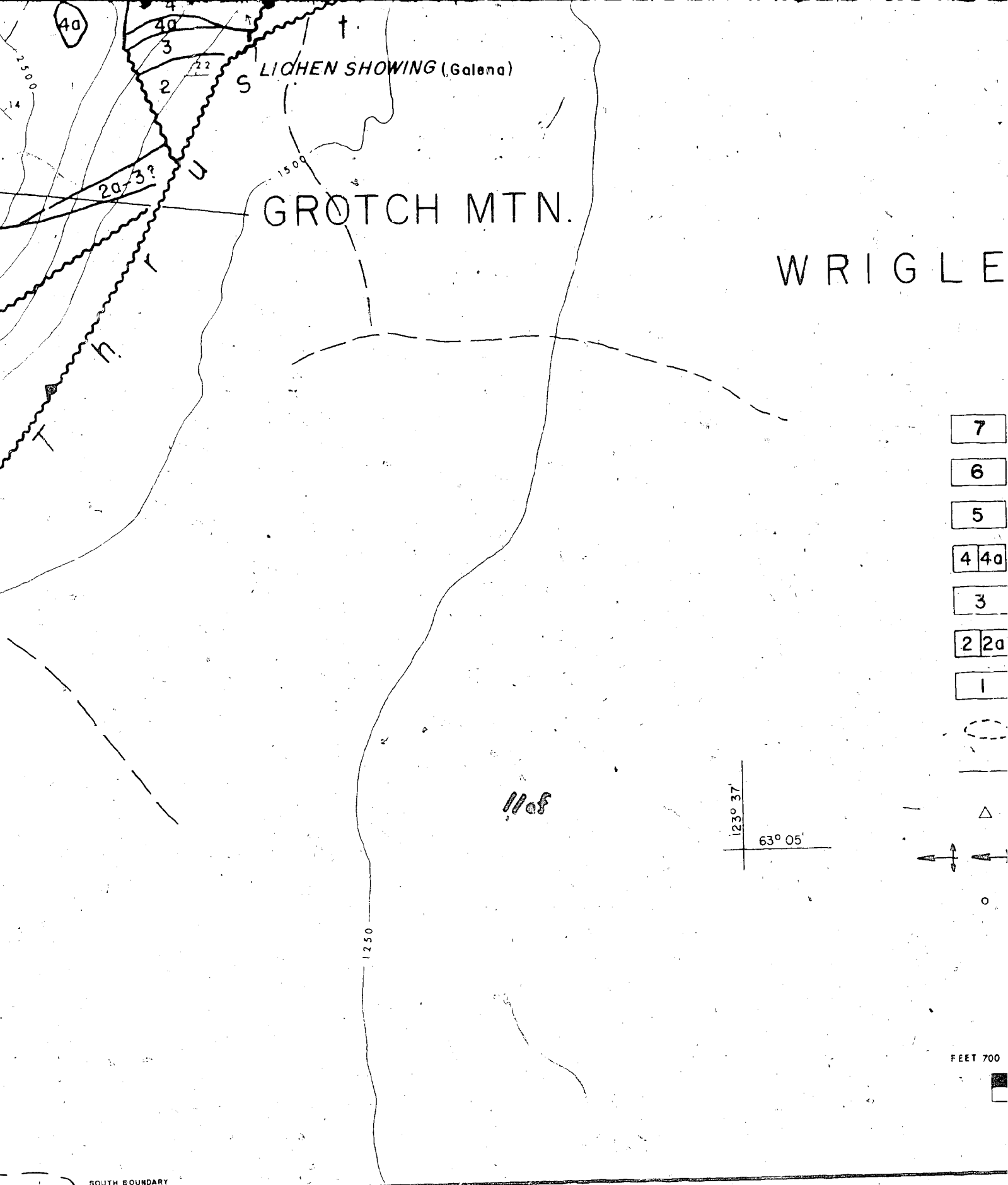


Fig. I-A

# WRIGLEY PROPERTY

## Legend

7

Hare Indian & Fort Simpson Shale

6

Nahanni Limestone

5

Headless Shale & Limestone

4 4a

Landry Limestone (4) : Transition Zone (4a)

3

Manetoe Dolomite

2 2a

Arnica Dolomite (2) : Late Stage Dolomite (2a)

1

Delorme Dolomite & Limestone

○

Pb-Zn Outcrop Showings

—

Faults and/or Linears

△

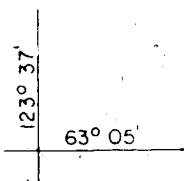
Collapse Breccia

↔

Anticlines, Synclines

○

Diamond Drill Holes



(adapted from map by  
E. Olfert, Cominco Ltd.)

12-8-12

SCALE

FEET 700

0

700

1400 FEET



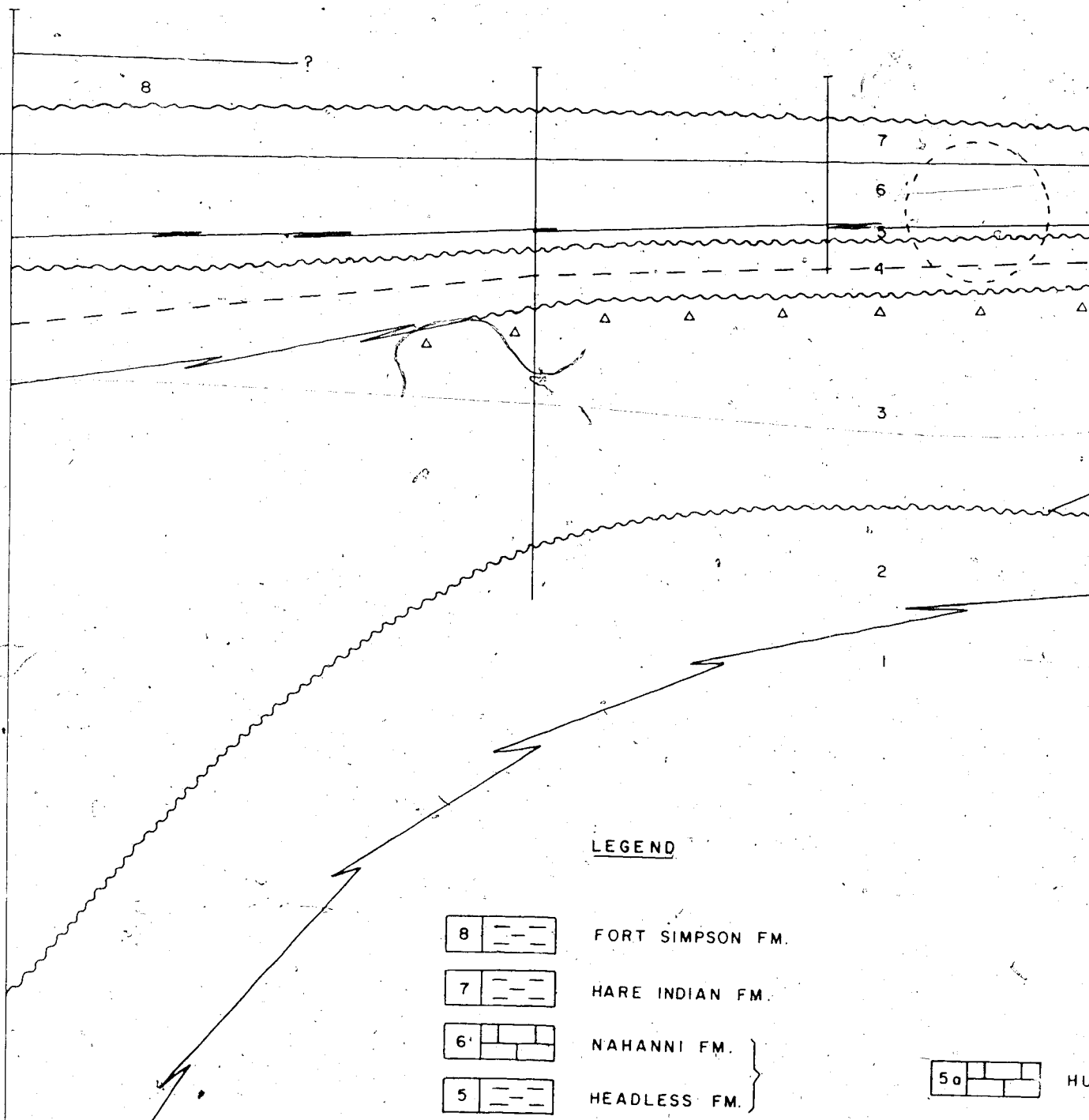
SHELL WRIGLEY

G-70

16F

MEASURED  
SECTION

DDH 28-1

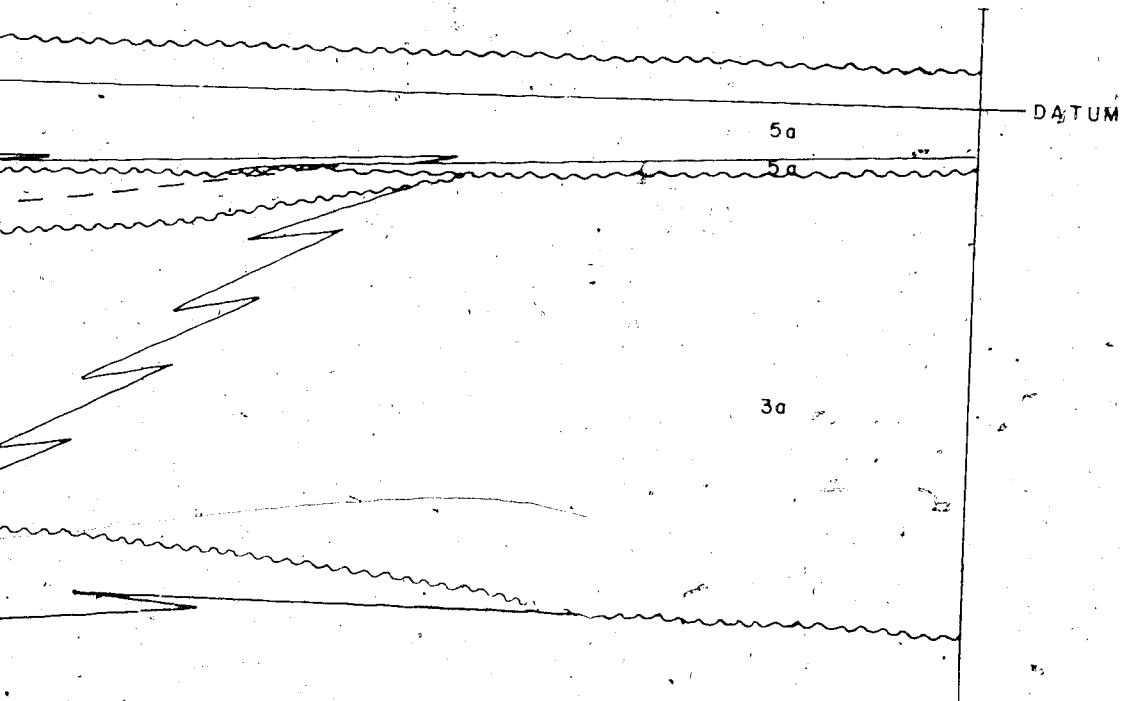


SHELL OCHRE

RIVER

1-15

2 of



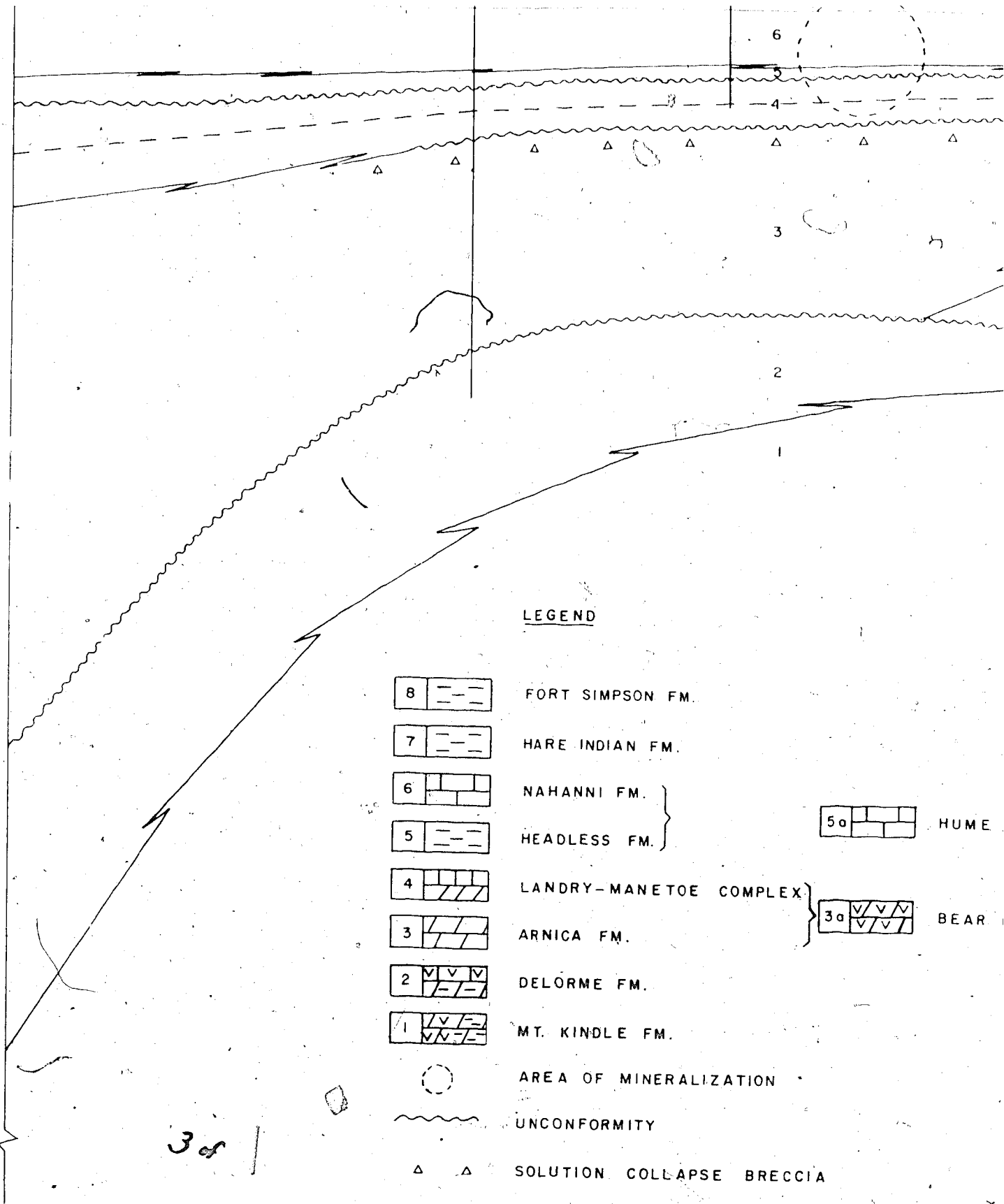
NORTH CAMSELL RANGE CROSS-SECTION

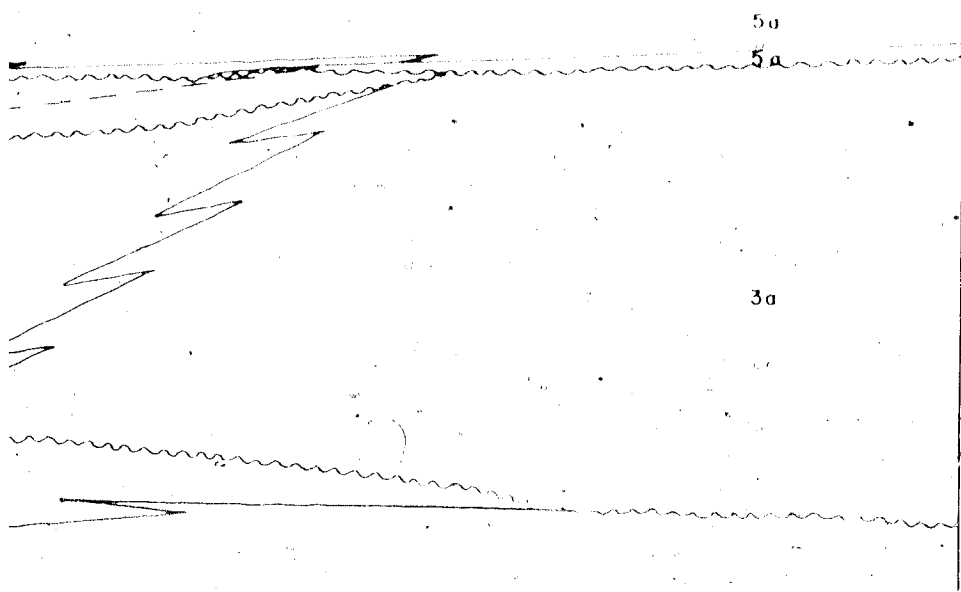
Fig. 4

SHELL OCHRE  
RIVER

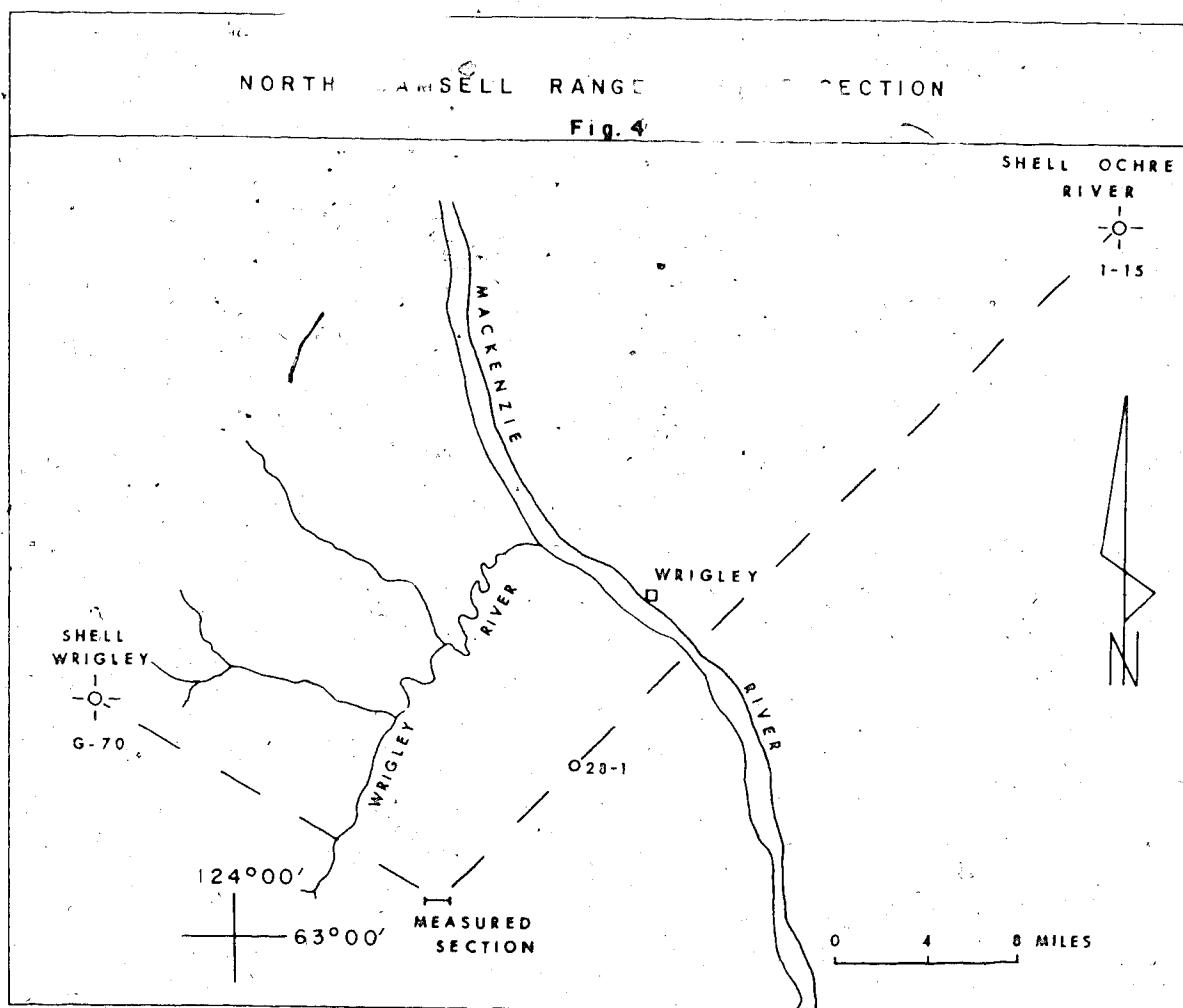
1-15

MACKENZIE





4 of 4



A

28-1

10F

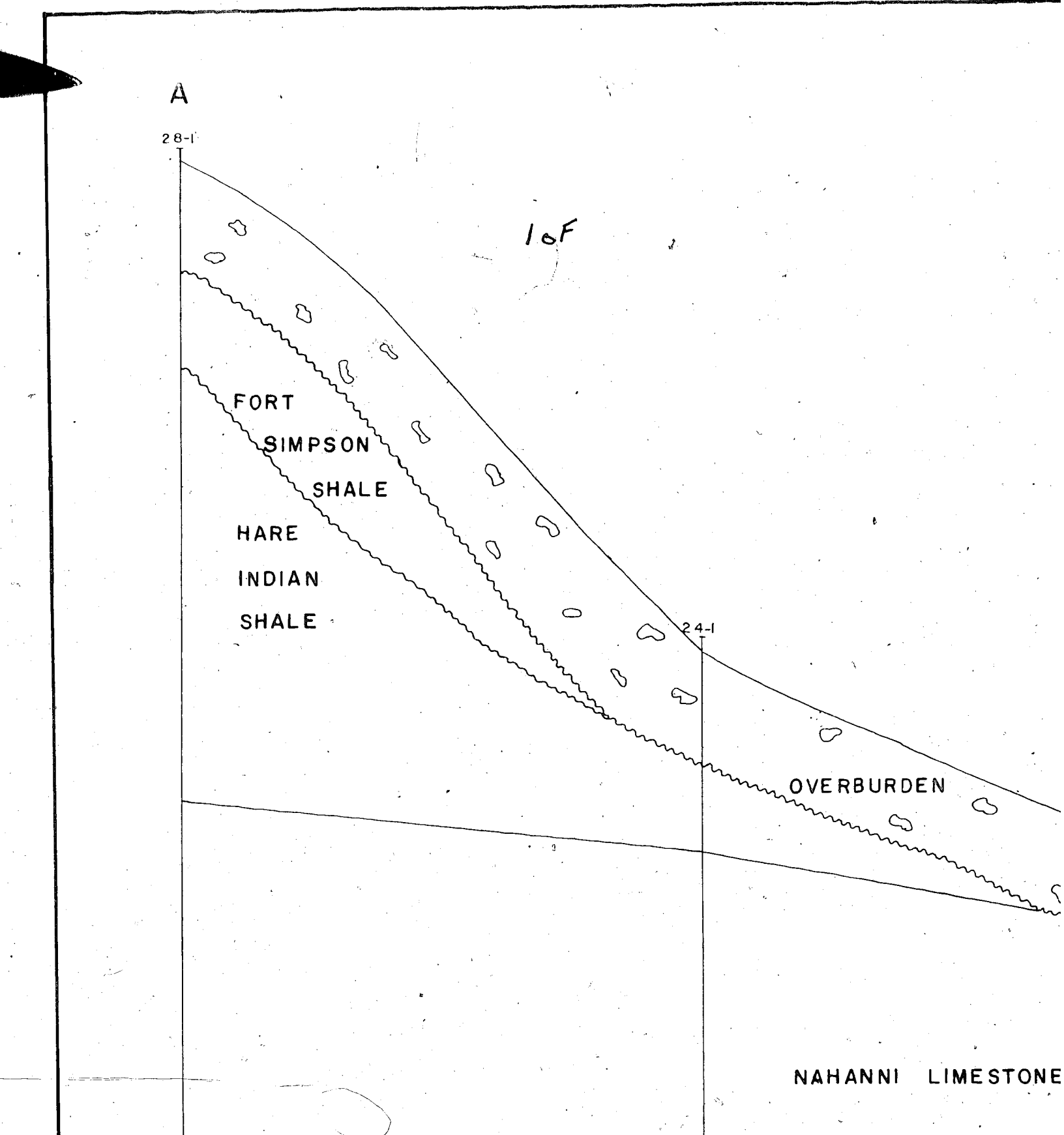
FORT  
SIMPSON  
SHALE

HARE  
INDIAN  
SHALE

24-1

OVERBURDEN

NAHANNI LIMESTONE

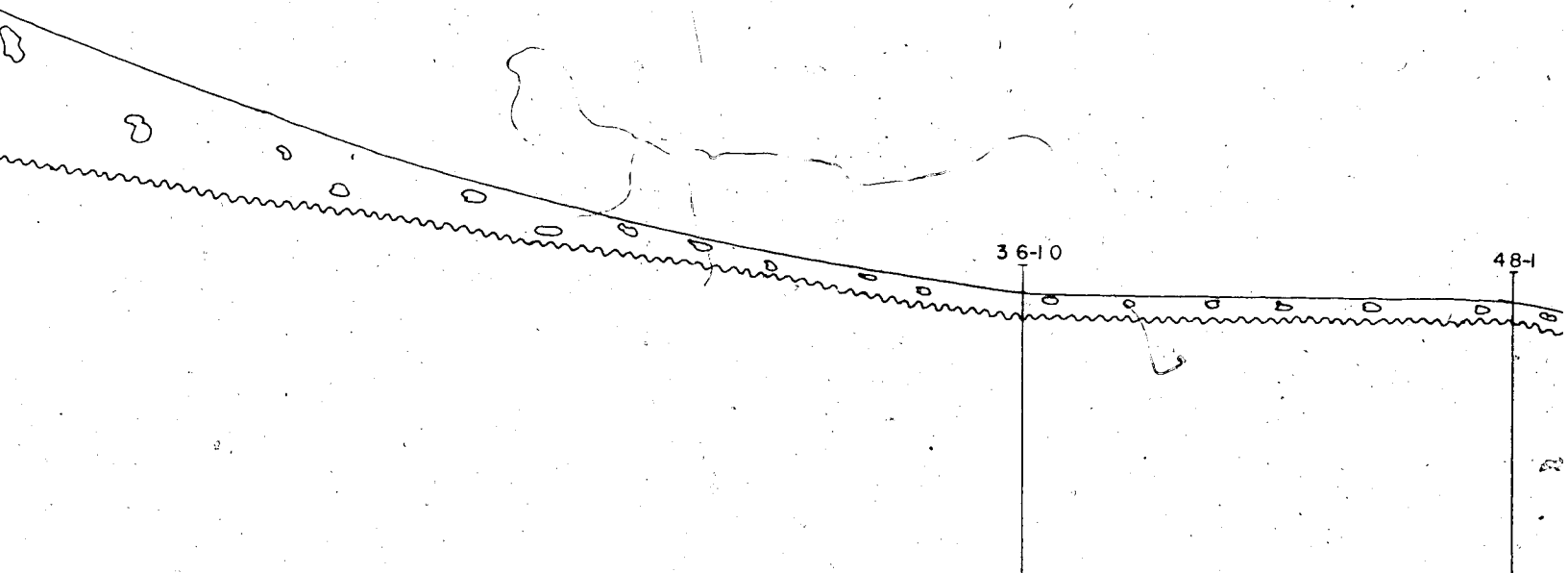




2 of

# WRIGLEY CROSS SECTION A — A'

Fig. 6

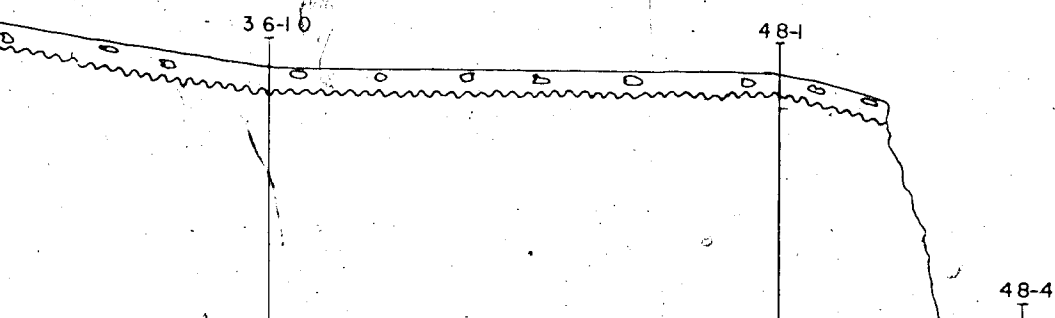


A'

3 of

SECTION A — A'

6



OVERBURDEN

4 of

NAHANNI LIMEST

HEADLESS SHALE

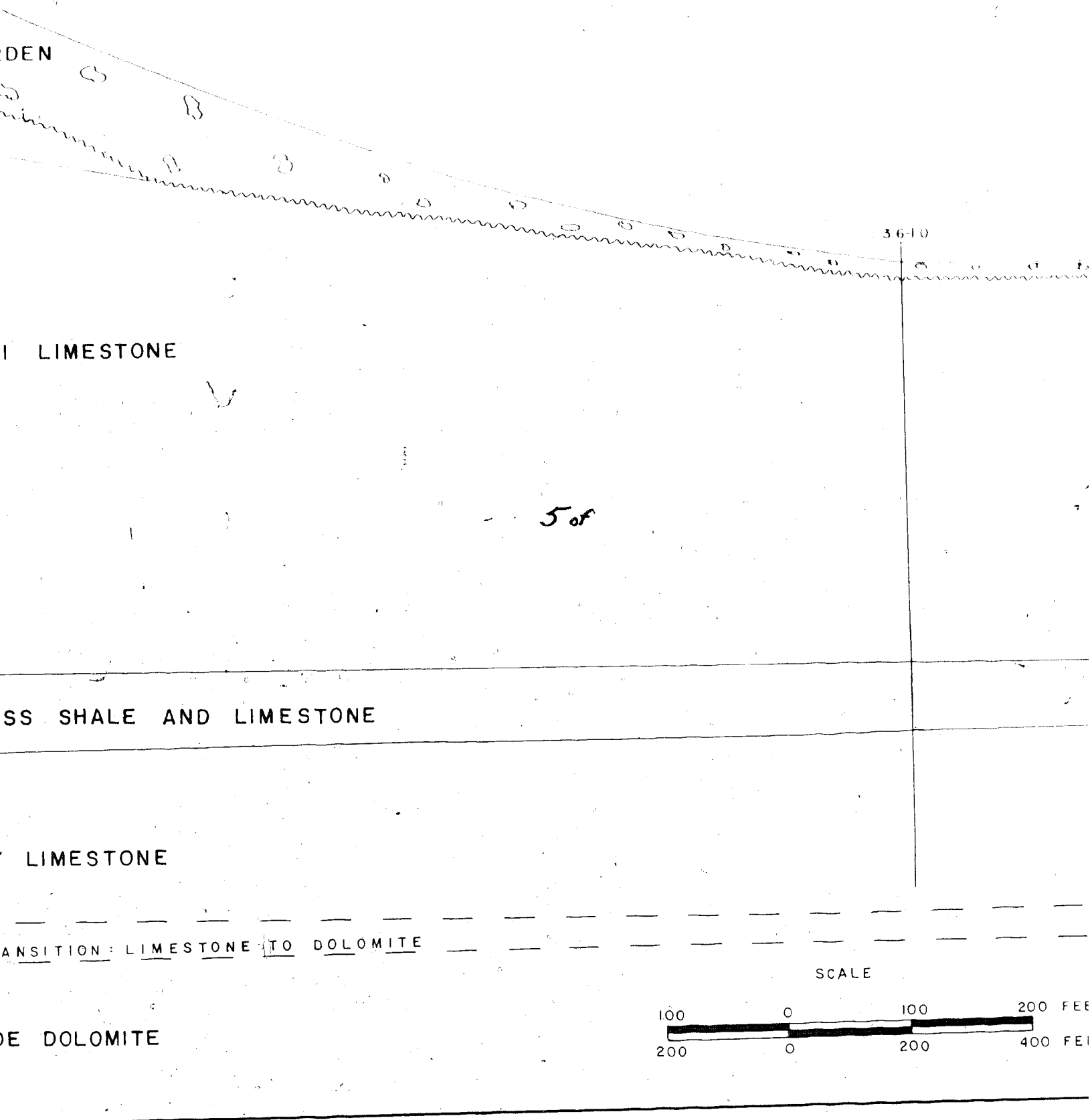
LANDRY LIMESTO

TRANSITION: L

MANETOE DOLOMIT

WRIGLEY CROSS SECTION A — A

Fig. 6



# CROSS SECTION A — A'

Fig. 6

